Applications Using a High Resolution Fluorescence Microscope

by

Şennur Turgut

A Thesis Submitted to the
Graduate School of Engineering
in Partial Fulfillment of the Requirements for
the Degree of

Master of Science
in
Materials Science and Engineering

Koc University

August 2006

Koc University

Graduate School of Sciences and Engineering

This is to certify that I have examined this copy of a master's thesis by

Şennur Turgut

and have found that it is complete and satisfactory in all respects,
and that any and all revisions required by the final
examining committee have been made.

Committee Members:

_____

Alper Kiraz, Ph. D. (Advisor)

_____

İ. Halil Kavaklı, Ph. D.

_____

A. Levent Demirel, Ph. D.

Date: _____

ABSTRACT

Confocal microscopy is a technique used for increasing the resolution of microscope images at the expense of the acquisition time. As compared with wide field microscopy, confocal microscopy provides a better resolution by rejecting out of focus fluorescent light. Despite this fact, smaller acquisition times can yield wide field microscopy superior to confocal microscopy in certain applications.

Fluorescence Resonance Energy Transfer (FRET) is the nonradiative energy transfer from an optically excited molecule (donor, D) to an unexcited nearby molecule (acceptor, A). Measurement of the FRET efficiency is a powerful tool in determining the relative localizations of the donor and acceptor molecules with nanometer (<10 nm) accuracy. We have used total internal reflection fluorescent microscopy to investigate the energy transfer between two fluorescent molecules Rhodamine B and Fluorescein Na in PMMA thin films. Following the steps of spectra FRET, the efficiency of FRET was quantified by the decrease in donor intensity after energy is transferred from donor to acceptor molecule.

We have used confocal microscopy to determine the exact localization of proteins in cells. It was observed that the melanopsin proteins are located in cell membrane, while the cry proteins are distributed in cytoplasm of the cell. Experiments were also performed using cells containing both melanopsin and cryptochrome tagged with red fluorescent protein (RFP) and green fluorescent protein (GFP), respectively. The ultimate goal of these experiments is to observe whether there is an interaction between these two proteins by measuring the FRET efficiency between GFP and RFP labels.

Finally, we observed the single molecule behavior of Rhodamine B molecules in PMMA thin films by wide field microscopy and confocal microscopy.

ÖZET

Eşodaklı mikroskopi tekniği görüntü alma süresini arttırmak pahasına görüntülerin çözünürlüğünü arttırmada kullanılan bir tekniktir. Bu teknik, arka plan gürültüsünü filtrelediği için geniş alanlı mikroskopi tekniğine göre daha yüksek bir çözünürlük sağlar. Buna rağmen veri alma süresinin kısa olması geniş alanlı mikroskopi tekniğini bazı uygulamalarda eşodaklı mikroskopi tekniğine göre üstün kılar.

Florışıl rezonans enerji geçişi (FRET), optik olarak uyarılmış molekülden (verici), bu molekülün yakının da bulunan uyarılmamış moleküle (alıcı) ışınım olmadan gercekleşen enerji transferidir. FRET verimliliginin ölçülmesi verici ve alıcı moleküllerin yerlerinin nanometre mertebesinde bir netlikte (<10 nm) belirlenmesinde kullanılan güçlü bir araçtır. PMMA ince filmi içerisindeki Rhodamine B ve Fluorescein Na floresan molekülleri arasındaki enerji transferini incelemek için toplam iç yansıma ışıma mikroskopi tekniğini kullanıldı. FRET sinyalini bulabilmek için spectraFRET yönteminin adımları takip edilerek, donor molekülünden acceptor molekülüne enerji geçişi olduktan sonra, donor ışımasındaki azalmaya bakılarak FRET verimliliği hesaplandı.

Eşodaklı mikroskopi tekniği kullanılarak, proteinlerin hücre içerisinde bulundukları yerler belirlendi. Melanopsin proteinleri hücre zarına yerleşirken, Cry proteinlerinin hücre sitoplazmasına dağıldıgı gözlemlendi. Deneyler ayrıca kırmızı ışıyan protein (RFP) ile etiketlenmiş melanopsin proteini ve yeşil ışıyan protein (GFP) ile etiketlenmiş cryptochrome proteinleri ile yapıldı. Amacımız bu iki protein arasında etkileşim olup olmadığına bu proteinleri etikelemekte kullanılan kırmızı ve yeşil ışıyan proteinler arasındaki enerji geçişi verimliliğine bakarak karar vermek.

Son olarak, eşodaklı mikroskopi ve geniş alanlı mikroskopi teknikleri kullanılarak PMMA ince film tabakası içersinde bulunan Rhodamine B molekülünün tek molekül davranışı gözlemlendi.

ACKNOWLEDGEMENTS

Firstly, I would like to thank my academic advisor, Professor Alper Kiraz, for the support and guidance he has provided me throughout my study. Beside, I am so thankfull to Professor Burak Erman, Professor İ. Halil Kavaklı and Dr. Şule Özdaş for their collabaration and guidance as well as providing me samples. Furthermore, I would like to thank to Professor Levent Demirel for providing me the materials I need for my experiments and letting me to use the devices in his laboratory.

Furthermore, I would like to thank to Adnan Kurt for helping us to build experimental set-up.

During my thesis work, I have enjoyed sharing ideas with other students of my group, Mehmet Ali Dündar and Sultan Doganay.

Outside of my group, I would like to thank my friends, for their friendship. I am fortunate to have met Evrim Besray Ünal, Ümit Demirbaş, Hüseyin Çankaya, Onur Akatlar, Oktay Aktaş.

In addition, I wish to thank my family, for their support, love and patience during my master study at Koç University. I wish to dedicate this thesis to them.

TABLE OF CONTENTS

LIST OF TABLES

LIST OF FIGURES

NOMENCLATURE

S_0	ground state
S_1	first energy level
S_2	second energy level
ΔE	energy difference
k	Boltzman constant
T_1	first triplet state
A°	Angstrom
k_t	energy transfer rate
r^-	the distance between the dipoles
τ_d	the lifetime of donor molecule
R_0	förster radius
$F(\lambda)$	the corrected fluorescence intensity of the donor
λ_d	the emissive rate of the donor
ϕ_d	quantum yield of the donor
$\varepsilon_a(\lambda)$	absorption coefficient of the acceptor at λ
K^2	orientation factor
Γ_d	decay rate of the donor
n	the refractive index of the sample
NA	numerical aperture
M	magnification
R	resolution
θ	half angle of the cone of light converging to an illuminated spot
ϕ	effective diameter
Γ	radiative
k	non-radiative processes

f	the ratio between the lens' focal length and the its clear aperture
ε_D	molar extinction coefficients for the donor
ε_A	molar extinction coefficients for the acceptor
Eapp	apparent FRET efficiency
F_D	donor intensity before photobleaching of the acceptor
$F_D^{'}$	donor intensity after photobleaching of the acceptor
I_{DA}	the donor emission intensity in the presence of the acceptor
I_D	the donor emission intensity in the presence and absence of the acceptor
r	the donor and acceptor separation

Chapter 1

INTRODUCTION

Fluorescence imaging techniques have become important experimental tools in modern biology. High resolution techniques such as X-ray crystallography and NMR spectroscopy determine three-dimensional structures of biological molecules, on the other hand, fluorescence imaging technology, reveals both temporal and spatial information on molecular structures in living cells [1].

Confocal microscopy, which is one of the most used microscopy methods, when combined with the technique of fluorescence resonance energy transfer (FRET) can provide powerful strategies to study molecular events in living cells. Confocal microscopy provides better resolution of microscope images as compared with wide field microscopy. Since it reduces background haze which results from the out of focus fluorescent light [2].

Nonetheless, both confocal and widefield microscopy techniques are used in detecting energy transfer between fluorescent molecules. Wide field microscopy provides faster detection of the samples than confocal microscopy. It illuminates the whole sample at the same time and detects simultaneously, to the contrary, the confocal microscopy has point detection. Thus, while a widefield microscopy image is obtained in tens of ms, obtaining a confocal image takes tens of seconds.

Fluorescence Resonance Energy Transfer (FRET) is a technique of nonradiative energy transfer from an optically excited molecule (donor, D) to an unexcited nearby molecule (acceptor, A). This method is a powerful tool in studies of protein-protein interactions in living cells and studying conformational distribution and dynamics of biological molecules [3, 4]. Until recently, there were few techniques such as

immunoprecipitation and affinity chromatography for molecular biologists to search for specific interactions between proteins depending on the use of chemical crosslinking agents and antibodies. However, these techniques do not preserve the physiological conditions when proteins undergo interactions within the cell. Moreover, these techniques do not provide information on the spatial distribution of interacting proteins. FRET measurements can solve these problems [5].

Each of the letters in the FRET acronym has significance. The first letter F stands for fluorescence because of the need for a fluorescent or light emitting donor to transmit energy to an acceptor according to some researchers whereas the others argue that it is the F of Förster and FRET Förster Resonance Energy Transfer since it is not the fluorescence that is transferred. Resonance is used because of the fact that the acceptor must be able to resonate with the donor oscillator, energy is used since the electronic energy resonates rather than the fluorescence. Transfer is included since FRET requires the resonance to be over distances that are much larger than the atomic distances.

There are many fluorescent probes, originally synthetic or natural, used to label specific molecules in FRET applications. Donor-acceptor pairs can be used to find proximity relationships in biological macromolecules and in measuring interactions between two proteins, DNA and a protein or other biological macromolecules [6]. In choosing fluorescent chromophores for a suitable application, a large overlap between the emission spectrum of donor and absorption of acceptor is crucial.

The discovery of green fluorescent protein (GFP) has revealed many opportunities for the analysis of gene function and protein-protein interactions [5]. The fluorophore can be fused to a wide variety of protein and enzyme targets, in order to monitor cellular processes in living systems using optical microscopy [7]. GFP and its derivatives are used to find localization of fusion proteins in cells by targeting the GFP to locations by fusing the mutants with organelle-specific localization signals [5].

In this study, FRET phenomenon between two dye molecules: Rhodamine B and Fluorescein Na is investigated. Furthermore, in vivo FRET experiments performed on the proteins: cryptochrome and melanopsin which are tagged with GFP and RFP respectively, will be discussed. Melanopsin and cryptochrome play roles in human biological clock, and FRET experiments should provide indications on the presence or absence of an interaction between them.

Chapter 2 describes the fluorescence mechanism and possible de-excitation pathways of excited molecules in detail. Then, the characteristics of fluorescence emission are given. Thereafter, nonradiative resonance energy transfer i.e. fluorescence resonance energy transfer and the theory behind the FRET technique is explained.

Two microscopy techniques: confocal and wide field microscopies that we used in our experiments are explained in Chapter 3. Especially, the emphasis on confocal microscopy is done with the components of microscopy technique as well as the working mechanism of the technique. After that, the differences between these techniques are discussed.

In Chapter 4, the applications of these two microscopy techniques to Rhodamine B molecules are given. The single molecule observation of Rhodamine B in thin films by confocal and wide field microscopy is provided with the discussion of these results.

In Chapter 5, before discussing the experimental results of the FRET mechanism between Rhodamine B and Fluorescein Na molecules, the information is provided on the characteristics of these fluorescent probes, which makes them a suitable FRET. Then, the energy transfer is discussed between Fluorescein Na and Rhodamine B prepared in thin films with experimental results provided by wide field microscopy.

In chapter 6, the biological experiments performed using GFP tagged cryptochrome and RFP tagged melanopsin proteins are discussed. First the locations of the proteins in

cells are verified by confocal microscopy. Then, FRET experiments are performed to assess the relative vicinity of melanopsin and cryptochrome.

The thesis is concluded with a short summary of the performed study and future research work.

.

Chapter 2

FLUORESCENCE RESONANCE ENERGY TRANSFER

2.1 Introduction

Luminescence, which was introduced by the physicist Eilhardt Wiedemann in 1888, has opened a new area in science. Luminescence is an emission of ultraviolet, visible or infrared photons from an electronically excited state. The types of luminescence can vary according to the mode of excitation. Fluorescence is a particular case of luminescence where the mode of excitation is the absorption of light. The absorbing species are excited into electronic excited states, and then the emission of photons occurs within an average excitation lifetime (typically 10^{-10}- 10^{-7} s for dye molecules). In fact, many pathways are also possible after the absorption of light such as internal conversion, intersystem crossing, intramolecular charge transfer and conformational change. The molecule in an excited state can interact with molecules in its close vicinity if the interaction takes place on a time-scale comparable with the average excited state lifetime during which the molecules stay in the excited state. The interactions can be in the form of proton transfer, electron transfer, energy transfer, excimer or exciplex formation.

Energy transfer is a dynamic process providing information on a molecule's close vicinity by affecting the characteristics of fluorescence such as spectrum, quantum yield, and lifetime [2]. Fluorescent resonance energy transfer (FRET) is a powerful technique which is widely used for studying biological systems on the nanometer scale. FRET occurs over distances similar to the Förster radius, which is ≈5 nm for common fluorophores [8].

FRET can function as a molecular ruler [6] because of being very sensitive to distances. In 1948, Förster proved that FRET efficiency between two fluorophores decreases with the sixth power of distance. Accurate knowledge on the fluorophore's orientation and position is needed for accurate measurement of the distance using the FRET efficiency [9].

In this chapter, the Fluorescence Resonance Energy Transfer mechanism is explained. First, fluorescence process is explained and followed by possible de-excitation pathways of excited molecules. Afterwards non-radiative resonance energy transfer between a donor and an acceptor fluorophore is explained. This is followed by the theory of FRET.

2.2 Fluorescence

2.2.1 Introduction to Fluorescence

Luminescence is the emission of photons from electronically excited states. It is divided into two types according to the nature of the ground and the excited states. In a singlet excited state, the electron in the higher-energy orbital has the spin orientation opposite to the spin orientation of the second electron in the lower orbital. In a triplet state these electrons are unpaired since their spins have the same orientation. While returning to ground state from an excited singlet state the electron does not change its spin orientation whereas returning from triplet state to singlet ground state requires a change in spin orientation. Fluorescence is the emission resulting from the return of the electron in a singlet excited state to the lower orbital. These transitions are quantum mechanically allowed and the emissive rates are near 10^{8} sec^{-1}. These high emissive rates cause fluorescence lifetimes to be around 10^{-8} sec or 10 nsec. The lifetime is the time that the electron stays in the excited state [8].

Substances that show high fluorescence generally have delocalized electrons present in conjugated double bonds. Namely, some of these fluorescent molecules are quinine, fluorescein, rhodamine B, anthracane.

2.2.2 Jablonski Diagram

Fluorescence occurs as an external light source provides a photon of energy that is absorbed by a fluorescent molecule raising it to an excited state. The electron stays in the excited state for a finite time before relaxing back to ground state, releasing a photon on doing so and generating fluorescence emission [10]. There are also many other pathways (Figure.2.1) for de-excitation: internal conversion (i.e. direct return to the ground state without emission of fluorescence), intercrossing (possibly followed by emission of phosphorescence), intermolecular charge transfer and conformational change. Furthermore, interactions in the excited state can compete with de-excitation: electron transfer, proton transfer, energy transfer, excimer or exciplex formation.

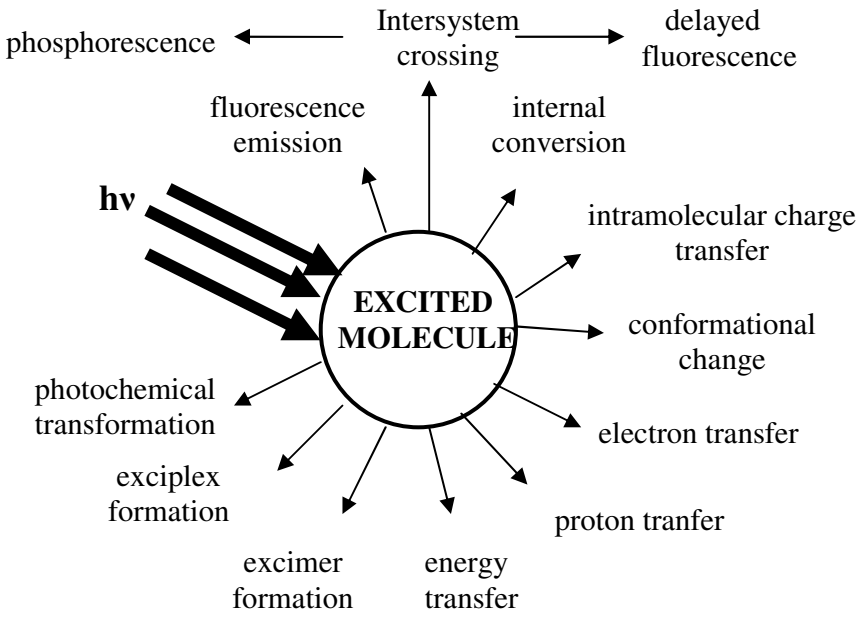

Figure 2.1 Possible de-excitation pathways of excited molecules

The diagram suggested by A. Jablonski is seen in Fig. 2.2. The possible energy transitions are illustrated in this figure. S_0, S_1, S_2 are the electronic states corresponding to the ground, first, and second level. The fluorophores can exist in a number of vibrational energy states shown by 0, 1, 2 at each of these electronic states.

The ratio of molecules in each state is given by the following formula

$$R = e^{-\Delta E/kT} \tag{2.1}$$

Where ΔE is the energy difference, k is the Boltzman constant, and T is the temperature in degrees Kelvin (K). According to this formula, most molecules are found in the lowest vibrational state. Thus, light absorption occurs in this energy level. Due to the large energy difference between first and ground levels fluorophores can not populate the higher energy

levels. However, owing to light absorption, several processes happen. A fluorophore molecule is excited to higher vibrational level of S_1 or S_2. Generally, molecules in condensed phases rapidly relax to the lowest vibrational level of S_1. This is known as internal conversion, which is non-radiative transition between two electronic states of the same spin multiplicity. The excess vibrational energy can be transferred to the solvent during collisions of the excited molecule with the surrounding solvent molecules [2]. This process occurs in time scales of 10^{-12} sec. Since internal conversion occurs within time intervals that are much smaller than the fluorescence lifetime (in the order of 10^{-8} sec), it is completed before emission. In general, electronic excitation does not change the spacing of vibrational energy levels so much. Thus, the vibrational structures seen in the emission and absorption spectra are similar [8].

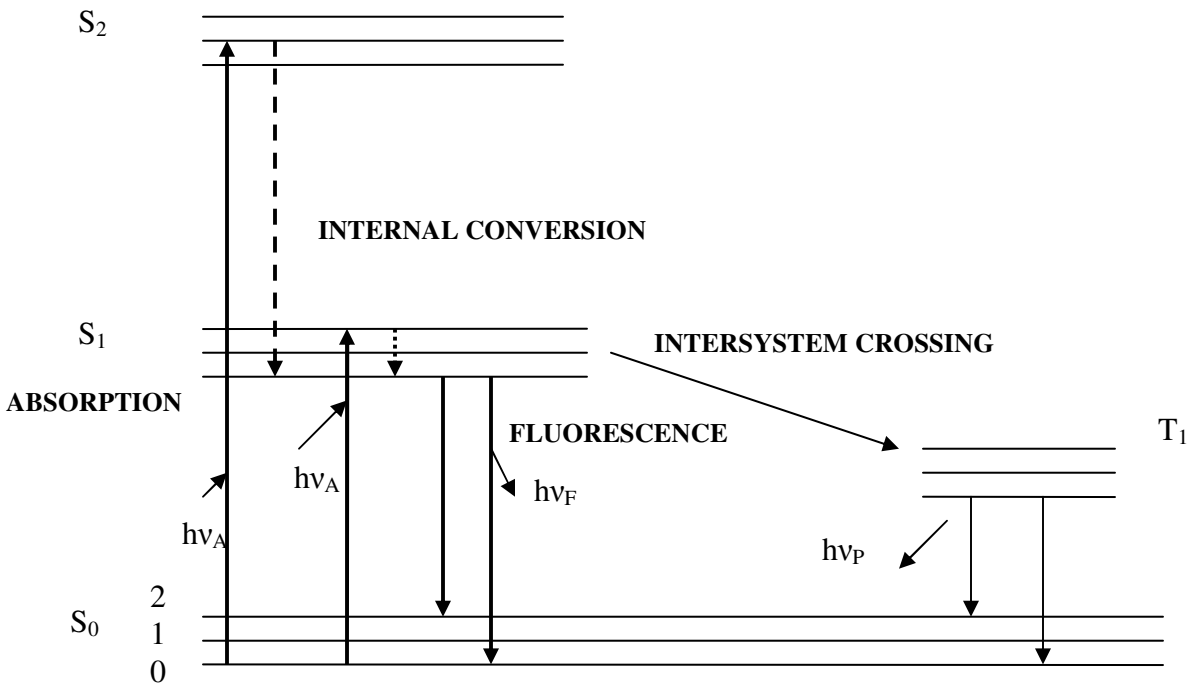

Figure 2.2. Jablonski Diagram

Furthermore, the molecules can undergo conversion to the first triplet state T_1. Emission from T_1 is called phosphorescence, which is shifted to longer wavelengths i.e. lower energy relative to fluorescence. The process is slow compared to fluorescence since the transition from T_1 to the ground state is forbidden. Therefore, numerous collisions with solvent molecules support intersystem crossing, which is the conversion of S_1 to T_1. In addition, there are also variety of factors affecting the fluorescence emission such as solvent effects, solvent relaxation, quenching, and numerous excited state reactions [2, 8].

2.2.3 Characteristics of Fluorescence Emission

2.2.3.1 Stokes' Shift

Fluorescence occurs when light absorbed by a molecule is emitted after a very short time period (approximately 10^{-8} s). Emitted light is always at a longer wavelength than the absorbed light. This phenomenon was first observed by Stokes in 1852, [8] hence the name of this phenomenon is Stokes shift. This shift is important for the detection of fluorescence as it helps to discriminate between the excitation and the emission signal [10].

Energy losses between excitation and emission are observed universally for fluorescing molecules in solution. One of the main causes of Stokes shift is the rapid decay to the lowest vibrational level of S_1. Moreover, fluorophores also decay to excited vibrational levels of S_0 which leads to more loss of vibrational energy. Beside this, fluorophores can show more Stokes shift because of solvent effects and excited state reactions [8].

2.2.3.2 Mirror Image Rule

In general, the fluorescence emission spectrum seems to be a mirror image of the absorption spectrum. Since the same transitions are involved in both absorption and emission, and the vibrational levels of S_0 and S_1 are similar. All electronic transitions are vertical according to Franck-Condon principle because they occur without change in the position of nuclei. However, there are some exceptions to this mirror image rule. Deviation from mirror image can result from different geometric arrangement of nuclei in the excited state as compared to the ground state. Nuclear displacement can occur due to the relatively long lifetime of the S_1 state. Furthermore, excited state reactions can also lead to deviation from mirror image rule [8].

2.3 Non-Radiative Energy Transfer

Non-radiative energy transfer occurs between a donor and acceptor molecule if the emission spectrum of the donor overlaps with the absorption spectrum of the acceptor (Fig. 2.3). Thus, several vibronic transitions in the donor have practically the same energy as the corresponding transitions in the acceptor. The coupling of transitions or resonance are seen in Fig. 2.4. This is known as resonance energy transfer, in some papers Fluorescence resonance Energy Transfer (FRET).

Non-radiative energy transfer can result from different interactions of molecules with their close microenvironment [2]. In Fig. 2.5 the coupled transitions involved between the donor emission and acceptor absorbance are shown on the Jablonski Diagram.

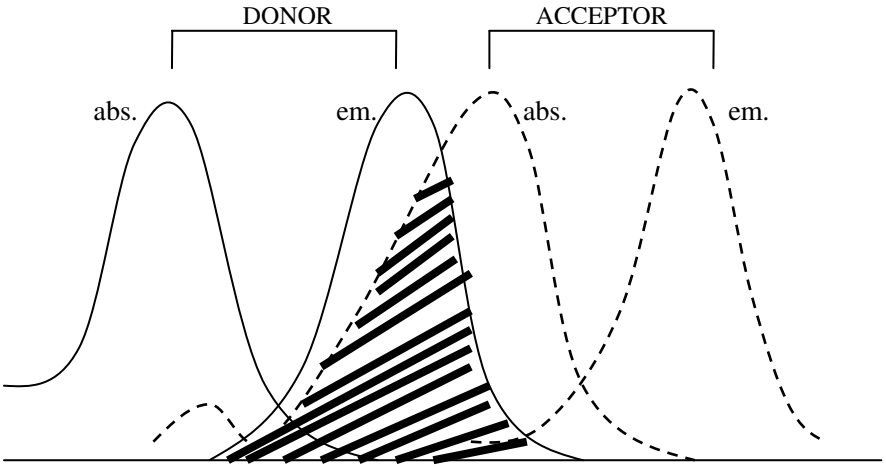

Figure 2.3. The spectral overlap between emission spectrum of the donor and the absorption spectrum of the acceptor

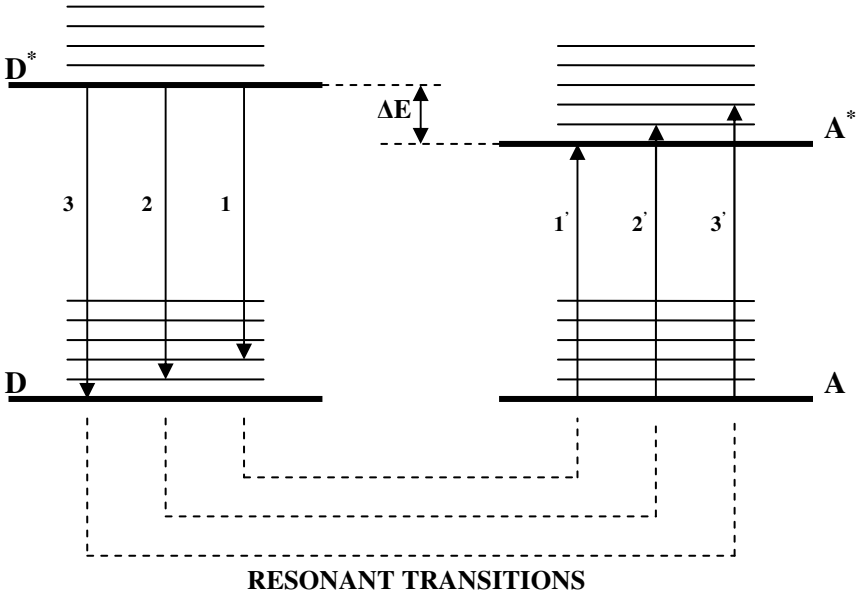

Figure 2.4. Coupled transitions in energy levels of donor and acceptor molecules

Resonance Energy Transfer Jablonski Diagram :

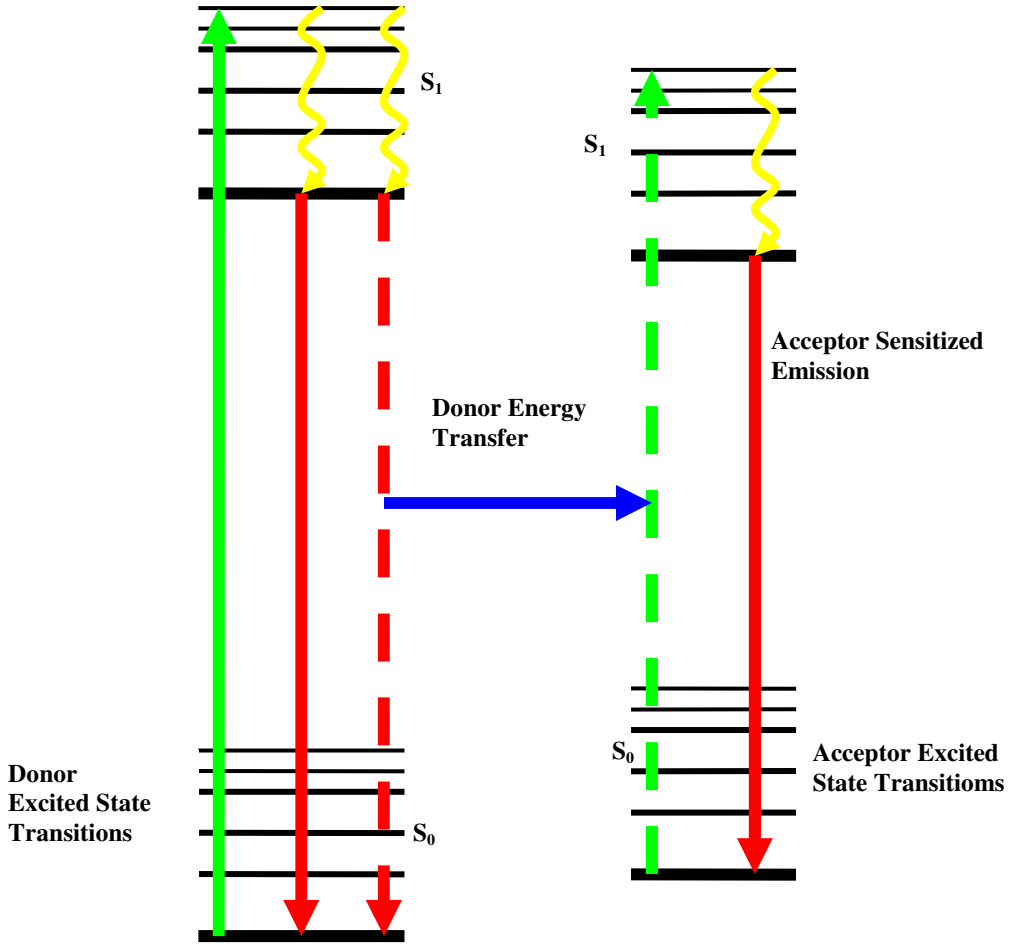

Figure 2.5 : Jablonski diagram illustrating the coupled transitions involved between the donor emission and acceptor absorbance in fluorescence resonance energy transfer

Donor Absorption (Excitation) :

Donor Fluorescence Emission :

Resonance Energy Transfer :

Non-Radiative Donor Energy Transfer :

Non-Radiative Acceptor Excitation :

Vibrational Excitation :

2.3.1 FLUORESCENCE RESONANCE ENERGY TRANSFER

Fluorescent resonance energy transfer (FRET) which is the radiationless transfer of resonance energy from an excited donor fluorophore separated by several atomic diameters [11] to a suitable acceptor fluorophore is a powerful technique in studies of protein-protein interactions, protein–DNA interactions, protein–membrane interactions and the three-dimensional structure of molecules in living cells [4]. Fluorescence spectroscopy can provide structural and functional information and the FRET spectroscopy is a valuable tool for measuring distances that can interpret conformational changes as small as 1 Aº [11, 12].

There are basic conditions in order for FRET to occur. Firstly, the donor molecule must be fluorescent. The distance between the donor and acceptor molecule is crucial. The efficiency of energy is inversely proportional to the sixth power of radius where radius is the distance between the centers of the donor and acceptor dipoles. The spectral overlap is another factor, which is one of the requirements of FRET. The emission spectra of donor must also overlap with the absorption spectra of acceptor [8].

2.3.2 The Förster Equation

The FRET technique, which is helpful in characterizing major conformational changes and determining molecular distances in macromolecules, is based on the theories of Förster who proposed that electronic excitation energy can be efficiently transferred through dipole-dipole interactions from a donor fluorophore to an acceptor fluorophore in a distance dependent manner.

Because the interaction between the donor and the acceptor fluorophore is a dipole-dipole interaction the distance between the centres of the dipoles is critical and proportional to r^{--3}.

$$V = -\frac{\mu_1 \mu_2}{4\pi\varepsilon_0} \times \frac{2}{r^3} \qquad (2.1)$$

Where V is the potential energy of dipole-dipole interaction.

Förster showed that the rate of energy transfer of the dipole-dipole mechanism is related to the square of this potential energy, and therefore energy transfer rate (k_t) is proportional to r^{-6}. Thus, he showed that the rate constant of transfer k_t is dependent on the distance between the dipoles.

$$k_T = \frac{1}{\tau_d}\left(\frac{R_0}{r}\right)^6 \tag{2.2}$$

The theory of radiationless dipole-dipole energy transfer predicts that, the efficiency of energy transfer depends on r^{-6}, where r is the distance between the donor and acceptor molecules for fixed donor-acceptor distances [8]. This predicted dependence on distance was confirmed by many researchers working on fluorescence spectroscopy. Stryer and Haugland [6], studied the dependence of energy transfer on the distance by using Oligomers of poly-L-proline. An a-naphthyl energy donor group and a dansyl energy acceptor group were attached to the ends of oligomers of poly-L-proline. They showed that the dependence of the transfer efficiency on distance is in excellent agreement with the r^{-6} dependence predicted by Förster. The efficiency of energy transfer decreased from 100 per cent at a distance of 12 Aº to 16 per cent at 46 Aº.

For efficient energy transfer, the emission spectra of donor must overlap the absorption spectra of acceptor [12].

The overlap integral can be calculated by the following formula:

$$J = \int_0^\infty F_d(\lambda)\varepsilon_a(\lambda)\lambda^4 d\lambda \tag{2.3}$$

where F(λ) is the corrected fluorescence intensity of the donor in the wave number range ν to $\nu + \mathrm{d}\nu$ with the total intensity normalized to unity, λ_d (=ϕ_d / τ_d) is the emissive rate of the donor. ϕ_d is the quantum yield of the donor in the absence of acceptor. $\varepsilon_a(\lambda)$ is absorption coefficient of the acceptor at λ.

The rate of energy transfer from a specific donor to a specific acceptor (k_T) is given by the following formula [8].

$$k_T = \frac{9000(\imath n 10)K^2\phi_d}{128\pi^5 n^4 N r^6 \tau_d} \int_0^\infty \frac{F_d(\nu)\varepsilon_a(\nu)}{\nu^4} d\nu \tag{2.4}$$

$$k_T = \left(r^{-6} J K^2 n^{-4} \lambda_d\right) \times 8.71 \times 10^{23} \sec^{-1} \tag{2.5}$$

where K^2 is the orientation factor, ϕ_d, the quantum yield or efficiency of the donor, which is defined as the number of light quanta emitted by a donor divided by the number of quanta absorbed by it, and ε_a is the absorption coefficient of the acceptor.

In order for FRET to occur donor and acceptor transition dipole orientations must be approximately parallel. Orientation factor K^2 effectively describes how the dipole moment of the donor is angularly oriented with respect to the dipole moment of the acceptor. This is the only term which can not be readily determined experimentally and is often assummed to be 2/3 for the experiments in solutions. This is the theoretically appropriate value if both the donor and the acceptor rotate freely, on a time scale which is short relative to the excited state lifetime of the donor. The orientation factor is given by

$$K^2 = (\cos\theta_T - 3\cos\theta_d \cos\theta_a)^2 \tag{2.6}$$

Where θ_T is the angle between the emission dipole of the donor and the absorption dipole of the acceptor, and θ_d and θ_a are angles between these dipoles and the vector joining the donor and acceptor.

Förster radius (Ro) for a given donor acceptor pair is the radius at which the energy transfer is 50%. Ro is dependent on the dipole orientation factor, quantum yield and the refractive index of the sample.

The constant terms in equation (2.4) are generally combined to define the Förster distance (R_0) at which the transfer rate (k_T) is equal to the decay rate of the donor in the absence of acceptor ($\Gamma_d = \tau_d^{-1}$). At this distance, one half of the donor molecules decay by energy transfer and one-half decay by the usual radiative and nonradiative rates. From equation (2.4) the following equation is obtained

$$R_0^6 = \frac{9000(\imath n 10)K^2\phi_d}{128\pi^4 n^4 N}\int_0^\infty \frac{F_d(\nu)\varepsilon_a(\nu)}{\nu^4}d\nu \qquad (2.7)$$

Using this definition of R_0, and equation (2.4), the rate of energy transfer is simply given by

$$k_T = \frac{1}{\tau_d}\left(\frac{R_0}{r}\right)^6 \qquad (2.8)$$

Which also verifies the Förster theory that the non-radiative energy transfer is strongly dependent on the distance between the fluorophores.

The constant terms in equation (2.7) can be used to find R_0

$$R_0 = 9.79\times10^3(K^2 n^{-4}\phi_d J)^{1/6} \quad \text{(in Å)} \qquad (2.9)$$

The measured parameter the efficiency of energy transfer (E) is the fraction of photons absorbed by the donor and transferred to the acceptor. E can be written as:

$$E = \frac{k_T}{\tau_d^{-1} + k_T} = \frac{k_T}{\Gamma_d + k_T} \tag{2.10}$$

$$\tau_{da} = (\Gamma_d + k_T)^{-1} \tag{2.11}$$

$$k_T = \tau_{da}^{-1} - \tau_d^{-1} \tag{2.12}$$

By substituting (2.11) and (2.12) into (2.10) one can get the transfer efficiency (2.13) depending on lifetimes τ_{da} and τ_d, lifetime of the donor molecule in the presence and absence of acceptor, respectively.

$$E = 1 - (\tau_{da} / \tau_d) \tag{2.13}$$

By using eqn. 2.14 the transfer efficiency which depends on the relative fluorescence yield in the presence (F_{da}) and absence of acceptor (F_d) is obtained as in eqn. 2.15.

$$\frac{F_{da}}{F_d} = \frac{\Gamma_d}{\Gamma_d + k_T} \tag{2.14}$$

By means of equation (2.14) the efficiency of energy transfer is found as the following

$$E = 1 - (F_{da} / F_d) \tag{2.15}$$

The transfer efficiency may be directly related to the distance by substituting equation (2.8) in to (2.13).

$$E = \frac{R_0^6}{R_0^6 + r^6} \tag{2.16}$$

Chapter 3

MICROSCOPY TECHNIQUES

3.1 Introduction

New intensity-based imaging techniques applying the method of FRET microscopy (wide field, confocal, and multiphoton [MP]) were developed with the development of new genetically encoded fluorescent labels and sensors and the increasing capability of computer software for image acquisition and analysis [13]. These techniques facilitate the study of the interactions of biological macromolecules in living cells [14].

We have used confocal and widefield microscopy techniques to detect FRET in our studies. In this chapter, first, a brief introduction is given to light microscopy. In the next part, confocal microscopy and detailed description of the elements of the confocal setup is discussed. After giving information on wide field microscopy, the differences between confocal microscopy and wide field microscopy are discussed. The experimental results obtained using these techniques are given in the following chapters.

3.2 Introduction to Light Microscopy

Light microscopes are the most widely used instruments to inspect structures down to the scale of a few micrometers. Although new techniques can be developed in the near future, light microscopy is the one used to image dynamic processes in biological macromolecules. Direct imaging of viruses, protein molecules, etc. is possible by using

fluorescent markers. Nowadays detection down to one fluorescent marker is routinely achieved thanks to the advanced technologies.

3.3 Confocal Microscopy

The confocal principle was first discovered by Marvin Minsky in 1957 [15]. Due to the lack of strong light sources and computers to handle the large amounts of data, it was not generally accepted as a technique in biological research until physicist Brakenhoff built a practical light microscope and imaged the three-dimensional chromatin distribution in the neuroblastoma in 1979 [16].

In Fig. 4.1 the schematic representation of a confocal microscope is illustrated. Light is directed via an illumination aperture and focused to a point in the specimen. Fluorescent light emitted from this point is focused, via a detector aperture, onto a detector (solid lines in fig. 4.4). The detector aperture (dotted lines in fig. 4.4) rejects fluorescence that arises from other points in the specimen [10].

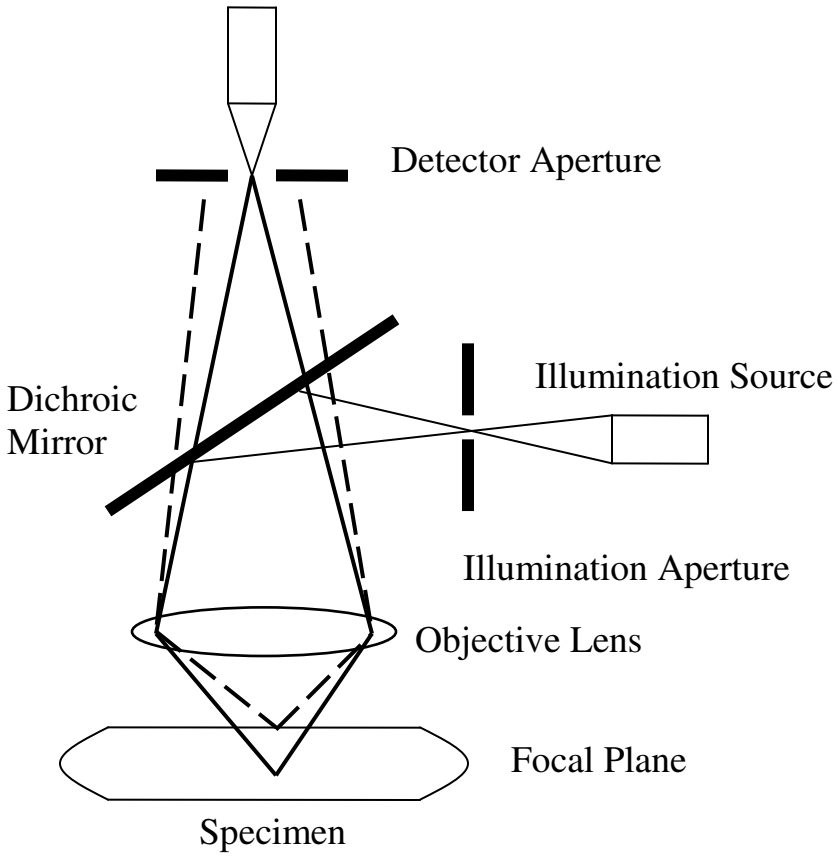

Figure 3.1 : Principle of the confocal microscope

In the figures 3.2.1, 3.2.2, 3.2.3 the operation principles of a confocal microscope are shown. The selection of light from one point and the rejection of light from all other points lead to the very high contrast images obtained using confocal microscopy. Confocal pinhole yields the microscope to be really efficient at rejecting out of focus fluorescent light which avoids background haze in the resulting image. By scanning many thin sections through the sample, very clean three-dimensional images of the sample can be obtained [13].

A cell (say), in a thick sample is imaged by a lens.

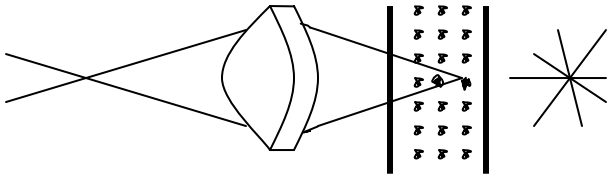

(1)

Another cell, elsewhere in the sample, is imaged at a different point.

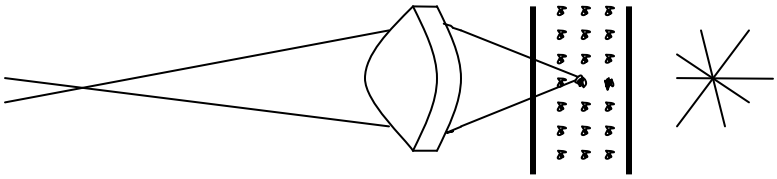

A pinhole in image space passes all the light from cell 1.

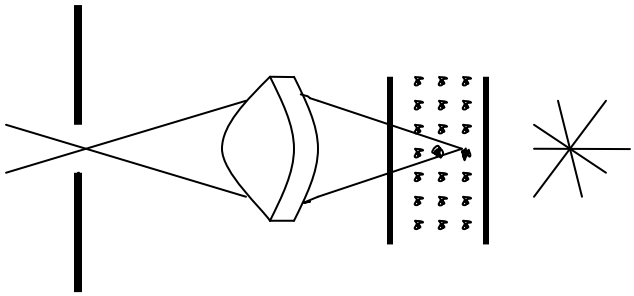

(2)

A pinhole blocks most of the light from cell 2.

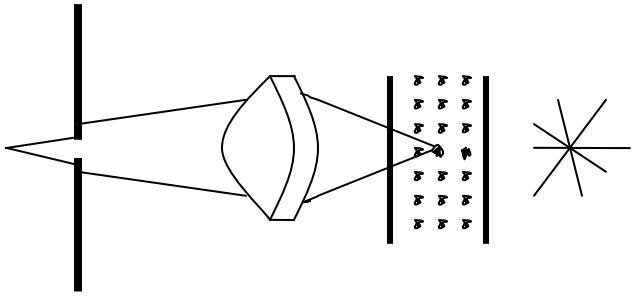

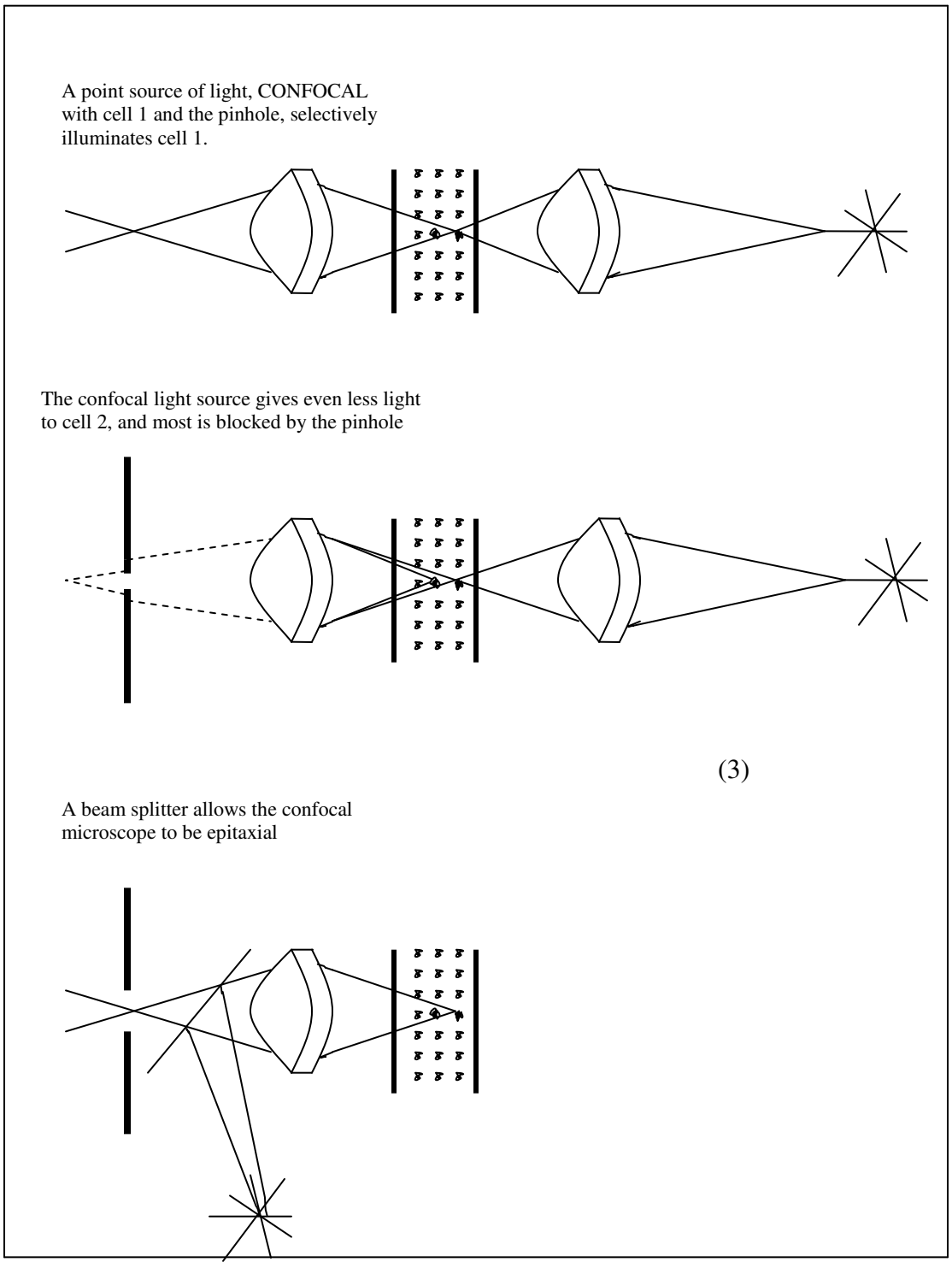

Figure. 3.2. A simple view of confocal microscope

3.3.1 Confocal Setup Components

Illumination sources, filters, pinholes, and electronic detectors constitute the important components of a confocal microscope. In this part, detailed description of these components will be discussed.

3.3.1.1 Light Sources

Illumination sources used in an optical microscope can be incoherent light from incandescent filaments as well as coherent light from lasers. The wavelength can range from the ultraviolet (250 nm) to the far infrared (~3 μm). Nowadays laser light is often used in confocal microscopy applications. Most confocal microscopes use epitaxial illumination. In this type of illumination, the same microscope objective is used for both focusing the excitation light and detecting the fluorescence.

3.3.1.2 Dichroic Mirror

In confocal microscopy, a dichroic mirror is used to reflect the excitation laser light into the optical path of the microscope and transmit the fluorescent wavelenghts. Specific dichroic mirrors can be made for the relevant wavelength regions of excitation and emission. Generally, in fluorescence applications, dichroic mirrors are used in combination with bandpass filters [17].

3.3.1.3 Microscope Objective

The objective lens is the most important element in every microscope. It determines the magnification, field of view and resolution, and its quality determines light transmission and the contrast and aberrations of the image [18]. These parameters and qualities are also critical in confocal microscopy. Microscope objective collects a fraction of the emitted photons in a random direction from the sample when it is excited and image onto the detector [13].

The numerical aperture is a measure for the optical resolution and the light sensitivity of the lens and is defined as follows:

$$NA = n\sin\theta \tag{3.1}$$

where NA is the numerical aperture, n the refractive index of the medium between lens and sample and θ is the half angle of the cone of light converging to an illuminated spot or diverging from one (Fig. 3.3). The concept of numerical aperture is closely related to that of the focal-ratio or f-number. In a simple lens the f-number is the ratio between the lens' focal length and its clear aperture ϕ (effective diameter) f-number = $f/_{\#.}$ and related to NA by the following formula [13]:

$$f/_{\#.} = n/_{2NA} \tag{3.2}$$

The relation between f-number and NA is given by the following equation [53] :

$$NA = \sin\theta = \phi/_{2f} \tag{3.3}$$

The working distance of the objective is a very important parameter, especially for confocal microscopy in thick biological samples. The working distance is the depth into the

sample to which the lens can focus before it runs into the sample. Magnification of an optical instrument is defined as the relative enlargement of the image over the object. Although the highest magnification seems to be the best, it is limited by the resolution of the imaging instrument. The field of view and the diffraction-limited resolution due to the finite aperture of the objective lens are illustrated in fig.4.4. The larger the cone of collected light, the higher the NA, since it depends on the half-angle of the objective's collection cone. As a result, the more light will be collected by the objective lens [18] .

Resolution limits the useful magnification in an optical microscope according to the basic diffraction principles of light. Resolution (R) is defined as the smallest distance that two objects can be apart and still be recognized as two separate objects. There are many mathematical definitions for resolution, but a simple and reasonable approximation is

$$R = \frac{\lambda}{2NA} \tag{3.4}$$

Where λ is the wavelength of the light.

Sometimes the lens design for confocal microscopy can be more important than either M or NA. This is especially true for co-localization experiments, in which the chromatic corrections of a planapochromat make it preferable in spite of its lower light collection efficiency [18].

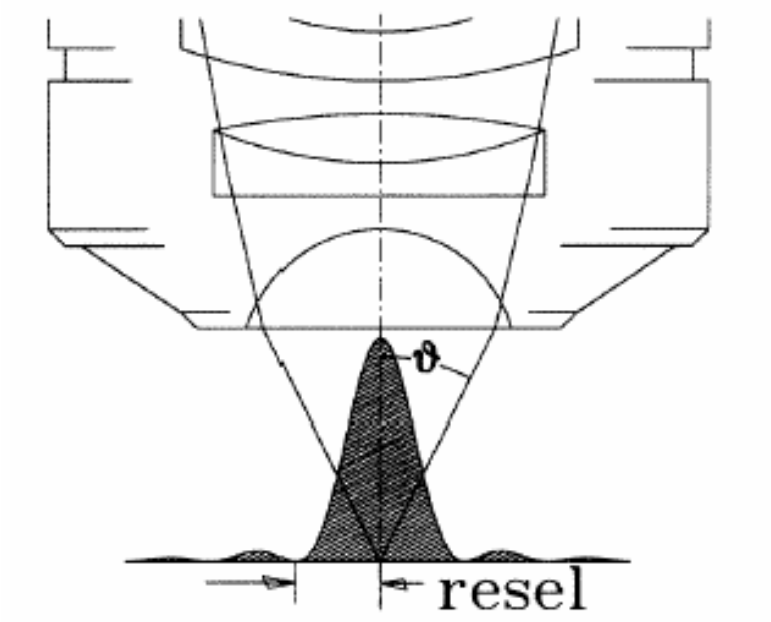

Figure 3.3. The resolution element due to a lens of $NA = n\sin\theta$ is called a resel: the radius of the first dark fringe in the diffraction pattern, or half the diameter of the Airy disc [13]

There can be several types of optical aberrations caused by a lens: spherical aberration, coma, field curvature distortion, longitudinal and lateral chromatic aberration and chromatic magnification difference. Not all of these aberrations can easily be overcome. The objectives are classified according to their optical aberration correction namely: achromat, apochromat, fluorite, planachromat and planapochromat [17].

Regardless of the lens design, a lower magnification lens (of equivalent NA) is almost always preferable, since it has a larger field-of-view, and better resolution [18].

3.3.1.4 Pinhole

The pinhole is a substantial component that makes confocal microscopy possible. It effects both the axial and the lateral resolution of the microscope. Typical pinhole diameters of 10 to 100 µm are used in confocal microscopy. The size of the pinhole determines how much background can be reduced. The smaller the pinhole, the better the discrimination against scattered light, but also the less light gets through to the detector. In practice, the pinhole should have approximately the same diameter as the FWHM (full width at half maximum) of the Airy diffraction pattern generated at the pinhole's position [17].

In confocal microscopy, the size of pinhole depends on magnification. Most confocal microscopes have an adjustable pinhole that is easily set to match the magnification (e.g., for equivalence, a 60x lens needs a pinhole 1.5-fold larger than a 40x lens) [18].

3.3.1.5 Scanning Stage

Confocal microcopy is a serial technique rather than a parallel one. For a specific setting of the microscope only a single point on the sample is detected at one time. Confocal image is obtained by the sequential illumination or sequential observation of small areas of a sample [13]. There are two techniques to obtain a complete two-dimensional image of the sample: sample scanning and laser scanning. Confocal microcopy is serial technique rather than a parallel one. For a specific setting of the microscope only a single point on the sample is imaged at one time. In laser scanning, the sample is kept fixed and the laser beam is moved. This is a form of scanning in confocal microscopy providing contrast enhancement [17].

In sample scanning, the beam is kept stationary and the sample is moved under the illuminating light beam. This has the advantage of providing constant axial illumination but

has the disadvantage of being slow or impractical if the specimen is likely to be disturbed by movement. Because of the fact that, the scan is demagnified by the objective lens, the mechanic tolerance of beam scanning systems are less critical than those for sample scanning [13].

3.3.1.6 Detectors

Mainly two types of detectors are used in confocal microscopy: Photo Multiplier Tube (PMT) and Avalanche Photo Diode (APD). The photomultiplier tube (PMT) is a vacuum tube device that uses the photoelectric effect to convert photons into electrons i.e. it converts the incident optical radiation to electronic current. A typical photomultiplier tube (PMT) consists of a photoemissive cathode (photocathode) followed by focusing electrodes, an electron multiplier and electron collector (anode) in a vacuum tube. Dynodes, which are series of electrodes, amplify these photoelectrons. PMTs can detect intensities as low as a few photons per second or as high as a billion photons per second. They are good for measurements that must be made in a short time or high frequency and for weak signals. Owing to its inherent high current amplification and low noise, the photomultiplier is one of the most sensitive instruments [17, 19].

The avalanche photodiode is a solid-state semiconductor device. An APD's working principle can be explained as follows. A photon hits the semiconductor and an electron-hole pair is generated, if the photon energy is higher than the band gap energy of the semiconductor [19]. Under the applied reverse voltage the electrons drift towards the anode while the holes drift towards the cathode, due to the electric field developed across the p-n junction. By increasing the reverse bias across a p-n junction, the field in the depletion layer can increase to a point at which electrons that are accelerated across the depletion layer gain enough kinetic energy to "kick" new electrons from the valence to the conduction band, while still traversing the layer. This process is referred to as avalanche multiplication of the photo-current [17, 19].

An avalanche photodiode (APD) is a detector combining the high quantum efficiency of a photodide with the high gain of a PMT. The build of electron avalanche as explained above causes a signal amplification with a gain between 50 and 1000. It has more noise than the dynodes in PMT but less noise than a photodiode's external amplifier. The gain is less than the gain of the PMT. However, the quantum efficiency of the APD is roughly an order of magnitude higher than PMT, e.g. APD with a gain of 10^3 corresponds to PMT with a gain of 10^4. APDs gain rely on operation temperature and they can endure high dark currents. They are kept usually at constant temperature.

3.4 Wide Field Microscopy

Wide-field fluorescence microscopy is a very widely used technique to obtain both topographical and dynamic information. It relies on the simultaneous illumination of the whole sample. This is the major drawback of this conventional microscopy causing generation of out of focus signal. Incoherent lamps together with proper optical filters (the excitation filter) or lasers can be used as excitation sources in wide field microscopy. Excitation light is directed to the sample via a dichroic mirror and the image is projected onto an imaging detector, usually a CCD camera. Therefore, the pixels on the detector must be matched to the desired image resolution, in order to optimize the information content of the resulting digital image. In practice, the pixel size is fixed by the camera used to image in wide field microscopy, thus the magnification is the only variable that can be adjusted [18]. The optimal magnification (M) to be used for a given pixel size can be determined by matching the sampling resolution in the image plane to the pixel size by

$$P = M * R_{samp} \tag{3.5}$$

3.4.1 Total Internal Reflection Microscopy

Total internal reflection fluorescent microscopy (TIRM) has attracted the attention of researchers owing to its ability to detect real-time events for studying the dynamics of various biological systems.

TIRFM, also known as evanescent wave microscopy, has been used in recent years due to its unique capabilities. The study of surface molecular dynamics is possible with TIRFM at the single molecule level through the generation of a thin evanescent wave at a glass/liquid interface by total internal reflection (TIR).

The incident angle of illumination, θ, in conjunction with the critical angle, θ_C, strongly influence the properties of the evanescent wave and are the most important variables when designing TIRFM configurations. TIRFM requires solely an excitation light beam traveling at a high incident angle through the solid coverglasses where the sample adhere. At a specific critical angle, the beam of light is totally reflected from the glass/water interface [20].

3.4.2 The Differences Between Confocal Microscopy and Wide-Field Microscopy

Wide-field microscopy is the simplest and most widely used technique. However, it has a major drawback due to the generation of out of focus signals. Confocal microscopy provide the advantage of rejecting out of focus information [21]. In wide-field microscopy, the whole sample is illuminated by the excitation light causing the entire sample to fluoresce. This results in background haze in the recorded image. However, rejecting out of focus fluorescent light using a pinhole, the confocal microscopy reduces the background haze in recorded image i.e. provides a higher resolution. Thus, a confocal microscope does have higher resolution than a wide field microscope [13].

High lateral resolution that gives a wealth of spectral information over a wide-field microscope, including controllable depth of field and the ability to collect serial optical sections from thick specimens. Furthermore, confocal FRET microscopy measure viscoelasticity and biochemical responses of living cells and real-time monitoring of cell membrane motion in natural environments owing to its nanometer depth resolution [21].

The point-spread function (psf) is a measure of resolution showing the intensity pattern illuminated or observed by a lens at its focal plane. Point-spread function defines the resel which is the resolution element transverse to the optical axis. The dramatic difference between the point-spread functions of a confocal microscope and wide-field microscope is seen in Figure 3.4. As it is shown in fig. 3.4b the confocal diffraction pattern has much less energy outside the central peak than does the single lens pattern shown in Fig 3.4a.

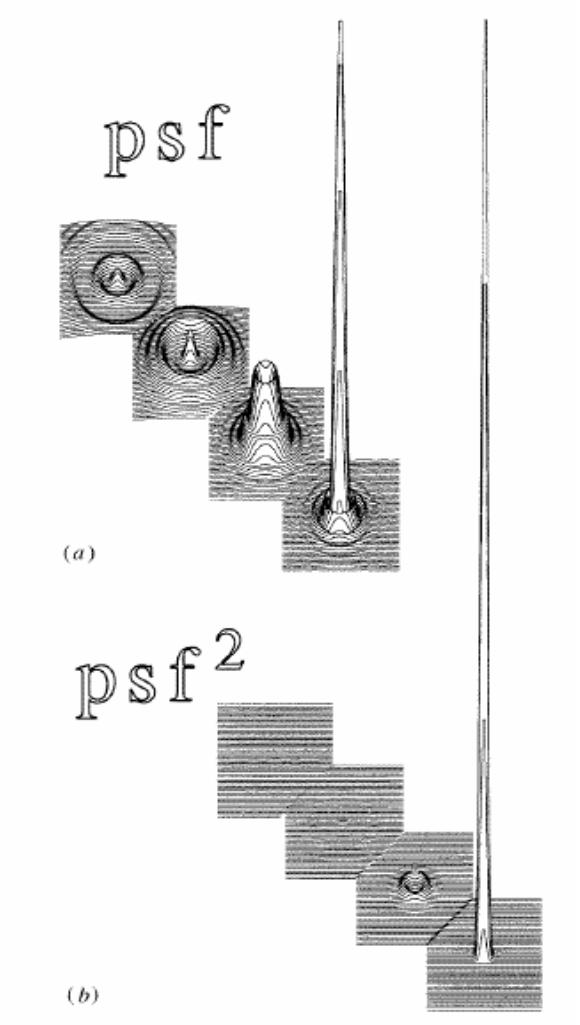

Figure 3.4. (a) conventional diffraction pattern, and in (b) it is for the confocal case [13].

Because of the sharper point-spread function a bright object near a dim one is less likely to contribute background light in a confocal microscope. In turn, that means that the resolved dim object can be seen as resolved. As an example, Figure 3.5 shows two point objects in the focal plane that are separated by 4.5 resels and differ in brightness (that is, in remission efficiency) by 200. When the diffraction pattern centres on the dim object, for a

conventional microscope the dim object is still obscured by the bright one, but in the confocal case both of the resolved points are visible [13].

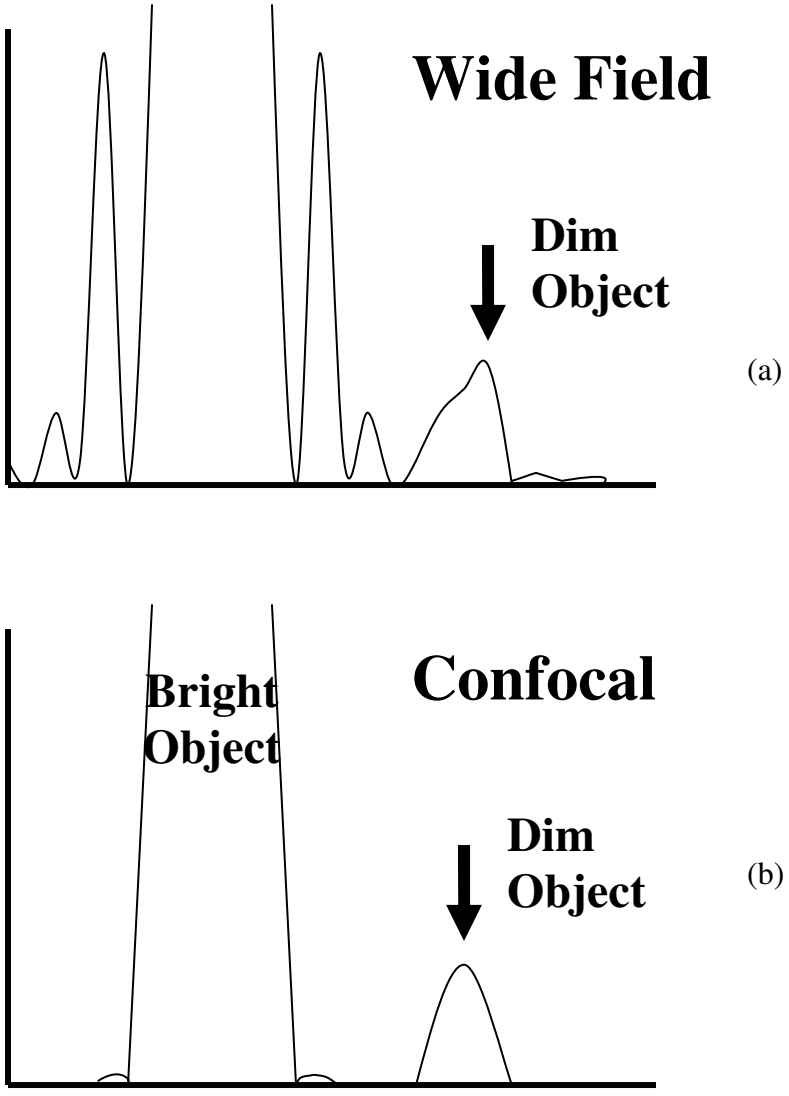

Figure 3.5. Two points of very different (200:1) remission intensity, are well resolved (4.5 resels). In (a) the conventional view leaves the dimmer point obscured, but in (b) the confocal contrast enhancement allows its display. Arrows indicate the weaker remitter

Despite its fundamental disadvantage in resolution wide-field microscopy possess an advantage over confocal microscopy. In wide field microscopy, the whole sample is detected simultanously, whereas in confocal microscopy the sample is detected point by point. Therefore, a wide-field microscopy image can be obtained much faster than a confocal image. A wide-field microscopy image can be typically obtained in tens of ms while at least tens of seconds are required to obtain a confocal image.

Chapter 4

SINGLE MOLECULE OBSERVATION

4.1 Introduction

Since the first fluorescence detection of single molecule in solution by Hirschfeld, the research on single molecule detection in solution and on surfaces has been developed for few decades by several researchers. The new generation of CCD cameras with high sensitivity, enabled the direct imaging and monitoring of single fluorophores [17].

The important characteristics of single molecules are blinking and photobleaching phenomena. By using the techniques of high resolution fluorescence microscopy it is possible to track the location of single molecules in amorphous hosts. Moving as well as stationary molecules can be observed by wide field fluorescence microscopy. Beside this confocal microscopy can also reveal their photobleaching and blinking mechanism in a time resolution analysis.

Single molecules can be used as fluorescent probes for labeling host biological molecules. Generally, two fluorophores are used in the form of Fluorescence Resonance Energy transfer (FRET) or Förster transfer. Actually, the sensitivity of FRET can be extended to the single molecule level by measuring energy transfer between single donor fluorophore and a single acceptor fluorophore. Energy transfer between a single donor and single acceptor reveals structural and conformational changes of biological macromolecules in real time without needing signal averaging over many molecules as in the case of ensemble studies [14, 22].

4.2 Room Temperature Single Molecule Detection

Two factors are important for the successful detection of a single molecule. These are the rate with which the fluorescence photons are detected and the total number of photons that are emitted before the molecule photobleaches, i.e, becomes photochemically nonfluorescent molecule [23]. Furthermore, it is essential for single molecule detection that the probability of finding molecule in the applied detection volume. It can be achieved by diluting the sample of interest sufficiently.

There are different kinds of CCD cameras which allows to direct imaging and monitoring of single fluorophores: state-of-the-art, cooled, back-illuminated [17].

4.3 Photophysical Properties of Single Molecules

4.3.1 Photobleaching

Photobleaching is an irreversible chemical reaction that occurs while the electron is in its excited state. Photobleaching occurs when a fluorophore permanently loses the ability to fluoresce due to photon-induced chemical damage and covalent modification. Covalent modifications results from interaction of fluorophores with another molecule upon transition from an excited singlet state to the excited triplet state. The triplet state is relatively long-lived with respect to the singlet state, thus excited molecules have much longer time frame to undergo chemical reactions with components in the environment [14]. Typical fluorescent dye molecules survive about 10^5 to 10^6 excitation cycles until photodestruction, although this number can vary widely and strongly depends on the nature of the embedding medium [17].

4.3.2 Triplet Blinking

In single molecule experiments most of the organic molecules are modeled by a three-level system, i.e. singlet ground state S_0 and excited state S_1 and a triplet excited state T_1. The transition from the singlet excited state to the triplet state via intersystem crossing is responsible for the on/off switching, known as triplet blinking. The transition accompanies by a spin flip of the excited electron and is thus symetrically disfavored. The lifetime of the triplet state determines for such a system, the duration of the dark intervals [24]. Intersystem crossing rates are low, one crossing for every 10^5-10^6 showing on/ off fluctuations with a period lasting milli seconds i.e. periods of sustained fluorescence emission and darkness. The average lifetime of triplet state is much higher then the fluorescence lifetime. The average fluorescence lifetime of Rhodamine B is ~2 ns [25].

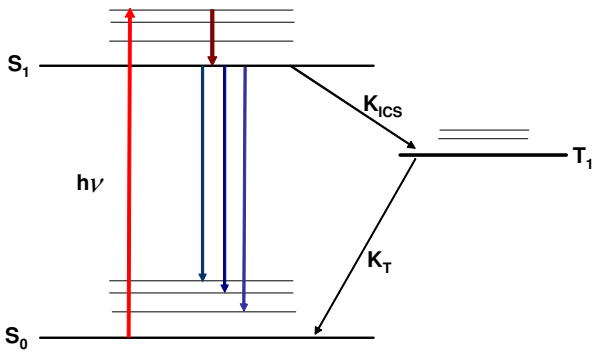

Figure 4.1. Three level system: triplet blinking

4.4 Experimental Materials and Methods

4.4.1 Materials

4.4.1.1 Polymer Thin Films

The dye molecules were put in amorphous PMMA (Poly (methyl methacrylate)) host by spin coating thin films from a solution containing PMMA and dye molecules in $CHCl_3$.

PMMA $(C_5\ O_2\ H_8)n$ is good candidate as a matrix since it is a clear, colorless polymer. It does not interact with the dye molecules and does not affect their characteristics such as quantum yield, absorption emission and decay time [2].

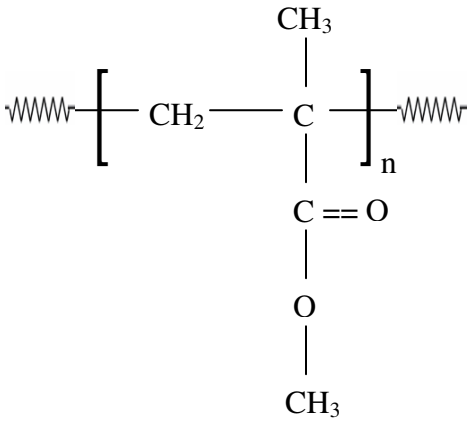

Figure 4.2. The chemical structure of PMMA (Poly (methyl methacrylate))

4.4.1.2 Rhodamine B

Rhodamine B is an organic molecule which emits light when excited by an excitation light at its absorption wavelength. It is highly fluorescent. Rhodamine B is generally toxic, and is soluble in water, methanol, and ethanol. Its absorption and emission spectra are quite narrow and the Stokes shift is small. They emit fluorescence in the range of 500-700 nm [2].

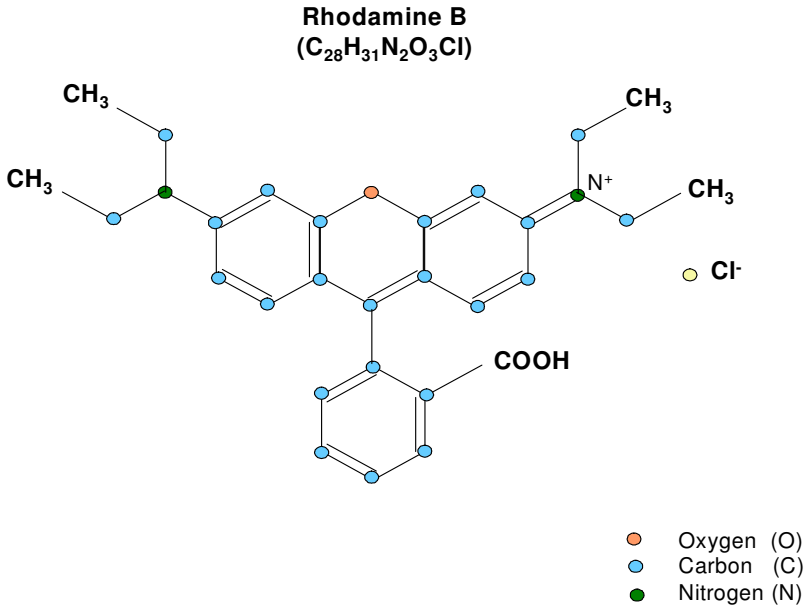

Figure 4.3 The chemical structure of Rhodamine B

4.4.2 Methods

4.4.2.1 The Preparation of Thin Films

Firstly, the cover glasses were cleaned by UV Ozone cleaner, which removes organic contaminations or organic thin films for 20 minutes. Secondly, 3 mg/ml solutions of PMMA polymer was prepared in Chloroform ($CHCl_3$). 20 µl of 20 nM Rhodamine B in methanol was added on to the 2 ml of PMMA in chloroform solution. The cover glasses were spin coated with the solution containing Rhodamine B and PMMA at 2000 rpm for one minute. The films of Rhodamine B molecules in the matrix of PMMA polymer was obtained after solvent evaporation. Lastly, the films were further dried in vacum oven in order to evaporate any trapped solvent molecules. The same procedure was repeated to prepare thin films containing less Rhodamine B using solution of 2 nM concentration. This time 20 µl of 2 nM Rhodamine B was added to 3 mg/ml Polymethylmethacrylate (PMMA) in Chloroform ($CHCl_3$). These films were used in total internal reflection fluorescence microscopy experiments.

4.4.2.2 Single Molecule Observation by Confocal Microscopy

Experiments were performed with a home-built inverted confocal microscope at room temperature. Excitation was provided by a 532-nm diode pumped Nd:YAG laser (Cyrsta Laser). The fluorescence emitted from Rhodamine B molecules was collected by a microscope objective, which has high numerical aperture objective (N.A.=1.4, 60x oil), a 1.5x magnification element and transmitted through a dichroic mirror and a bandpass filter and is focused onto the pinhole. The Rhodamine B fluorescence passed through the pinhole and detected by an avalanche photodetector (APD). A piezoelectric translation stage was used for confocal scanning. The experimental set up is seen in Fig. 4.4.

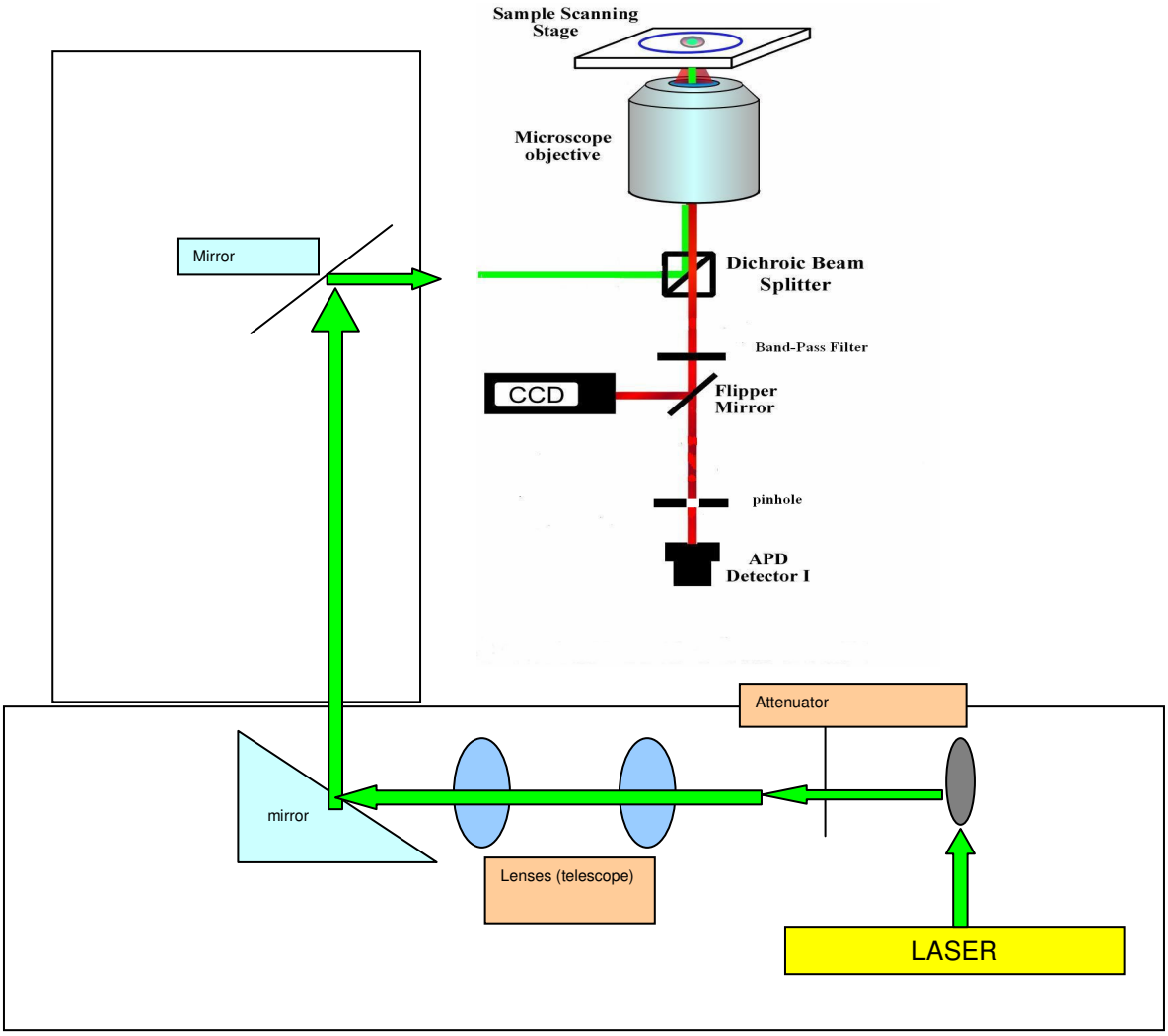

Figure 4.4 The set up of confocal microscopy

4.4.2.3 Single Molecule observation by wide field microscopy

Experiments were performed with home built confocal microscope and 532 nm Nd-YAG laser was used as an excitation source. High numerical aperture objective (N.A.=1.4, 60x oil), a 1.5x magnification element were used to collect collimated light. The angle of incidence of the laser beam to the polymer-air interface was adjusted to observe total internal reflection. The light was collected by objective and transmitted through a dichroic mirror and a band pass filter and then is focused onto the CCD camera. The experimental set up is shown in Fig. 4.5.

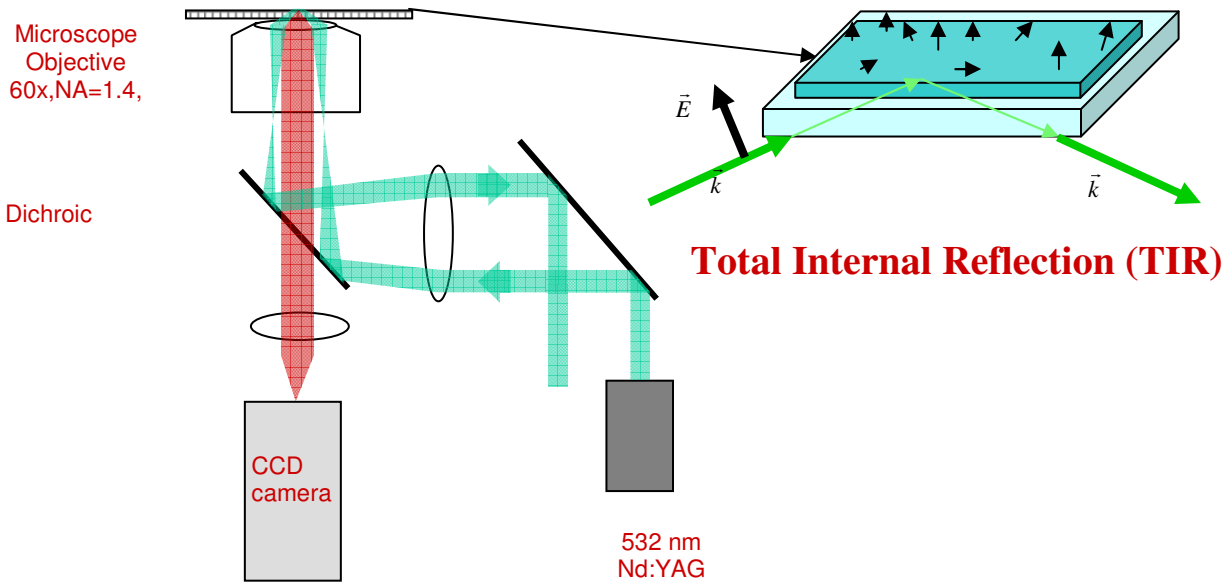

Figure 4.5 The set up of wide field microscopy

4.5 Results

We were able to detect single dye molecules by confocal microscopy. We observed photobleaching as well as blinking in the fluorescent spots of Rhodamine B molecules in the confocal images. These are strong indications for the observation of single molecules.

Figure 4.6 shows 5 µm-5 µm confocal images of Rhodamine B doped PMMA sample. There are 100-100 pixels at each image and integration time to record the intensity at each pixel is 100 ms. The molecule encirculated in red color fluoresces for 4-5 traces, afterwards a sudden drop is observed in intensity. This is the indication of photobleaching. In the same figure the Rhodamine B molecule encirculated in blue color fluoresces for 3 traces, then no intensity is detected for one and half traces and the molecule restarts fluorescing. This is the indication of blinking.

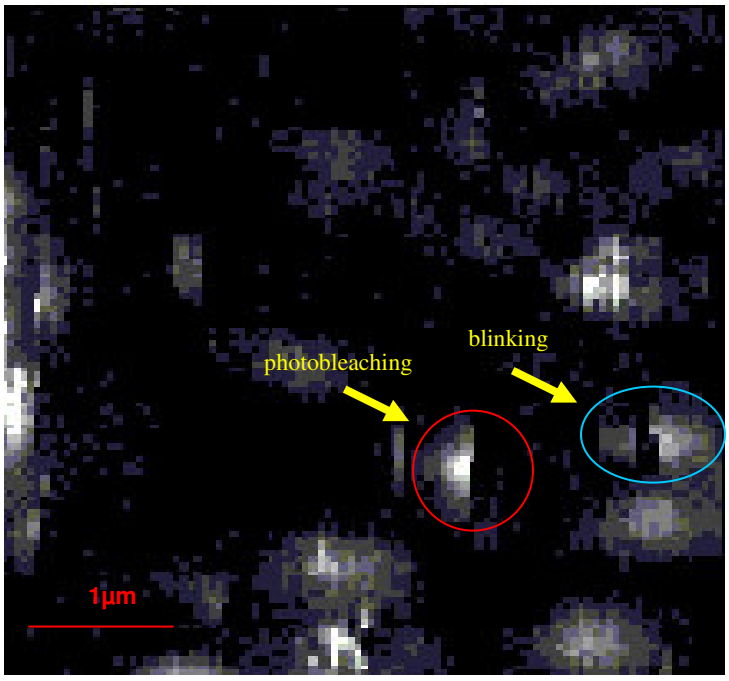

Figure 4.6. Photobleaching and blinking phenomena by confocal microscopy

The single molecule observation was also verified by wide field microscopy as shown in Fig. 4.7. In this figure, wide-field fluorescence images of the Rhodamine B doped PMMA sample are plotted. 3 consecutive images in Fig. 4.7a are seperated by a time interval of 3 seconds. The encirculated donut shaped fluorescence spot is observed in the first and third images while being absent in the second image. This is an indication for blinking. Figure 4.7b shows the wide-field fluorescence images of the same area on the sample as in Fig. 4.7a. These consecutive images are recorded after 20 sec constant laser illumination, and they are seperated by 3 sec time interval. The encirculated donut shaped spot stems from a single molecule and its absence in the 2nd and 3rd images is due to photobleaching.

The fluorescence images of single molecules reveal the three dimensional dipole orientations. Single molecules have different emission patterns (donut-like structures, rings, asymmetric rings, or spots) due to the different dipole orientations. Single molecules having dipole moments in a direction perpendicular to the substrate have donut shape. In contrast single molecules having dipole moments in a direction parallel to the substrate have point-like images.

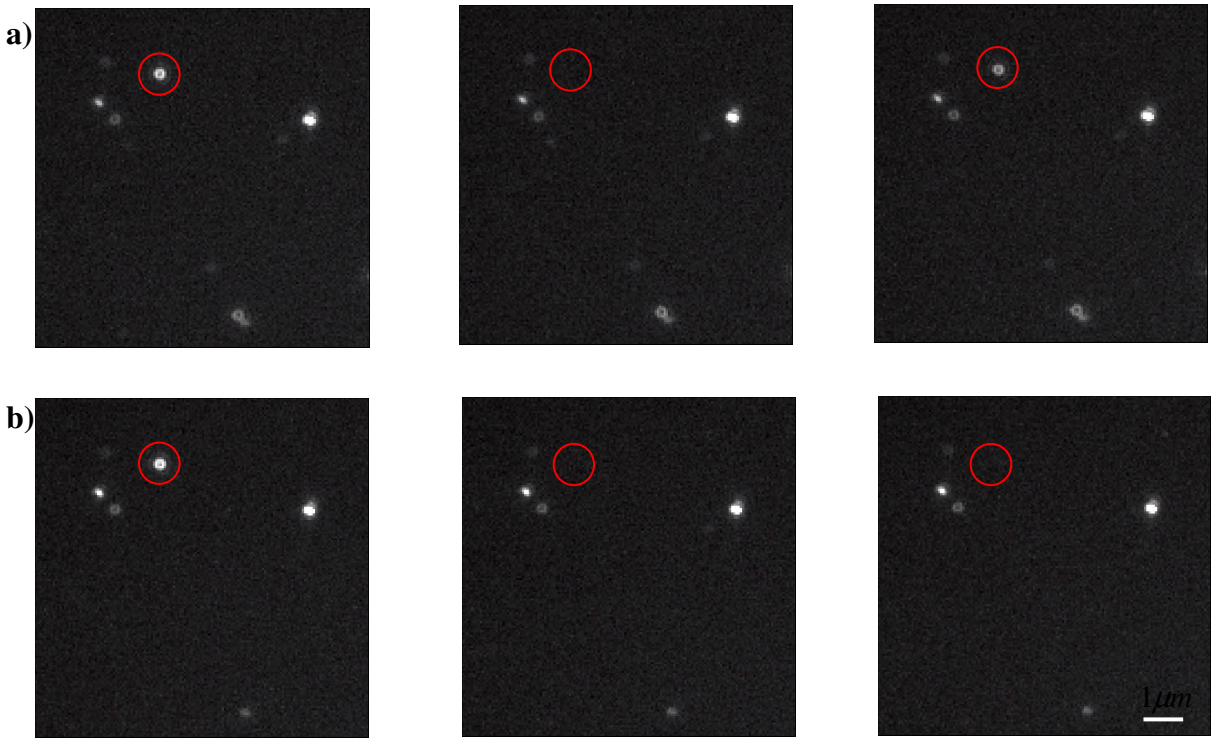

Figure 4.7. a) Blinking phenomenon b) photobleaching phenomenon by wide field microscopy

Chapter 5

FRET between Rhodamine B and Fluorescein Na

5.1 Introduction

In a FRET pair, the fluorescent donor is selected for its absorption, emission, quantum yield and decay time characteristics. On the other hand, the acceptor is selected for its absorption in the wavelength range of donor emission and its photostablity. In some experiments the donor and acceptor molecules can be covalently linked by a flexible or rigid spacer, conjugated to macromolecules, or simply mixed together [26].

In our studies we have chosen Rhodamine B and Fluorescein Na as the FRET pair. As it is explained in this chapter these two dye molecules constitute a suitable FRET pair owing to their photophysical and spectral properties.

In this chapter, the characteristic properties of fluorescein and rhodamine B molecules are given. Then, the Förster radius of this FRET pair, which depends on the spectral overlap of donor emission band and acceptor absoption band, and quantum yield of donor and relative orientations of donor and acceptor molecules with respect to each other, is explained.

This is followed by the explanation of the light contaminations in FRET measurements and how they are resolved in a variety of FRET approaches. Next, the experimental results of the energy transfer between Fluorescein Na and Rhodamine B and the methodology to determine the FRET efficiency are discussed.

5.2 Fluorescent Probes

Fluorescent molecules are used as probes for the investigation of physicochemical, biochemical and biological systems. They can be classified into three groups as i) intrinsic probes; ii) extrinsic covalently bound probes; and iii) extrinsic associating probes [2]. A variety of biological molecules contains naturally occurring or intrinsic fluorophores. Namely, the aminoacids such as tryptophan and tyrosine in proteins, nucleic acids such as Yeast $tRNA^{PHE,}$, cofactors such as NADH, riboflavin and FAD are all examples of intrinsic fluorophores already existing in biological molecules thus contributing to background fluorescence.

Although the intrinsic probes are ideal, few of them can be used in investigation of biological systems. Since their natural fluorescence properties are not generally sufficient for the experimentation. Thus, the fluorophores that are not natural but have improved spectral properties are chosen for specific applications [8]. These fluorophores can be attached covalently or noncovalently associating. The covalently bound probes are advantegous over the associating probes because the locations of the covalently bound probes are known. However, it is difficult to synthesize molecules or macromolecules with covalently bound specific proteins. These macromolecules can be surfactant, polymer chains, phospholipids, proteins, polynucleotids, etc. Protein tagging is possible on amino groups and on sulfhydryl groups by means of labeling reagents having functional groups. Fluorescein, rhodamine and erythrosine derivatives with these functional groups are used [2].

There are also intrinsic probes such as GFP and its mutants that are used in real time imaging and tracking of cellular events. The fluorophore can be fused to a wide variety of protein and enzyme targets [7]. By means of these markers, it is possible to detect the localization of proteins in living cells and monitoring more cellular events such as small molecule messenger dynamics, enzyme activation and protein- protein interactions [27].

5.3 The Properties of Fluorescent Dyes

Fluorescent dyes absorb light at a characteristic wavelength and re-emit light at a second lower energy, longer wavelength. The wavelength (nm) where photon energy is most efficiently captured is defined as the Absorbancemax. The wavelength (nm) where light is most efficiently released is defined as the Emissionmax [28].

5.3.1 Quantum Yield

The fluorescence quantum yield Q is the fraction of excited molecules that return to the ground state S_0 with the emission of fluorescence photons [2]. In other words, Quantum yield is the ratio of number of photons emitted to the number of photons absorbed by the sample:

$$Q = \frac{photons_{emitted}}{photons_{absorbed}} \tag{5.1}$$

It can also be described by the relative rates of the radiative and non-radiative pathways, which deactivate the excited state:

$$Q = \frac{\Gamma}{\Gamma + k} \tag{5.2}$$

where Γ and k correspond to radiative and non-radiative processes, respectively.

k describes the sum of the rate constants for the various processes that compete with the emission process. These processes include photochemical, and non-radiative transitions of which two types have been recognized: intersystem crossing and internal conversion which is the return to ground state without emission of photon. Intersystem crossing is related to the radiationless spin inversion of a singlet state (S_1) in the excited state into a triplet state (T_1).

The quantum yield can be close to unity if the radiationless rate of deactivation is much smaller than the rate of radiative decay, that is $k \langle\langle \Gamma$. However, the energy yield of fluorescence is always less than unity because of Stokes' losses [8].

Quantum yield of fluorescent dyes depend on the concentration of dye solutions. The peak wavelength at which the fluorescence or absorbance is maximum changes with different solution concentrations, this is illustrated in Figure 5.2 and 5.3. Beside this, the fluorescent intensity or absorbance efficiency alters and peak wavelength changes slightly in a variety of solvents. As an illustration, the absorption spectrum of Rhodamine B and in methanol and water is shown in Fig. 5.5, Fig. 5.6 respectively.

A group in India showed that the absorption spectrum of methanol has very low absorption at 514 nm and hence any signal from methanol can be neglected. Furthermore, They studied the concentration-dependence of the quantum yield of rhodamine B in methanol. As it is shown in Figure 5.1 the quantum yield decreases with increasing concentration [29].

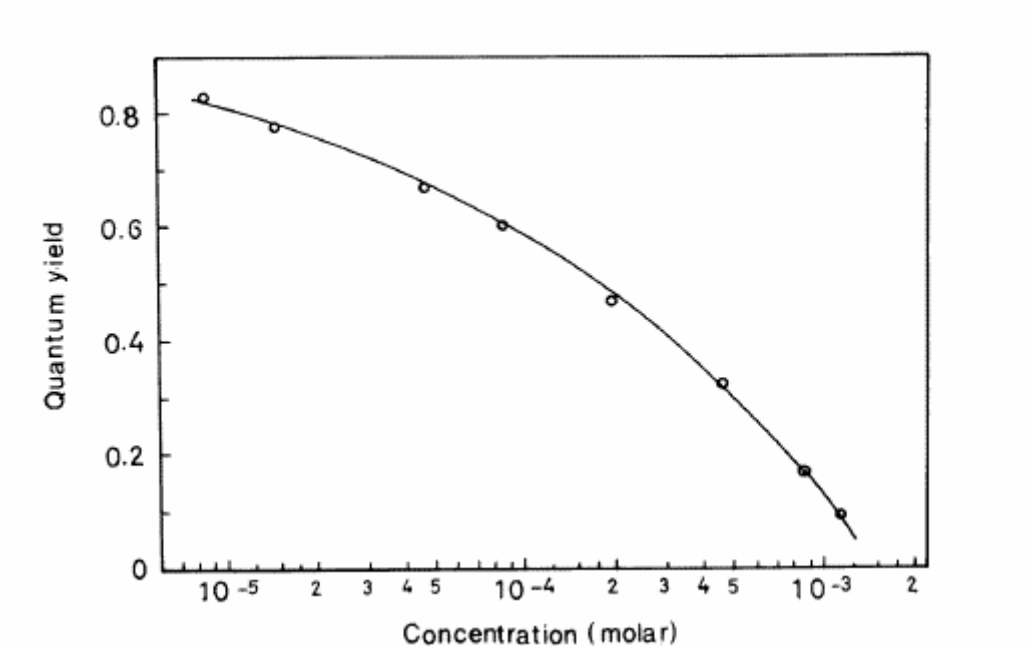

Figure 5.1 The variation in quantum yield of rhodamine B in methanol with concentration [29]

5.3.2 The Spectra of Fluorescein and Rhodamine B

Fluorescein and Rhodamine B were dissolved in methanol separately and placed in quartz cuvettes (optical path: 1 cm). Absorption spectrum measurements were done using a Shimadzu spectrometer. The samples used in this work were prepared at different concentrations and the dependence of the absorption maximum to concentration was tested [29]. The absorption peak was observed at 495.2 nm (Fig. 5.2) and 488 nm (Fig. 5.3) for 8 µM and 80 µM Fluorescein solution, respectively. The absorption peak of Rhodamine B was observed at 545.6 nm (Fig. 5.5) and 546.4 nm (Fig. 5.4) for 20 µM solution and 2 µM solutions respectively. Thus, the change in the absorption spectrum of Rhodamine B was observed to be less significant as compared to the change in the absorption spectrum of Fluorescein [30],[31].

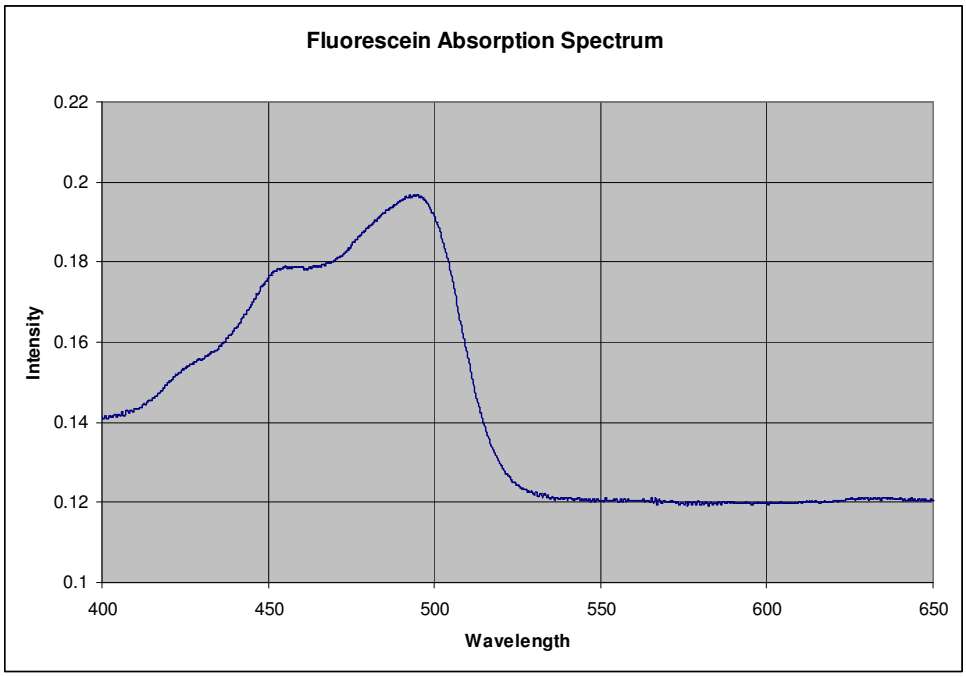

Figure 5.2 The absorption spectrum of Fluorescein 8 µM concentration in methanol

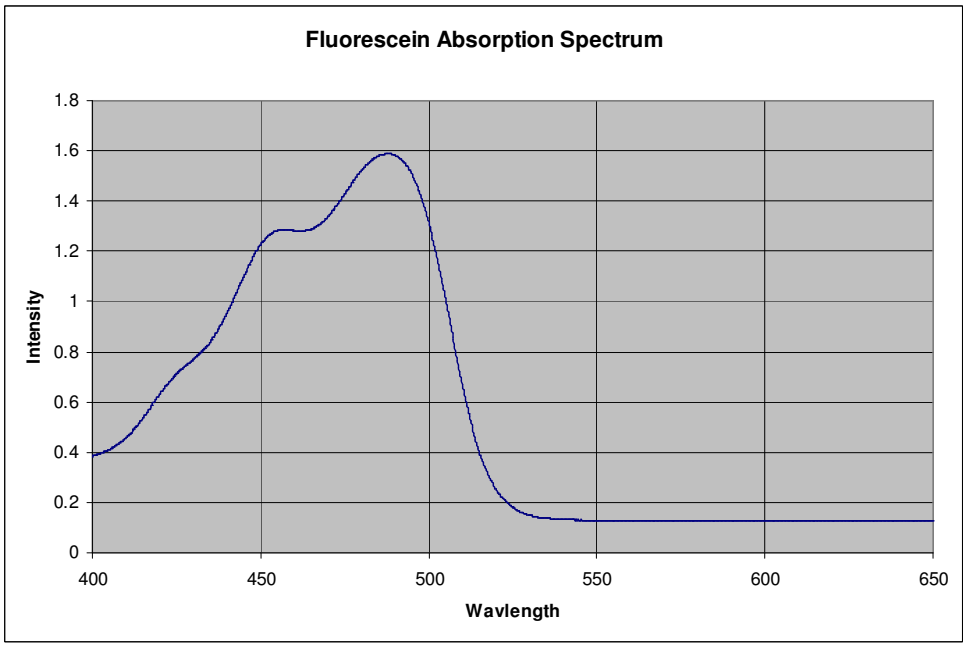

Figure 5.3 The absorption spectrum of Fluorescein 80 µM concentration in methanol

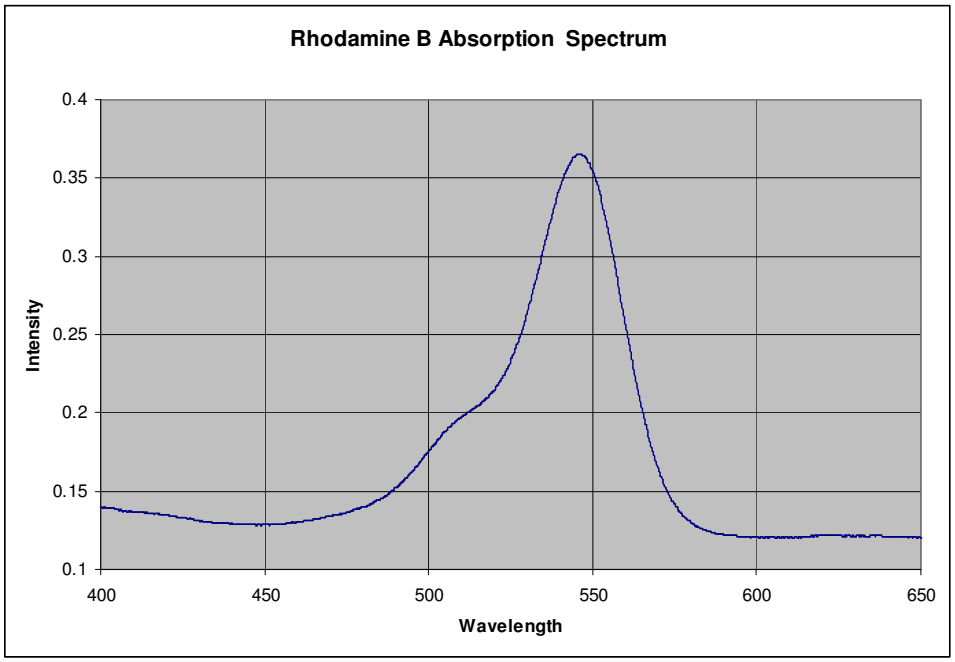

Figure 5.4 The absorption spectrum of Rhodamine B 2μM in methanol

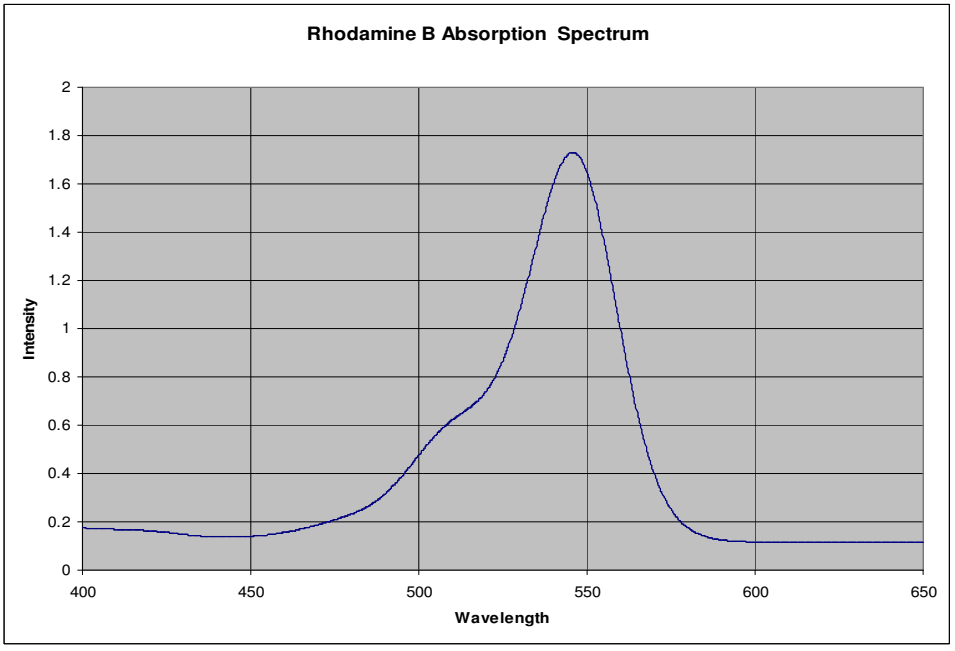

Figure 5.5 The absorption spectrum of Rhodamine B 20 μM in methanol

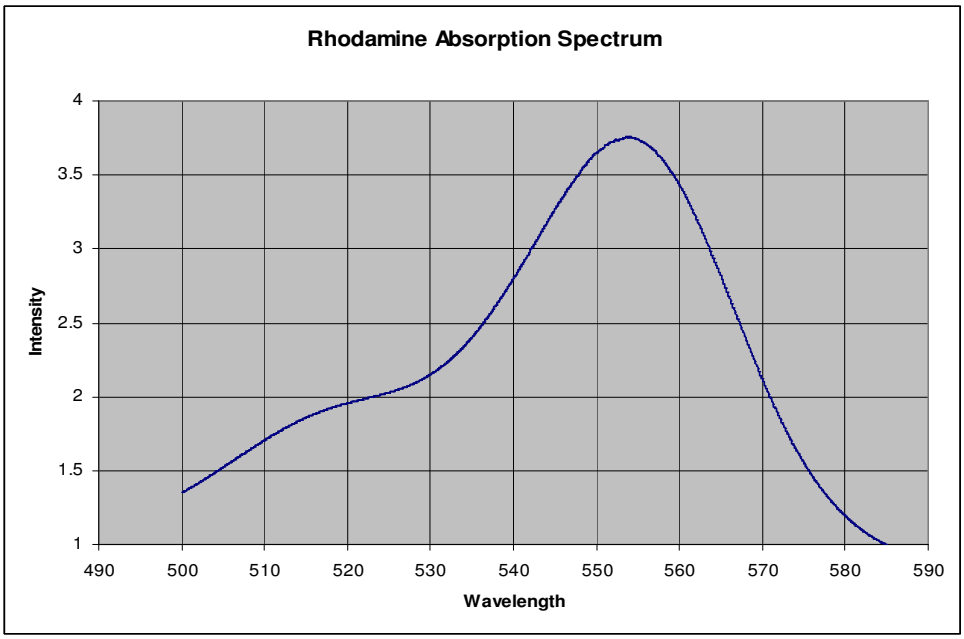

Figure 5.6 The absorption spectrum of Rhodamine B 25 µM in water

5.3.3 Förster Radius

Förster radius is defined as the distance between a given donor acceptor pair where the energy transfer is 50%. Förster radius (Ro) depends on the dipole orientation factor, quantum yield and the refractive index of the sample. The overlap integral is the area of overlap between the emission spectrum of donor and the absorption spectrum of acceptor, as it is seen in equation 5.6.

The rate of energy transfer between donor and acceptor pairs depends on the extent of overlap of the emission spectrum of the donor with the absorption spectrum of the acceptor, the relative orientation of the donor and acceptor transition dipoles and the distance between these molecules.

In fact, the rate of energy formulas are as the following:

$$k_T = \frac{1}{\tau_d}\left(\frac{R_0}{r}\right)^6 \tag{5.3}$$

$$k_T = \frac{9000(\iota n 10)K^2\phi_d}{128\pi^5 n^4 N\tau_D} J(\lambda) \tag{5.4}$$

By equating these energy rate formulas, we can get R_0 Förster Radius formula as in equation 5.9.

$$R_0^6 = Q_D K^2\left(\frac{9000(\iota n 10)}{128\pi^5 n^4 N}\right)J(\lambda) \tag{5.5}$$

$$R_0 = 0.211(\kappa^2 n^{-4}\phi_d J)^{1/6} \quad (\text{in } \mathring{\text{A}}) \tag{5.6}$$

R_0 value is specific to a given set of donor and acceptor molecules. The förster radius of FRET pairs are known in literature. However, it can slightly vary by altering the quantum yield of the donor or the absorption spectrum of the acceptor [6].

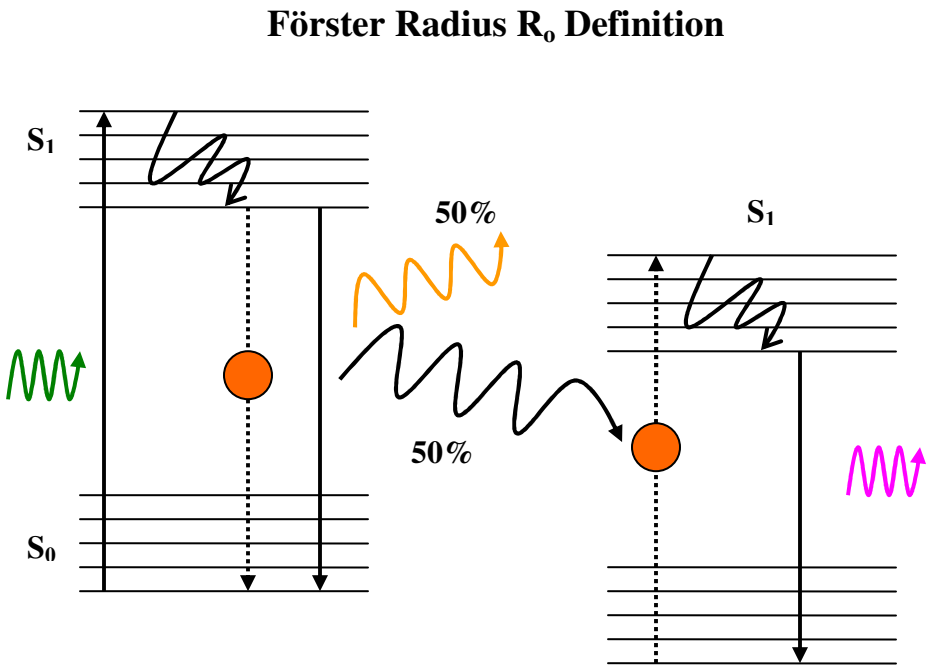

Figure 5.7 Förster Radius where the energy transfer is 50%

Thus, in selecting a suitable FRET pair, it is crucial to consider two factors affecting the optimization of R_0: 1) the quantum yield of donor 2) the spectral overlap between donor emission and acceptor absorption which is dependent on the acceptor extinction coefficient. The higher the R_0, the larger the distance over which FRET can be detected. For example, the use of sulfoindocyanine dye which has large extinction coefficient and spectral overlap makes Cy3 a suitable acceptor with the donor EGFP. The R_0 of this pair is 6 nm, which enables the FRET detection over distances ~1.6× R_0 =9.6 nm [5]. In general, even under optimal donor-acceptor spectral conditions, R never exceeds 7 nm, thus enables one to detect almost 11 nm limit distances.

5.4 FRET Quantification Techniques

The popularity of FRET as a method for measuring distances and interactions in biological macromolecules has lead to the development of several techniques for the measurement and quantification of FRET efficiency.

FRET can be measured by either the decrease in the donor fluorescent emission or the increase in the acceptor fluorescent emission. There are various FRET quantification techniques. Namely, Some of the widely used techniques are 1) donor de-quenching, 2) enhanced acceptor emissions, 3) comparison of donor-acceptor emission ratios, and 4) spectral FRET methods will be given by emphasizing the approaches of each method towards light contaminations i.e. potential problems in FRET experiments. To have accurate FRET measurements and calculations, one must be aware of the potential light contaminations affecting the FRET calculations. These contaminating factors are 1) cross talk, 2) bleed-through, 3) non-specific FRET, 4) mixture of fluorophore populations, and 5) variable expression levels of donor and acceptor.

5.4.1 Potential Problems in FRET

5.4.1.1 Cross Talk

Cross Talk is the overlap of the donor emission and acceptor absorbance bands. That is to say, direct excitation of acceptor by donor excitation light that can cause contaminating fluorescence signal in FRET [7].

Cross-talk can be experimentally determined by comparing the fluorescence intensity of an acceptor-only sample excited with the donor excitation light to that of the same sample excited with the acceptor excitation light [32].

5.4.1.2 Bleed-Through

Bleed through is the overlap in the emission spectra of donor and acceptor molecules. The amount of bleed through can be estimated by examining the emission spectrum of the donor.

There is also backgroud light problem exist identical experimental conditions. This amount of light contamination can be evaluated by several approaches and subtracted from FRET signal [32].

5.4.1.3 Non-Specific FRET

In FRET experiments there can be light contamination from unassociated donor and acceptor fluorophores. As the number of fluorophores from which fluorescence emission is recorded increases and the power of excitation light increases, the average distance between unassociated donor and acceptor fluorophores decreases. Hence, the probability of finding a donor and an acceptor within the FRET distance increases.

Existence of non-specific FRET can be found when the measured FRET values are plotted against the fluorescence intensity of either the donor or the acceptor (the fluorescence intensity is used to represent roughly the fluorophore density in Fig. 5.8. The detectable dependence of FRET on the fluorescence intensity may suggest the occurrence of non-specific FRET [32].

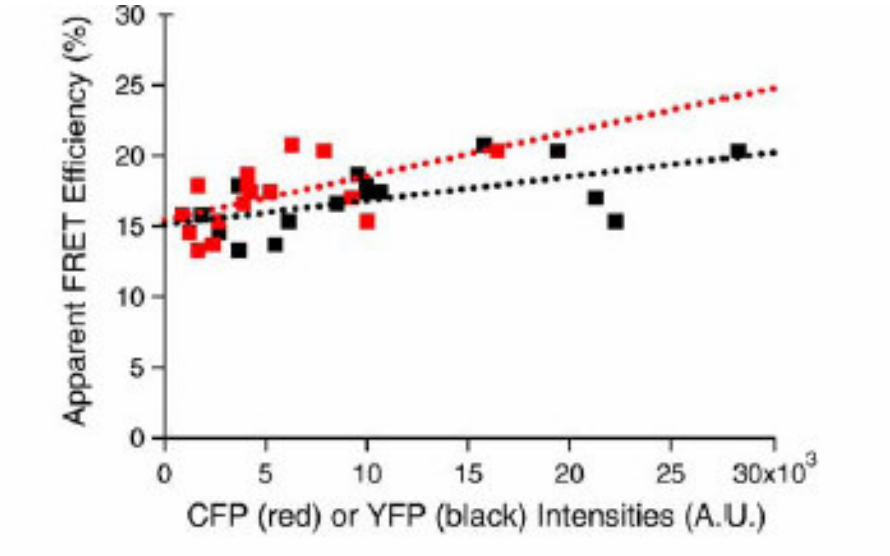

Figure 5.8 Non-Specific FRET CFP(donor) and YFP(acceptor)[32]

5.4.1.4 Mixture of Fluorophore Populations

All the fluorescence emisision collected from a sample is not always due to FRET. Uncoupled fluorophores and pairs of like fluorophores contributes to the total fluorescence intensity and reduces the apparent FRET efficiency since free or unpaired fluorophores contribute to the total fluorescence intensity but not to the FRET signal. The dependence of FRET to the concentrations of donor and acceptor molecules can be explained with the following formulas. Without FRET, the donor and acceptor fluorescence intensities, F_D and F_A, respectively, would be directly proportional to the fluorophore concentrations:

$$F_D = (D + DA) \cdot S_D \tag{5.7}$$

$$F_A = (A + DA) \cdot S_A \tag{5.8}$$

where the donor–acceptor pair, the free donor and the free acceptor at concentrations of DA, D, and A, respectively. Furthermore, S_D and S_A are constants that reflect the properties of the recording system and the fluorophore, such as the transfer function of the

fluorescence detector, excitation light intensity, the fluorophore extinction coefficient, and the quantum yield.

FRET causes a decrease in the donor intensity and an increase in the acceptor intensity. These changes in the fluorescence intensity are determined by the FRET efficiency, E, and the concentration of donor–acceptor pairs:

$$F_D^{FRET} = DA \cdot E \cdot S_D \tag{5.9}$$

$$F_A^{FRET} = DA \cdot E \cdot \frac{\varepsilon_D}{\varepsilon_A} \cdot S_A \tag{5.10}$$

where ε_D and ε_A are molar extinction coefficients for the donor and acceptor, respectively, at the donor excitation wavelength.

FRET can be measured by two ways. Firstly, it can be quantified by the fractional decrease in the donor intensity. Secondly, it can be found by the fractional increase in the acceptor intensity.

The apparent FRET efficiency, E_{app}, of the system by first way as the following equation:

$$E^{app} = \frac{F_D^{FRET}}{F_D} = \frac{DA}{D + DA} \cdot E \tag{5.11}$$

As an example of this approach is the acceptor photobleaching i.e. donor de-quenching.

Another way to measure FRET is to use enhanced acceptor emission, in which the apparent FRET efficiency will be:

$$E^{app} = \frac{F_A^{FRET}}{F_A} \cdot \frac{\varepsilon_A}{\varepsilon_D} = \frac{DA}{DA + A} \cdot E \tag{5.12}$$

Several methods such as “netFRET” method and the “three-cube” method and “spectra FRET” use this way to quantify FRET.

Since the FRET efficiency depends on the concentration of the donor and acceptor molecules as it is seen in the previous formulas, the problem arises when the expression levels of the donor and the acceptor fluorophore vary from one sample to another. If all the

fluorophores are not correctly paired, the observed FRET efficiency will always be lower than the true efficiency, E.

The relationship between the apparent FRET efficiency and the concentrations of the donor and acceptor fluorophores is seen in Fig. 5.9.

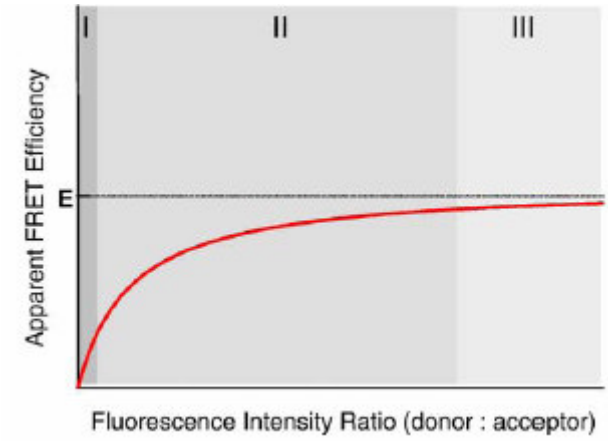

Figure 5.9 FRET efficiency versus donor:acceptor concentration ratio [32]

In the Figure 5.9 , The apparent FRET efficiency is calculated from the enhanced acceptor emission according to Eq. 5.12 and is plotted against the fluorescence intensity ratio between the donor and acceptor. The figure can be investigated in three parts. In first part shown with I label, there are lots of uncoupled acceptor molecules that do not contribute to FRET (DA << A). Thus, the apparent FRET efficiency is much lower than the true efficiency. On the other hand, in region III most of the acceptor fluorophores should be coupled to a donor (DA >> A) and the apparent efficiency approaches the true value. However, in order for the apparent efficiency to be close to the true efficiency, the donor-to-acceptor ratio needs to be quite high. That means the low acceptor intensity in the presence of the high donor intensity which are hard to quantify accurately and more prone to contaminations from autofluorescence and background light. Therefore, the calculated FRET efficiency values are not so reliable. In region II, where the donor intensity and the acceptor intensity are comparable and easy to measure. Here the apparent efficiency

depends strongly on the donor-to-acceptor ratio as in the case of first region. For accurate estimation of the intrinsic FRET efficiency, data is taken from all three regions [32].

5.4.2 FRET Methods

5.4.2.1 Acceptor Photobleach FRET

In this technique FRET can be quantified by observing an increase in the fluorescence intensity of the donor measured after the acceptor is photobleached. After the acceptor is quenched, the energy transfer does not occur thus, the donor emission is expected to increase. By this way FRET can be measured using the following formula:

$$E = 1 - \frac{F_D}{F_D^{'}} \tag{5.13}$$

where F_D and $F_D{}'$ are the donor intensity before and after photobleaching of the acceptor, respectively. Measurements can only be taken once from each sample since the photobleaching process is irreversible. In addition, incomplete acceptor photobleaching can lead to underestimation of FRET. It is not affected by either cross-talk or bleed-through so much. Since the excitation light used to bleach the acceptor usually does not bleach the donor efficiently and donor emission can be measured at a wavelength range away from the acceptor emission. However, mixtures of fluorophore populations will cause underestimation of the FRET efficiency. Therefore, it is better to use samples having less donor-acceptor ratios.

In fact, the relationship between the apparent FRET efficiency and the expression level of the fluorophores are used to determine the true FRET efficiency [32].

5.4.2.2 Sensitized Emission FRET

In FRET calculations, the enhancement of acceptor emission can be used instead of measuring the increase in fluorescence of the donor, as with donor de-quenching. When the donor fluorophore transfers energy to the acceptor fluorophore i.e. FRET occurs, an increase in fluorescence of the acceptor is observed and can be measured by the following formula:

$$E = \frac{\varepsilon_A}{\varepsilon_D}\left(\frac{F_A^{'}}{F_A} - 1\right) \tag{5.14}$$

where F_A and $F_A{}'$ are the acceptor intensity in the absence and in the presence of the donor, respectively. There are several different methods designed to measure FRET in this way. Common to these methods, light contaminations due to cross-talk and bleed-through are estimated separately from acceptor-only and donor-only samples using the same equipment setting for FRET measurements. These contaminating fluorescent emissions are subsequently subtracted from the total fluorescent signal measured from the donor-plus-acceptor samples [7].

In netFRET, FRET is assumed to arise from the bimolecular interaction with a certain equilibrium constant in the form D + A ↔ DA. Algorithms are developed to correct for variable protein expression levels with a ratio that compares the concentration of donor–acceptor molecules (donor-tagged molecules associated with acceptor-tagged molecules) to the concentration of free donors and free acceptors. A general approach is applied in the spectra FRET method, for which no specific form of interaction is assumed. The mixture of fluorophore populations and variable donor-to-acceptor ratios is dealt with by analyzing the dependence of the apparent FRET to the donor-to-acceptor ratio.

There is a simple way to detect sensitized emission FRET just getting two images: one of donor alone excited by donor excitation wavelength, and one of donor and acceptor excited by the same wavelength. A confocal microscope or the standard mercury source can be used as excitation source with appropriate excitation and emission filters. An ideal FRET pair for this analysis would have an extensive overlap between the donor emission and acceptor absorption in order to promote FRET but no overlap of absorbance bands of donor and acceptor as well as no overlap of emission bands of donor and acceptor. However, there is no ideal FRET pair. The donor excitation can excite the acceptor and also the acceptor excitation can excite the donor. Thus, it is difficult to design filter sets to seperate the donor and acceptor emission [32].

The protein-protein interactions can be studied by Fluorescence-activated cell sorting (FACS) method. Fluorescence is quantified first for donor alone, acceptor alone, and for untransfected cells to establish background levels. The fluorescence emission from doubly transfected cells are obtained for acceptor emission for acceptor excitation, and for donor and acceptor emission using donor excitation. FACS helps to quantify the percentage of cells showing FRET which shows that the interaction occurs [7].

5.4.2.3 Donor-acceptor emission peak ratio

Another simple technique for rapid detection of FRET changes is to compare donor-acceptor emission peak ratios with and without FRET. Since FRET is the transfer of energy from a donor to an acceptor, the fluorescence intensity of the donor will diminish while the fluorescence intensity of the acceptor will raise. The ratio between the acceptor intensity over the donor intensity before FRET can be quantified according to the eqn. 5.15. The ratio between the acceptor intensity over the donor intensity before FRET is expected to be smaller to the ratio after FRET. Since as the numerator increases and the denominator

decreases in opposite directions, the ratio increases if there is an energy transfer from donor to acceptor.

$$FRET\_index = \frac{F_A}{F_D} \tag{5.15}$$

The measurement of fluorescence ratio is not as complicated as the techniques previously described. It can be determined at the peak emission of each flurorophore. Since it is a quick test for FRET changes, contaminations such as cross-talk and bleed-through normally not corrected. In addition, mixed flurophore populations and variable expression levels affect the FRET signal measured from the donor-to-acceptor ratio [27].

5.4.2.4 Spectral FRET Methods

Researchers have found a new method, which is more reliable and avoids the problems resulting from the difficulty of separating fluorophores in FRET studies. It is possible to measure enhanced acceptor emission or the decrease in donor emission after photobleaching. The underlying principle behind the various spectral methods is the same: if the spectra of two fluorophores are known, the observed spectrum at any pixel is the sum of the spectra of the component fluorophores, weighted by linear coefficients:

for wavelengths $\lambda = \lambda_1, ..., \lambda_n$

$$S(\lambda) = A \times Donor(\lambda) + B \times Acceptor(\lambda),$$

where S(λ) is the spectrum observed at the pixel, Donor(λ) and Acceptor(λ) are the spectra for the donor and acceptor over the same wavelength range, and A and B are constants. The goal is to determine A and B from the set of linear equations above. This can be readily achieved by least-squares fitting and is referred to as linear unmixing.

For applying this method one needs a spectrograph and a detector and an epi-fluorescence microscope, excitation light source, two filter cubes (for donor and acceptor excitation). The spectrograph is attached to the output port of the microscope via a

compatible mounting mechanism. The CCD camera is attached to output port of the spectrograph. The use of spectrograph has many advantages, such as accurate subtraction of bleed-through and cross talk light contaminations. Recently, this technique has been applied to both membrane and cytosolic proteins expressed in cultured cells. To record FRET, a fluorescent cell is brought into the field-of-view of the camera. The slit is then moved into the light path to cover the region of the cell from which fluorescence signals are to be measured. The grating is rotated to the desired angle for light of a selected wavelength range to be projected to the camera. Two spectroscopic images are taken using the donor and the acceptor excitation filter cube. A fluorescence emission spectrum is constructed from each image using the fluorescence intensity values along a horizontal line whose position corresponds to the part of the cell to be measured.

They quantified FRET after correcting the contaminations using the spectroscopic data taken from only donor fluorophores or only acceptor fluorophores and donor and acceptor fluorophores together. First contribution from bleed-through is removed from the donor-acceptor emission spectrum (Fig. 5.10, red curve) by subtracting from it a donor spectrum that has been normalized to the peak fluorescence in the donor emission region. Thus, an extracted acceptor spectrum which is free of donor contamination is get (Fig. 5.10, blue curve). After that, the contribution from cross-talk is removed from this extracted spectrum. The amount of cross-talk can be estimated from the two spectra collected from acceptor-only cells using the donor and the acceptor excitation light, respectively. The ratio between these two spectra, which is termed RatioA0, represents the efficiency of cross-talk that is specific to the donor–acceptor pair and the recording system. Multiplying RatioA0 to the total acceptor emission from a donor–acceptor sample in respond to the acceptor excitation light (not shown) yields the amount of the cross-talk signal (Fig 5.10, yellow dotted curve).The difference between the extracted acceptor spectrum and the cross-talk is the FRET signal. In Spectra FRET, the ratio between the

extracted acceptor spectrum and the total acceptor emission spectrum with the acceptor excitation is calculated, which is termed RatioA, and compared to RatioA0 as in equation 5.16. The apparent FRET efficiency from an individual cell, Eapp, can be calculated as

$$E^{app} = \left(\frac{RatioA}{RatioAO} - 1 \right) \frac{\varepsilon_A}{\varepsilon_D} \tag{5.16}$$

The FRET spectra method is more tolerant to low signal-to-noise ratios and more reliable since both bleed-through and cross-talk are subtracted from the whole wavelength range[7,27].

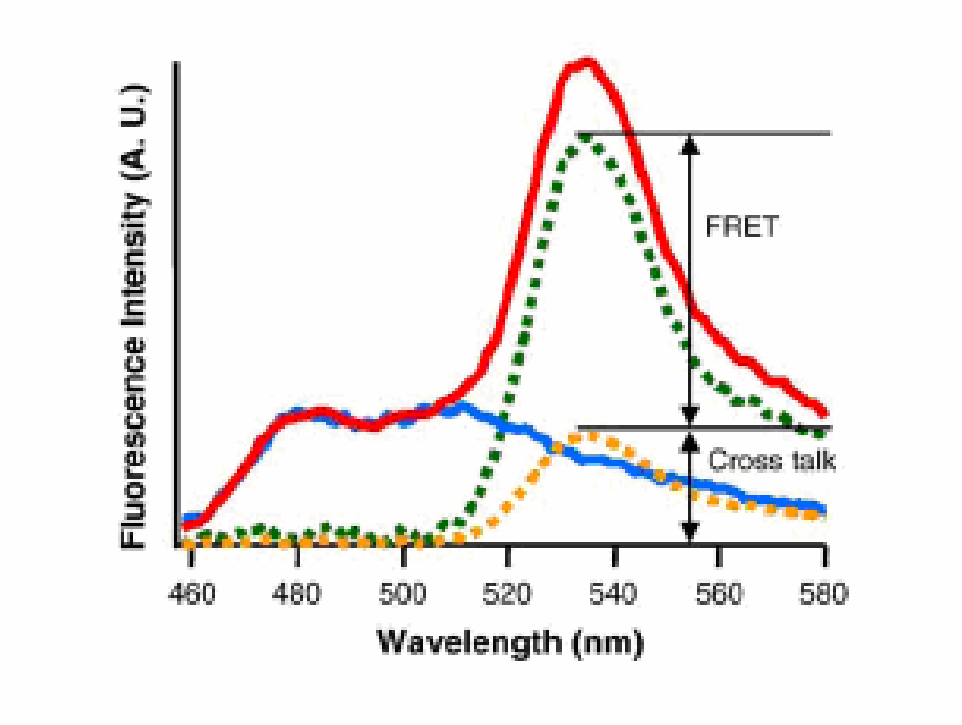

Figure 5.10 FRET signal [32]

5.5 Materials and Methods

5.5.1 Materials

5.5.1.1 Fluorescein

Fluorescein and its derivatives are second family of xanthene dyes (Fig. 5.11). Fluorescein is a fluorophore commonly used in microscopy and dye laser as the gain medium. Fluorescein itself is only slightly fluorescent in alcohol solution. On the contrary, the alkali salt obtained by addition of alkali shows the well-known yellow-green fluorescence characteristic of the fluorescein dianion (uranin). There are also other derivatives of fluorescein e.g. eosin Y and erythrosine Y which are very sensitive to pH, thus used as pH fluorescent probes [2]. The structure of fluorescein is seen in Fig. 5.12. The fluorescent properties of fluorescein have been shown to change dramatically in low pH. Therefore, all studies done using fluorescein should be done at pH 7.0 or higher. Fluorescein has excellent fluorescence quantum yield and good water solubility as well as its relatively high absorptivity.

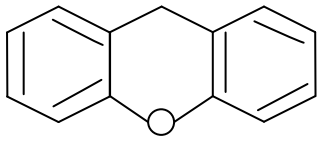

Figure 5.11 Xanthene

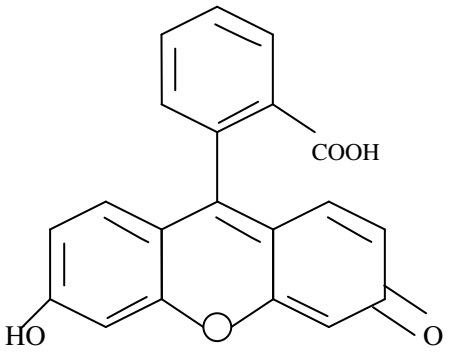

Figure 5.12 Fluorescein

5.5.1.2 Rhodamine B

Rhodamines (e.g. rhodamine 6G, rhodamine B) are also highly fluorescent dye molecules which are derivatives of xanthene. They are used as a dye or laser dyes. Their absorption and emission spectra are quite narrow and the Stokes shift is small. They emit fluorescence in the range 500-700 nm. Rhodamine dyes are generally toxic, and are soluble in water, methanol, and ethanol [2].

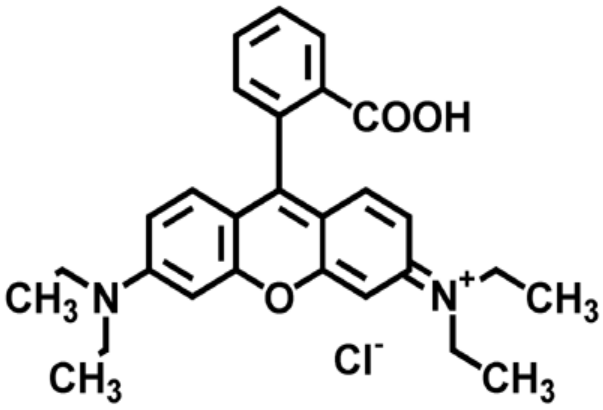

Figure 5.13 Rhodamine B

5.5.2 Methods

5.5.2.1 Choosing Suitable Probes

We have used Fluorescein Na and Rhodamine B as an acceptor-donor pair in order to get FRET efficiency owing to their spectral properties. There are two important factors affecting the efficiency of energy transfer. Firstly, the donor must have high quantum yield in order to have a high efficiency. The other factor is, the acceptor molecule must have high absorption coefficient regardless of being fluorescent or nonfluorescent. Fluorescein, the donor molecule, has high quantum yield and Rhodamine B, acceptor molecule, has a high absorption coefficient verified by several researchers using these FRET pairs as probes in their work (Table 5.1).

Table 5.1 Quantum yield for different chemical compounds. Molar absorption coefficient in correspondence of the wavelength of the absorption peak [33].

	ε (liter moles^{-1} cm^{-1})	λ (nm)	quantum yield	solvent
Coumarin 1	23,500	373.25	0.73 at 360 nm	ethanol
Coumarin 6	54,000	459.25	0.78 at 420 nm	ethanol
Coumarin 30	42,800	407	0.67 at 380 nm	acetonitrile
Fluorescein	92,300	482.5	0.79 at 425 nm	ethanol
Rhodamine B	106,000	542.75	0.70 at 510 nm	ethanol
Rhodamine 6G	116,000	529.75	0.95 at 480 nm	ethanol

Actually, in selecting fluorescent probes as workable FRET pairs the spectroscopic properties of fluorophores are crucial. First, there must be sufficient separation in excitation spectra of fluorophores i.e. not much overlap between absorption spectra of the molecules. We have verified this by obtaining the absorption spectra of Fluorescein and Rhodamine B at different molarities (Fig. 5.14 and Fig. 5.15). Secondly, there must be high overlap between the emission spectrum of the donor and the absorption spectrum of the acceptor to

obtain efficient energy transfer, which is the main requirement of FRET. Finally, there must not be much overlap in emission spectra between donor and acceptor molecules to allow independent measurement of the fluorescence of each fluorophore. In fact, the overlap between the absorption and emission spectra are unavoidable known as cross talk and bleed through causing light contaminations in FRET measurements. Nonetheless, these contaminating factors can be corrected by several methods developed to measure exact FRET efficiency as explained in previous sections. However, one can be careful while choosing the fluorescent probes, which has the lowest overlap between excitation and emission spectra.

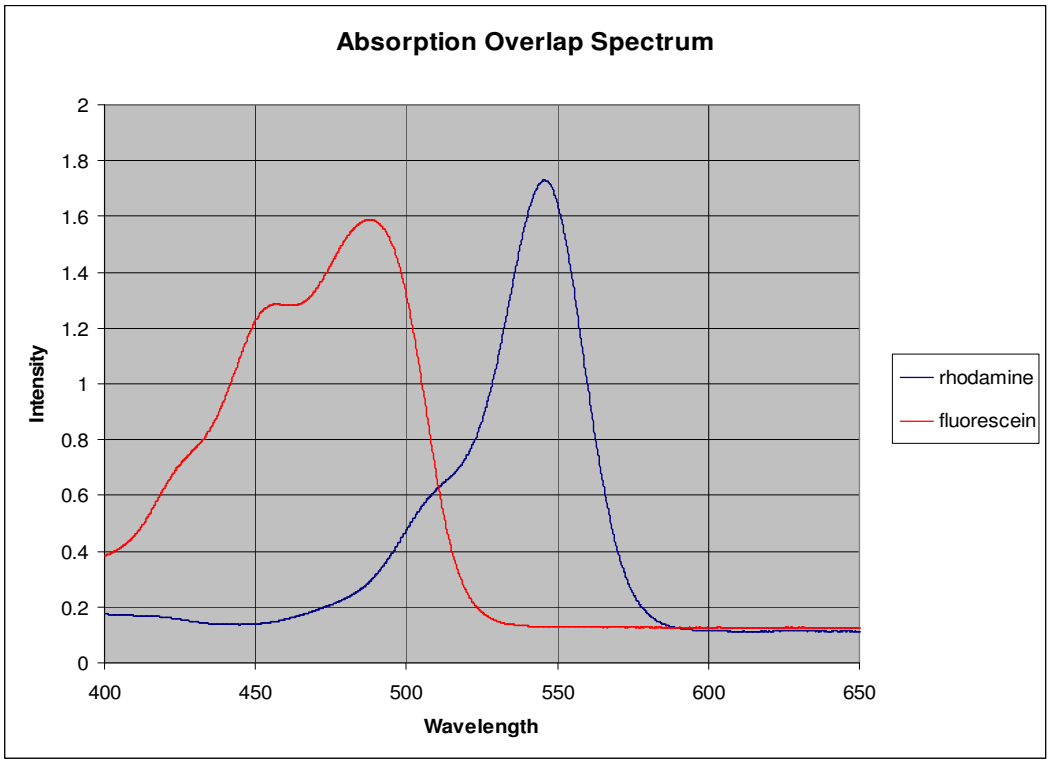

Figure 5.14 The overlap of the absorption spectra of Rhodamine B 20 µM and Fluorescein Na 80µM

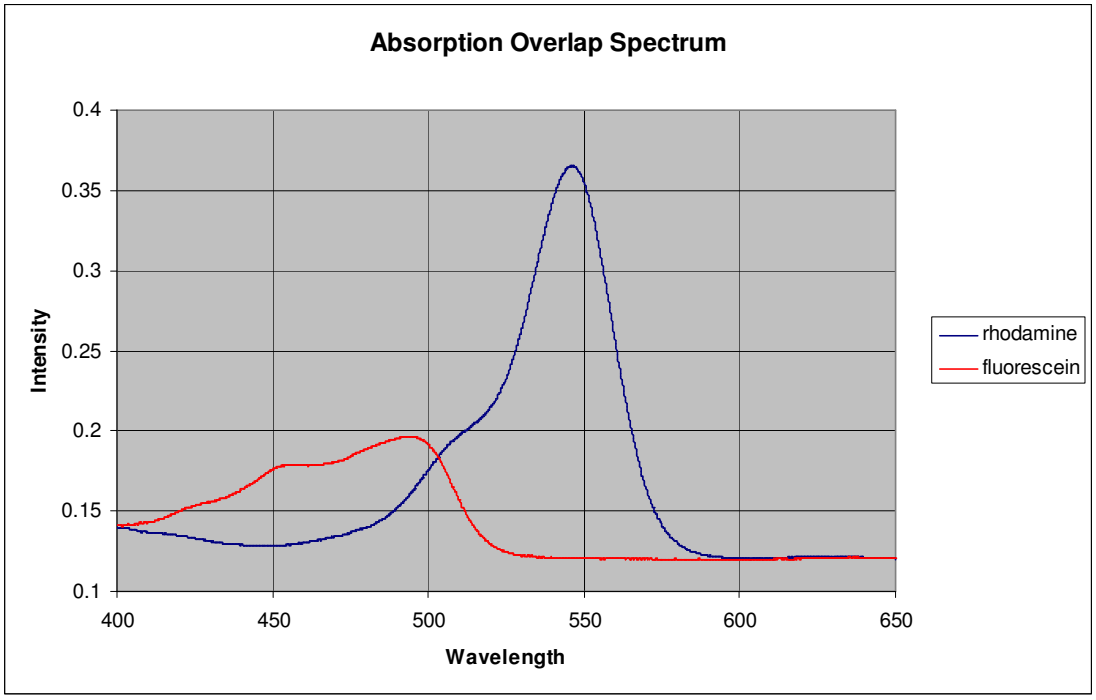

Figure 5.15 The overlap of absorption spectra of Rhodamine B 2 µM and Fluorescein Na 8µM

The emission spectra of Rhodamine B and Fluorescein Na could be obtained by attaching a spectrograph to the output port of the microscope and attaching a CCD camera to the output port of the spectrograph. However, in literature their emission spectra are known. Actually, the emission spectra depends on the concentration of dye solutions and the solvent used to dissolve the dye molecules. Thus, the spectrum of a fluorescent dye alters with different solution concentrations as well as in a variety of solvents. However , it can be concluded that these two fluorophores are suitable FRET pairs to be used in FRET calculations.

5.5.2.2 The Sample Preparation

We have prepared three samples, which contain only donor molecules and only acceptor molecules, and the mixture of donor and acceptor molecules in thin films in order to use them in FRET experiments. Firstly, the cover glasses were cleaned by UV Ozone cleaner , which removes organic contaminations or organic thin films for 20 minutes. For preparing the donor only molecules, 20 µl of 800 nM Fluorescein Na in methanol was added to 1 ml of 3 mg/ml Polymethylmethacrylate (PMMA) in Chloroform ($CHCl_3$), while preparing the acceptor only molecules 20 µl of 200 nM Rhodamine B was added to 1 ml of 3 mg/ml Polymethylmethacrylate (PMMA) in Chloroform ($CHCl_3$). In addition, the mixture of 20 µl of 200 nM and 20 µl of 800 nM Fluorescein were added to 2 ml of PMMA in chloroform solution so as to prepare sample containing both donor and acceptor molecules. Then the cover glasses were spin coated with the solutions containing Rhodamine B and PMMA and Fluorescein Na and PMMA, and both Rhodamine B, Fluorescein Na and PMMA at 2000 rpm for one minute. The films of only Rhodamine B molecules and only Fluorescein Na molecules and both Rhodamine B and Fluorescein Na molecules in the matrix of PMMA polymer were obtained after solvent evaporation. Lastly, the films were dried in vacum oven in order to evaporate any trapped solvent molecules.

5.5.2.3 FRET Quantification

The FRET efficiency *E*, defined as the fraction of donor excitation events that result in the excitation of the acceptor. The FRET efficiency can be quantified by two ways: first, a decrease in donor intensity (eqn 5.17) and second, an increase in the acceptor intensity after some energy transferred from donor to acceptor molecule (eqn. 5.18).

FRET efficiency E may be quantified from images of FRET pairs as follows:

Decrease in fluorescence intensity of donor after donor fluorophore transfers energy to the acceptor fluorophore during the occurence of FRET:

$$E = 1 - \left(I_{DA} \middle/ I_D \right) \tag{5.17}$$

where I_{DA} and I_D are the donor emission intensity in the presence and absence of the acceptor, respectively.

Increase in fluorescence intensity of acceptor after FRET occurs:

$$E = \frac{\varepsilon_A}{\varepsilon_D}\left(\frac{F_A^{'}}{F_A} - 1 \right) \tag{5.18}$$

Where F_A and F_A ' are the acceptor intensity in the absence and in the presence of the donor, respectively.

The donor and acceptor separation, r, can also be calculated from the following relationship:

$$E = \frac{R_0^6}{R_0^6 + r^6} \tag{5.19}$$

$$r = R_0 \left\{ \left(1 \middle/ E \right) - 1 \right\}^{1/6} \tag{5.20}$$

Where R_0 is a coefficient called the förster radius, which has been determined for many fluorophores [7, 27].

5.5.2.4 FRET Experiment

Total Internal Reflection Microscopy technique was used to look for energy tranfer between Fluorescein Na and Rhodamine B. Experiments were performed with home built confocal microscope. Donor and acceptor excitation was provided by 488 nm Ar ion laser. It was used to excite samples containing donor molecules only, acceptor molecules only, and the mixture of donor and acceptor molecules. The angle of incidence of the laser beam to the polymer-air interface was adjusted to observe total internal reflection. High numerical aperture objective (N.A.=1.4, 60x oil), a 1.5x magnification element were used to collect collimated light. Furthermore, we have collected the emissions from donor and acceptor molecules using donor and FRET filters. As a donor filter and FRET filter, we

have used HQ Chroma 525/50, 620/60 bandpass filters, respectively. A cooled charge-coupled device (CCD) camera was used to detect signals emitted from the samples.

5.6 Results and Discussion

The images of the samples containing both donor and acceptor using the donor filter (Fig. 16a), using the FRET filter (Fig.16b) were plotted and the substraction of donor from acceptor molecule were done by means of labview program. In Fig. 5.16c we see the difference between donor and acceptor fluorescence where the intensity of light emitted from acceptor molecule is more than the intensity of light emitted from donor molecule. These images display that there are some points on the sample where the acceptor molecule emits more fluorescence light than the donor molecule does. It can result from energy transfer from a donor molecule to an acceptor molecule. However, we can not quantify energy transfer by solely looking at the intensity differences of light emission in the donor and FRET channel. Since the bleed through from both donor and acceptor emission through FRET channel is possible. The acceptor molecule, Rhodamine B can also be excited by donor excitation light as well as the donor molecule, Fluorescein can emit light in the range of wavelenghts corresponding to acceptor emission both of which contributes to FRET signal.

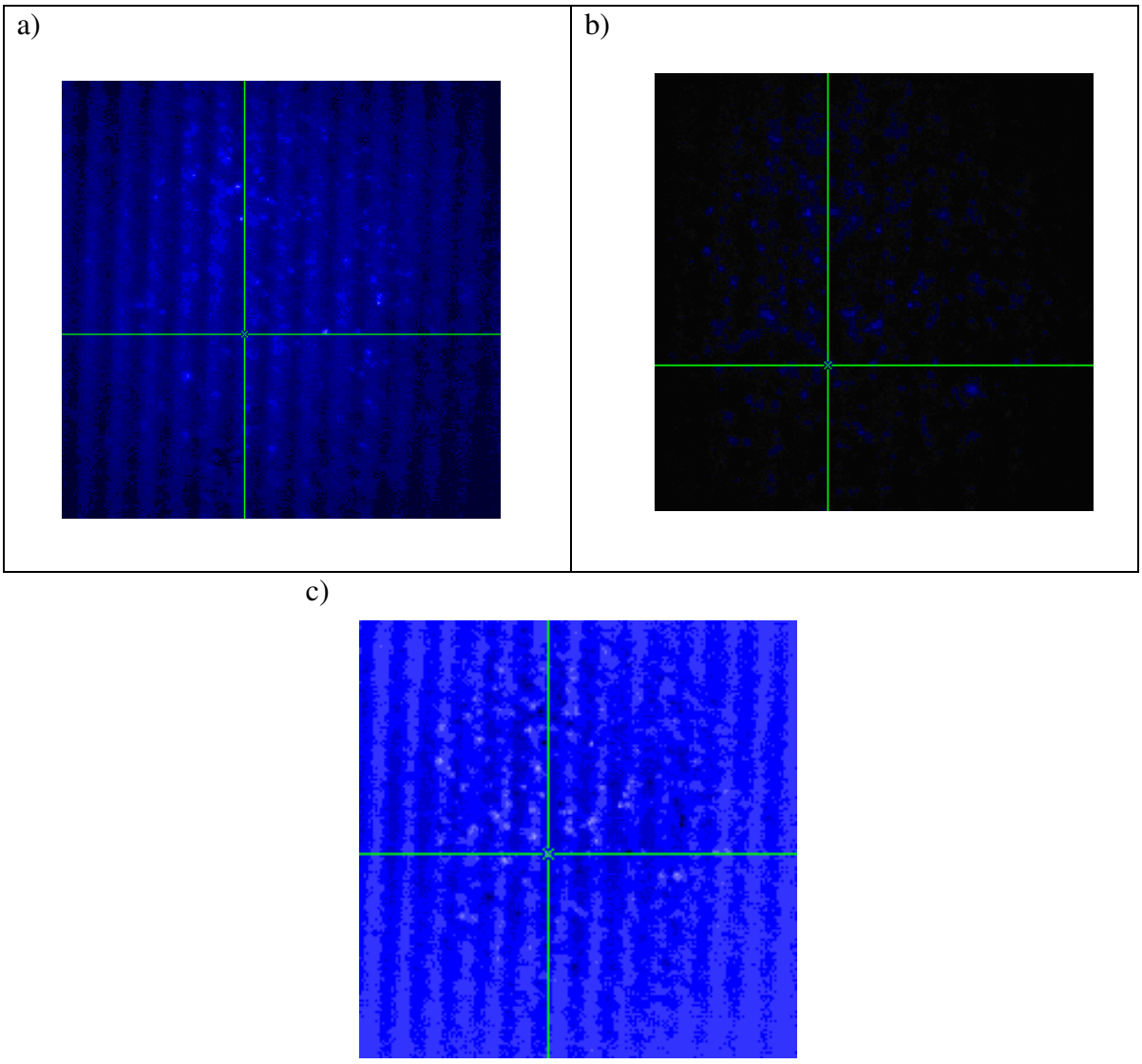

Figure 5.16 a) Fluorescence intensity image of a sample containing donor and acceptor molecules obtained by donor filter **b)** Fluorescence intensity image of the sample containing the mixture of donor and acceptor fluorophores obtained by fret filter **c)** The substraction of donor fluorescence from acceptor fluorescence.

Thus, further experiments with samples containing 800 nM Fluorescein Na, donor molecules and 200 nM Rhodamine B, acceptor molecules were done in order to find the light contaminations in FRET channel.

The observed FRET signal is higher than the actual signal. Since donor excitation can also excite the acceptor molecule which is known as cross talk and emission bands also overlap. Therefore, contributions of donor and acceptor fluorescence emission into the FRET channel is a major problem. Furthermore, there are other factors existing in intensity-based FRET imaging microscopy such as detector noise, optical noise, and photobleaching. To correct these problems, various methods of FRET data analysis for wide-field microscopy have been developed. These methods remove bleed-through and cross talk light contaminations. One of the new and reliable method developed to remove the unwanted contaminating signals in FRET calculations is spectra FRET method which is explained in Sec. 5.4.2.4. in detail. In fact, we followed the steps of spectra FRET methods in a spatial region not in the spectral region as in spectra FRET method. We get FRET intensity profile of images and did substractions of undesired contaminating signals which results from the overlap between absorption and emission spectra of fluorophores. Thus, we get the actual FRET signal at the end. In order to calculate the apparent energy transfer, we have used eqn 5.17.

The steps of the method that has been inspired from the spectra FRET method [7] are shown as the following:

Firstly, the subtraction of donor bleed-through from donor-acceptor emission intensity profile is done. This is achieved by subtracting the donor emission in the FRET channel i.e. donor fluorescence emission obtained by using FRET filter. This data refers to Fluorescein emission, flu_f, this is subtracted from the donor intensity profile in the donor emission region which is the data of the mixture of donor and acceptor molecules taken by using donor filter, fret_d.

fret_d :

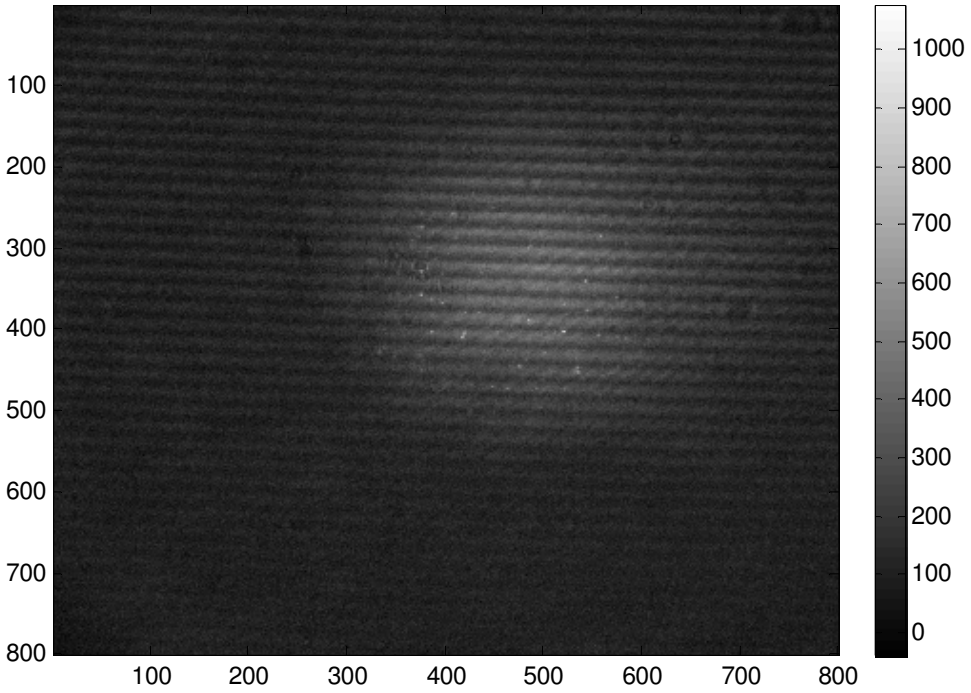

Figure 5.17 Donor emission from sample containing donor and acceptor

Then, one line is selected on the image by means of improfile command existing in image processing toolbox menu of matlab.

profile line for fret_d (profile line contains 400 pixels) :

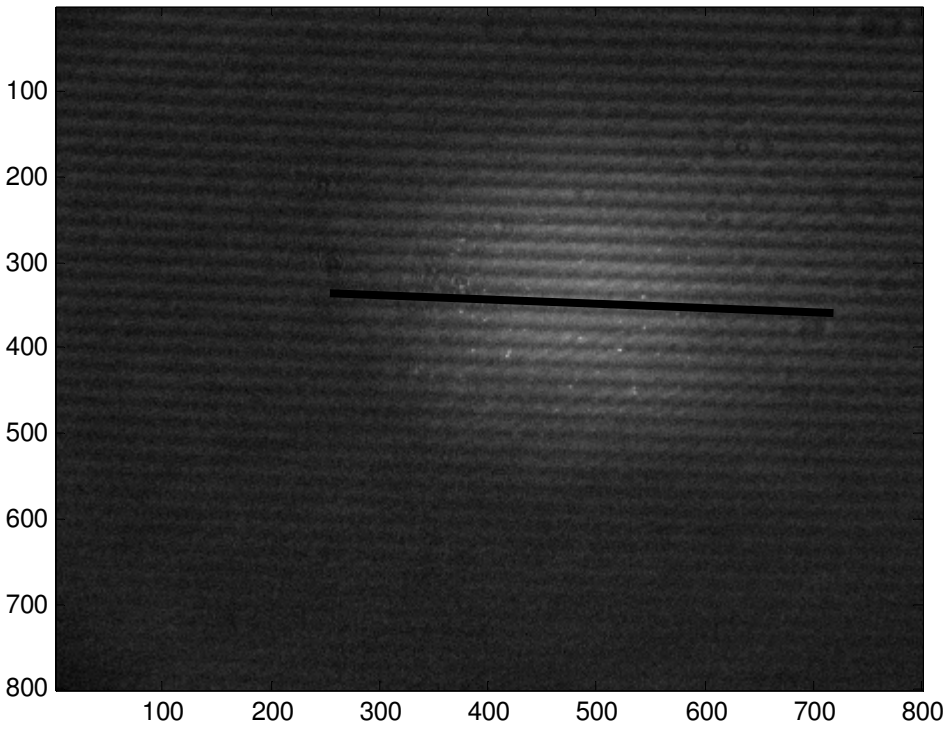

Figure 5.18 Profile line draw on donor acceptor sample

Then, the intensity profile of the image along the selected line is obtained.

profile of fret_d :

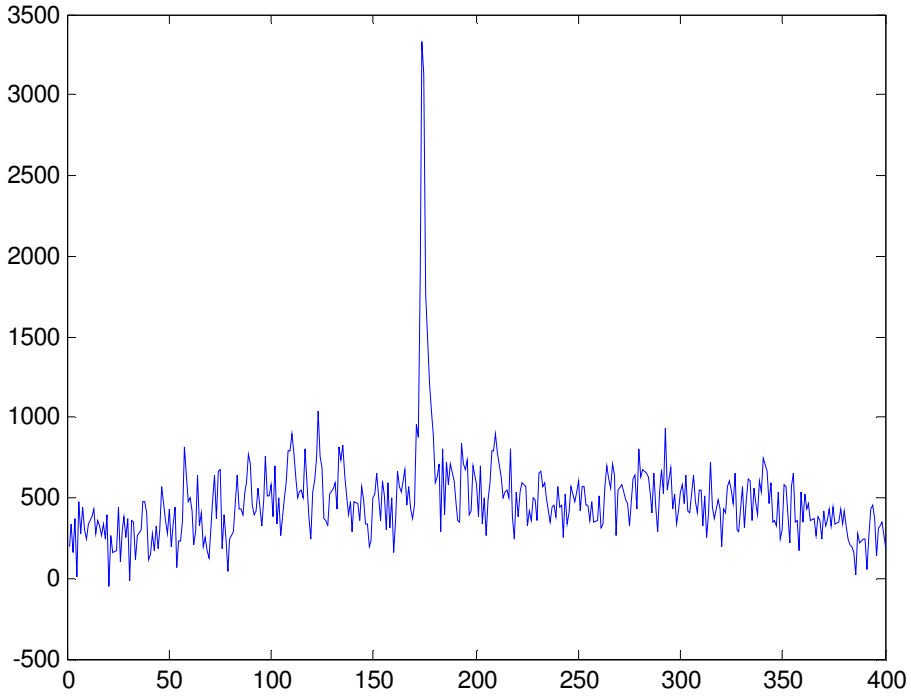

Figure 5.19 Intensity profile of donor emission from donor and acceptor sample

After that, the image of donor molecule, Fluorescein Na showing the intensity of fluorescence emission from donor molecules obtained by using FRET filter is plotted.

flu_f :

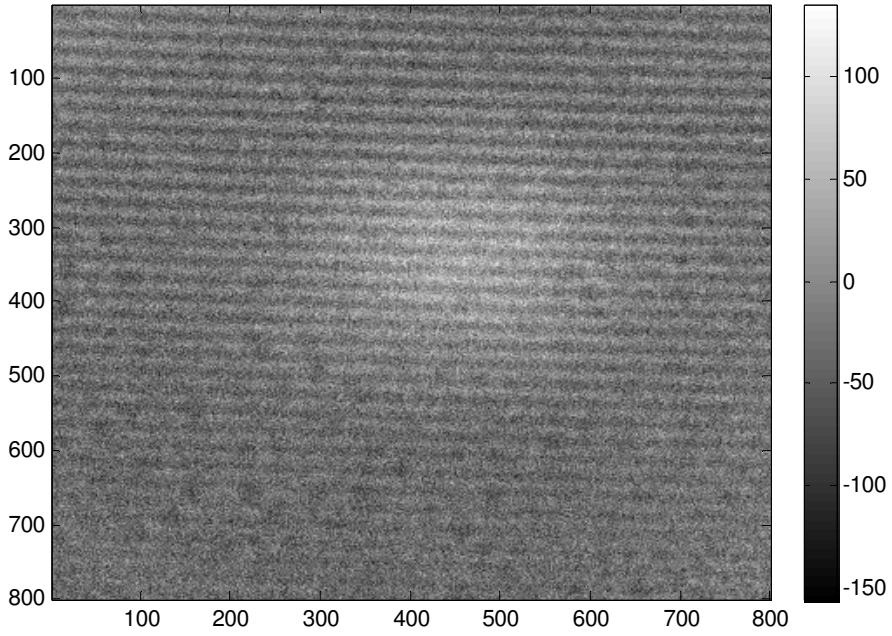

Figure 5.20 Donor bleed through in to FRET channel

A line is selected on the image again to get intensity profile of the donor molecule.

profile line for flu_f (profile line contains 400 pixels) :

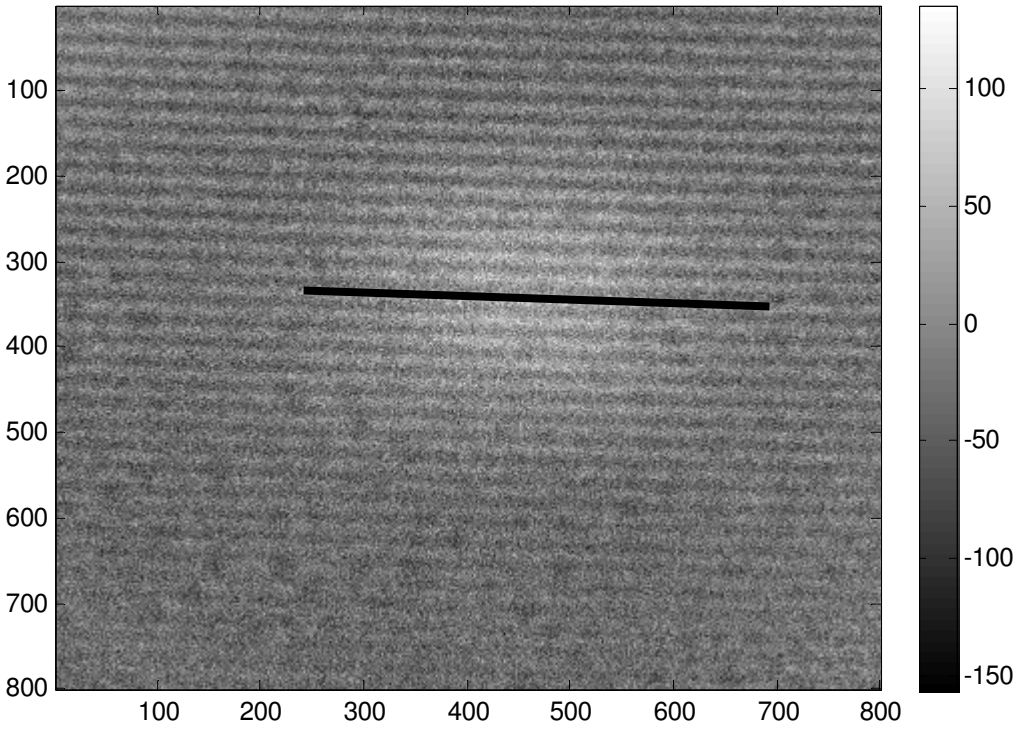

Figure 5.21 Profile line on donor sample

Then the intensity profile of donor molecule in acceptor emission region that is bleed through is obtained.

profile of flu_f :

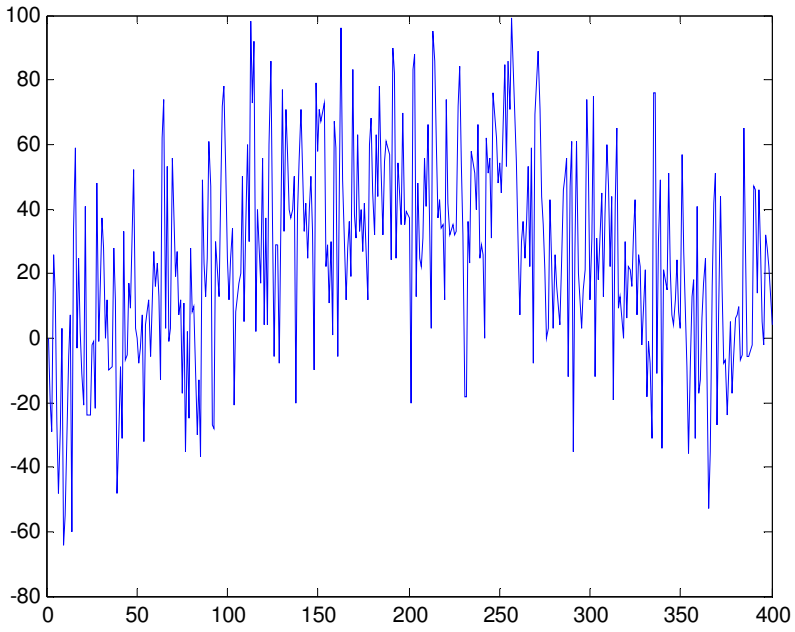

Figure 5.22 The intensity profile of donor emission in the range of acceptor

Lastly, the substraction of bleed through from donor emission is realized. The result gives us the extracted acceptor profile that is free of donor contamination.

extracted acceptor profile = profile of fret_d – profile of flu_f :

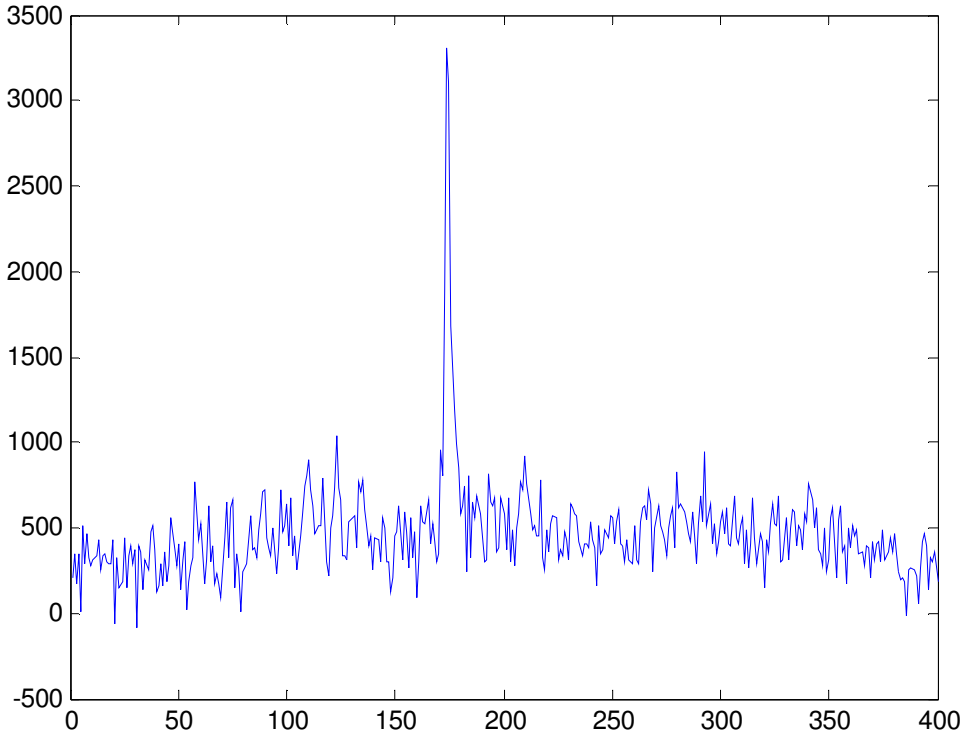

Figure 5.23 Extracted acceptor profile

Secondly, the following steps calculate cross talk, which is the overlap between the donor and acceptor absorption spectra. First, the ratio AO is obtained by dividing the acceptor only sample's emission in donor channel to acceptor only sample's emission in FRET channel. It gives the efficiency of cross-talk. Then this is multiplied to the total acceptor

emission from a donor-acceptor sample taken by FRET filter. This result is the cross-talk signal.

In order to find the ratio AO, that is the ratio between acceptor emission obtained by using donor filter and FRET filter. The images of acceptor only samples, Rhodamine B obtained by using these filters consecutively are plotted.

Rhb_d :

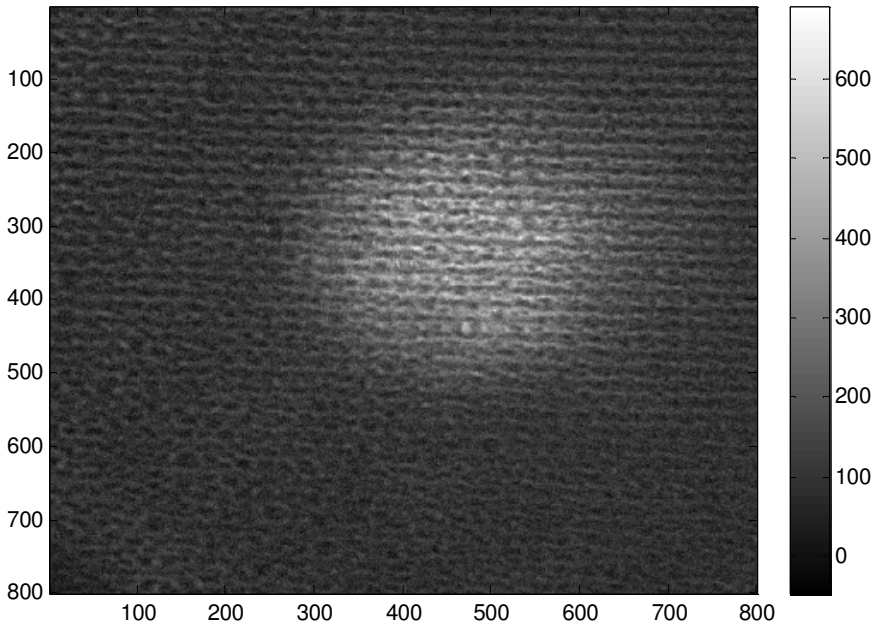

Figure 5.24 Acceptor emission with donor filter

Rhb_f :

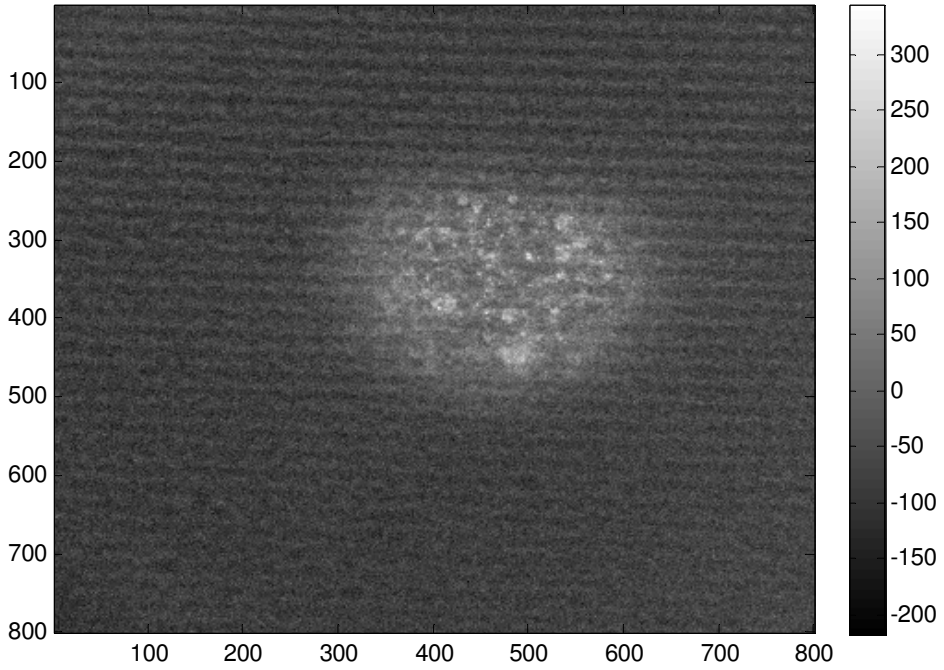

Figure 5.25 Acceptor emission with FRET filter

norm of Rhb_a03_d = norm(Rhb_a03_d) = 1.1963e+005

norm of Rhb_a03_f = norm(Rhb_a03_f) = 5.0432e+004

ratioAO = 1.1963e+005 / 5.0432e+004

ratioAO = 2.3721

This ratio gives us a constant and it is multiplied by the total acceptor emission from a donor-acceptor sample. The image of donor-acceptor sample showing the intensity of fluorescence emission from donor molecules obtained by using FRET filter is as the following.

The image of acceptor emission from donor-acceptor sample is plotted.

fret_f :

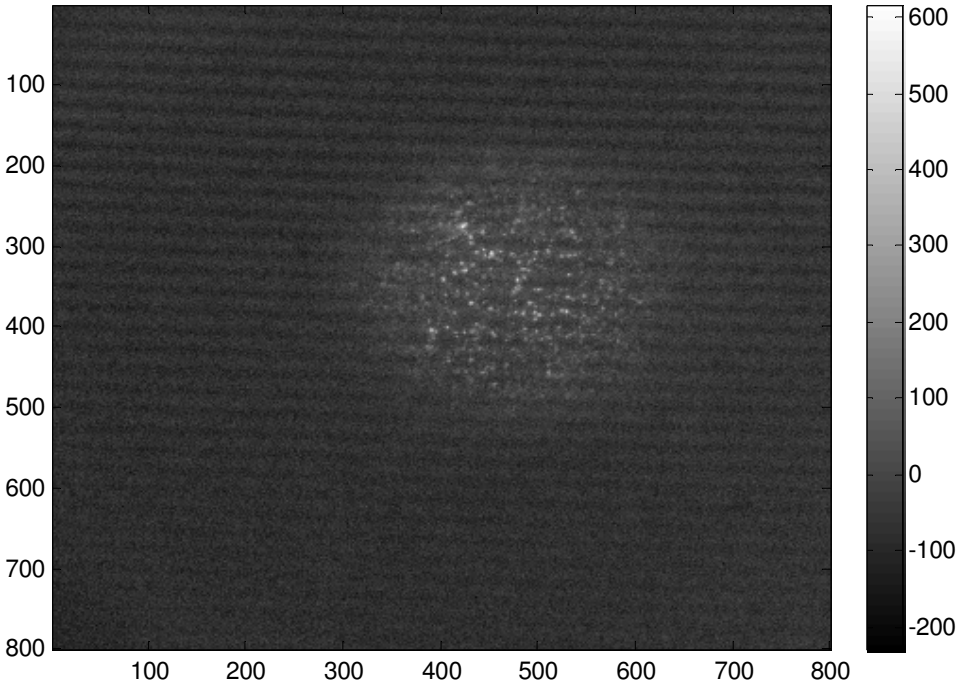

Figure 5.26 Acceptor emission from donor and acceptor sample

Then the intensity profile of donor-acceptor sample is found again drawing a line on the image.

profile line for fret_f (profile line contains 400 pixels) :

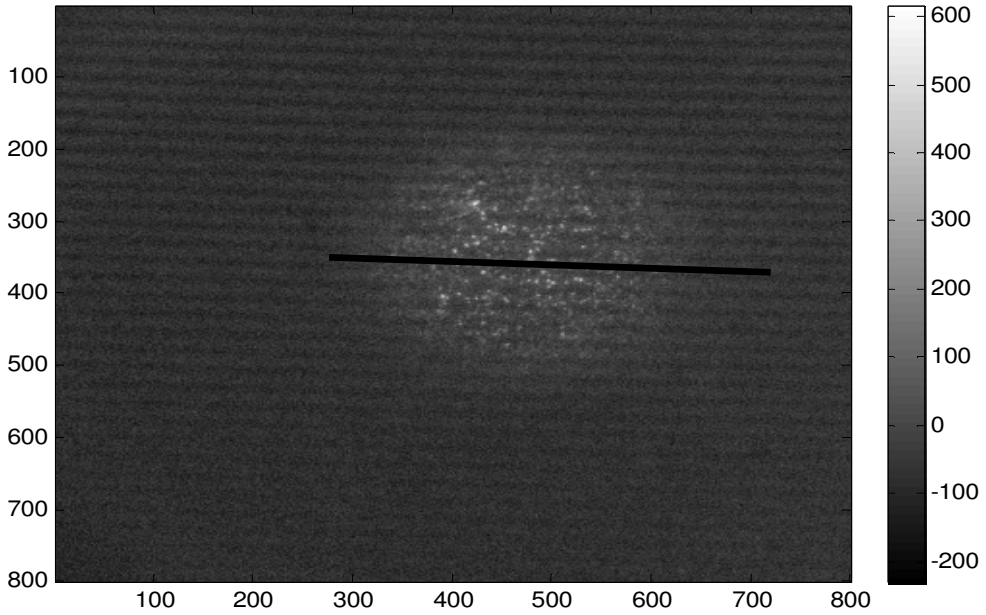

Figure 5.27 Profile line on sample containing donor and acceptor

Lastly, the cross talk is calculated by multiplying this ratio to the acceptor emission from the sample containing both donor and acceptor molecules.

crosstalk = ratioAO * profile of fret_a15_f

The difference between the extracted acceptor signal and cross-talk is the FRET signal.

fret = extracted acceptor profile – crosstalk

fret = extracted acceptor profile – (ratioAO * profile of fret_a15_f)

The fret signal is obtained at the end.

fret :

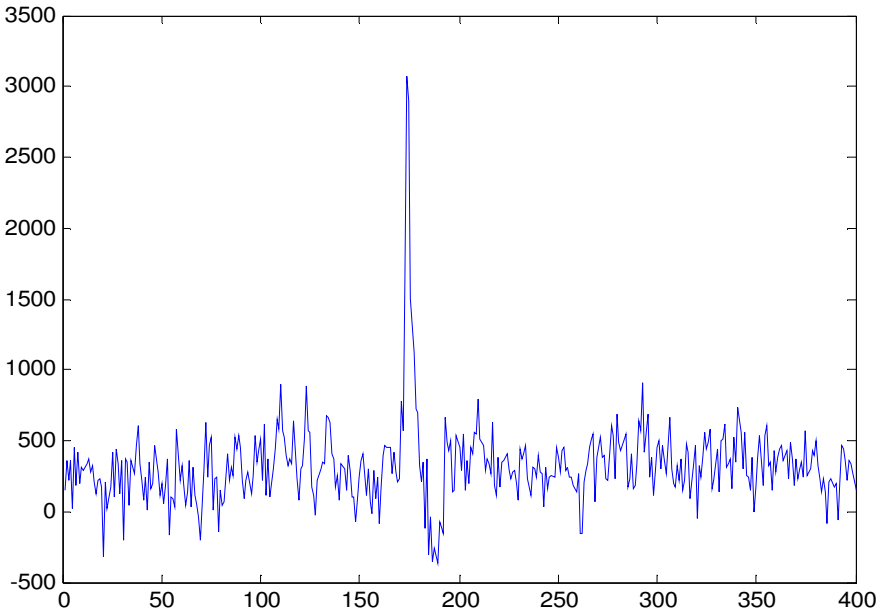

Figure 5.28 FRET signal

Furthermore, the resulting FRET signals of the same donor-acceptor sample with different samples containing donor only and acceptor only molecules are given in the following figures.

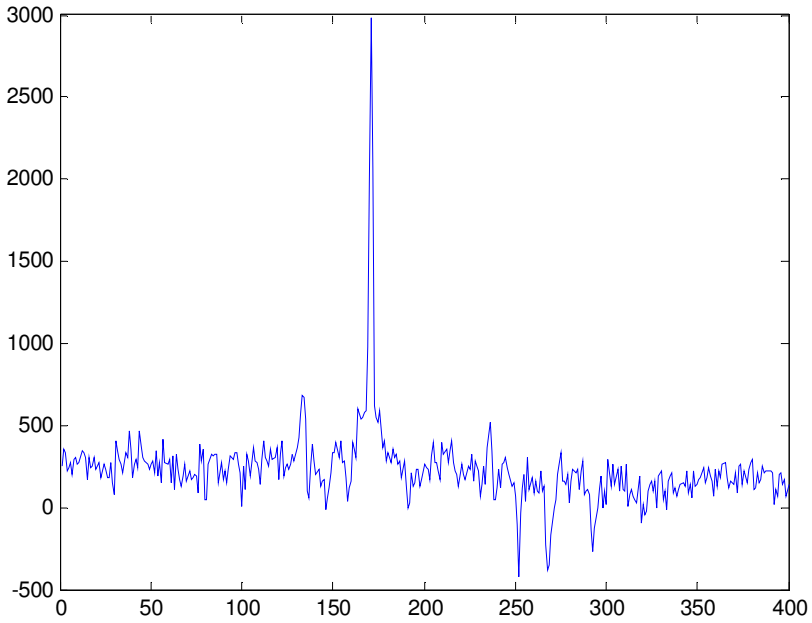

Figure 5.29 FRET signal

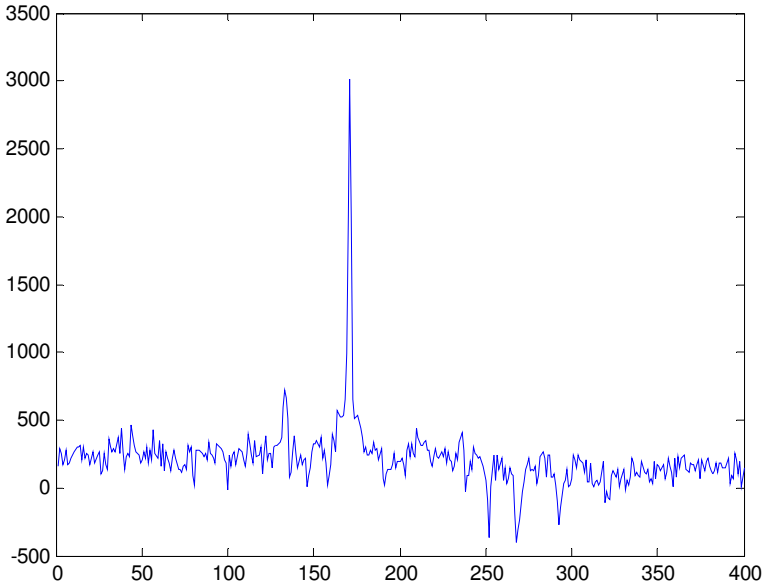

Figure 5.30 FRET signal

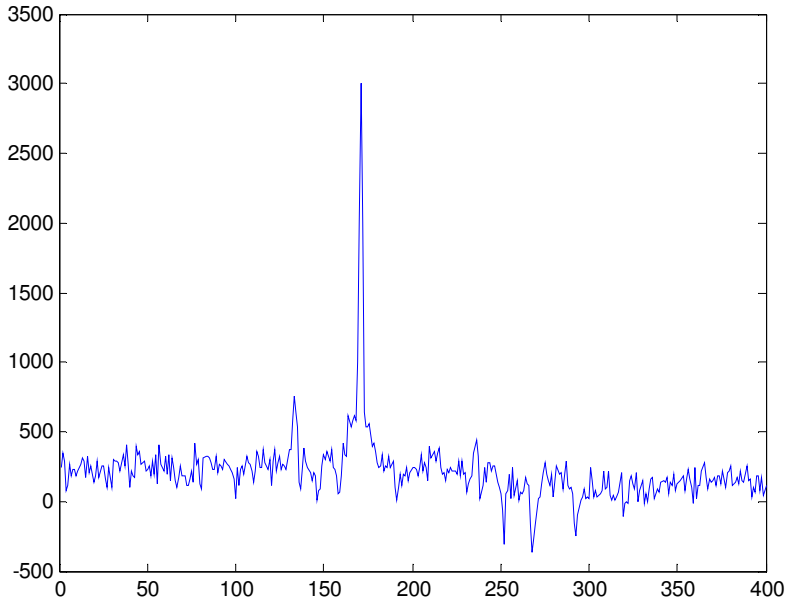

Figure 5.31 FRET signal

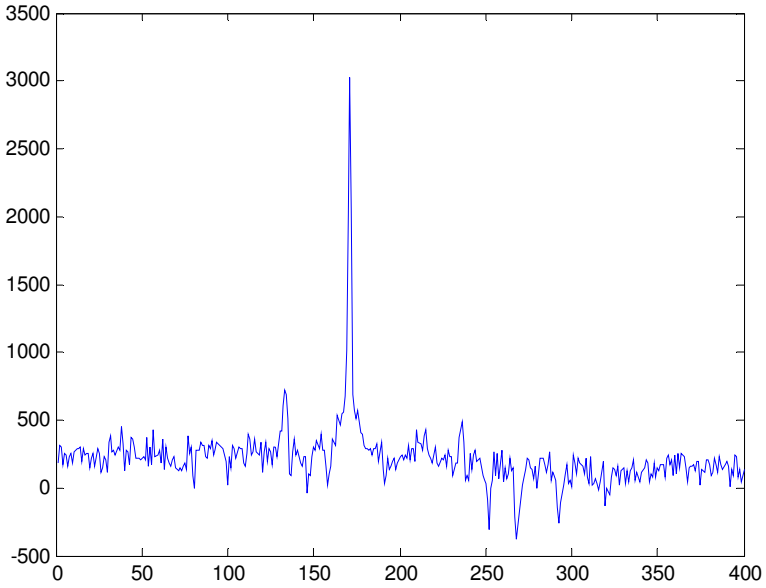

Figure 5.32 FRET signal

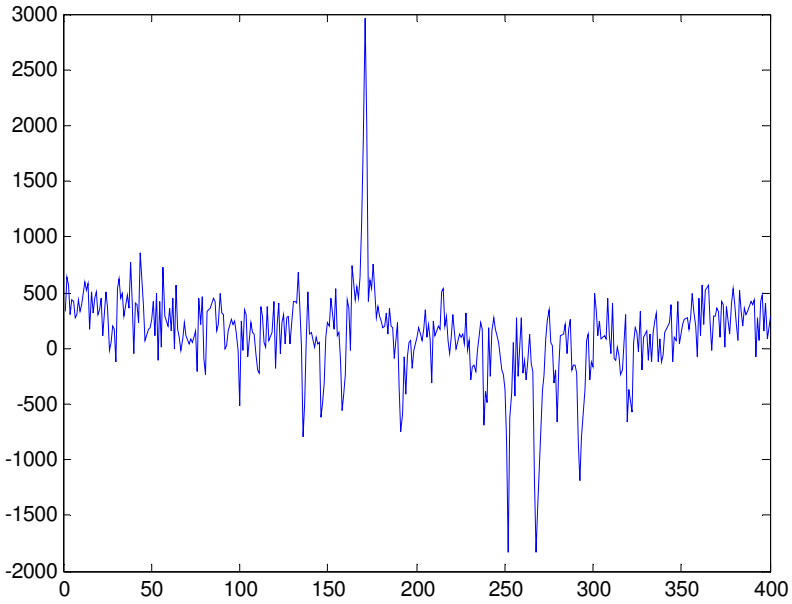

Figure 5.33 FRET signal

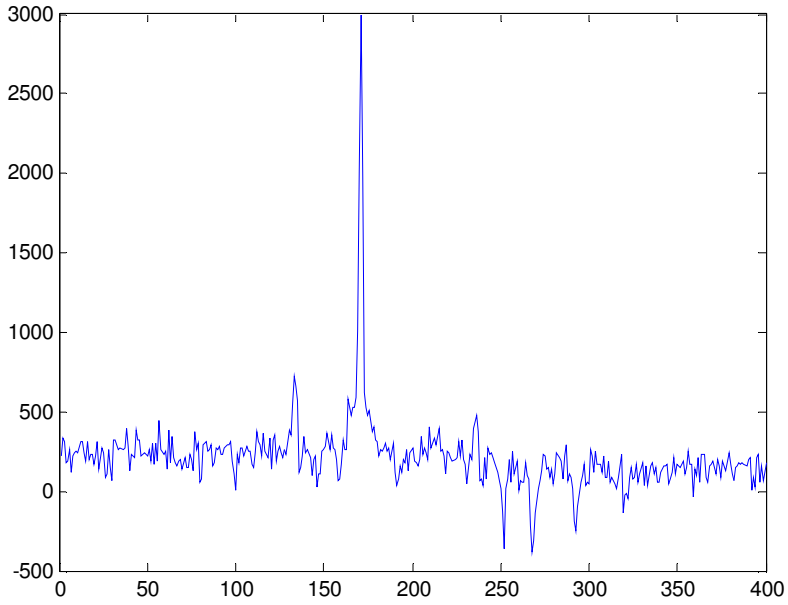

Figure 5.34 FRET signal

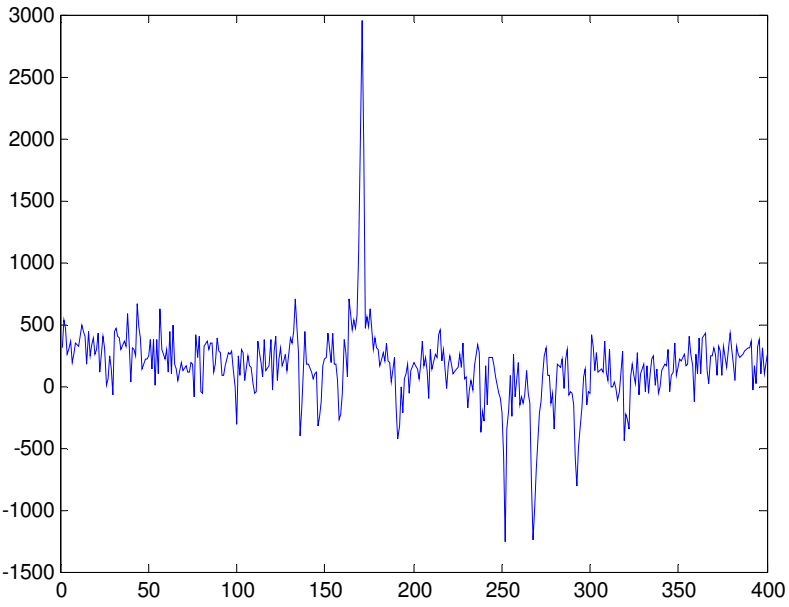

Figure 5.35 FRET signal

The efficiency of FRET of the same sample with different donor emission from donor only sample was calculated according to following the formula based on the decrease in donor emission after energy is transferred to the acceptor fluorophore.

$$\text{Efficiency} = \left(1 - \frac{I_{DA}}{I_D}\right)$$

Where I_{DA} and I_D are the donor emission intensity in the presence and absence of the acceptor, respectively.

eff_15_1 = 0.3703 (fret_a15_d, flu_a01_d)
eff_15_2 = 0.2749 (fret_a15_d, flu_a02_d)
eff_15_3 = 0.4051 (fret_a15_d, flu_a03_d)
eff_15_4 = 0.3057 (fret_a15_d, flu_a04_d)
eff_15_5 = 0.3662 (fret_a15_d, flu_a05_d)
eff_15_6 = 0.4249 (fret_a15_d, flu_a06_d)
eff_15_7 = 0.1612 (fret_a15_d, flu_a07_d)
eff_15_8 = 0.3076 (fret_a15_d, flu_a08_d)
eff_15_9 = 0.2761 (fret_a15_d, flu_a09_d)
eff_15_10 = 0.5807 (fret_a15_d, flu_a10_d)

In average, the efficiency of energy transfer was calculated to be 34.73 %.

Chapter 6

PROTEIN-PROTEIN INTERACTIONS

6.1 Introduction

Optical techniques relying on the property of fluorescence resonance energy transfer (FRET) between closely spaced fluorescent molecules are becoming more widely used for co-localization and functional interaction studies. Traditional approaches for studying protein-protein interactions such as Western-based pull-down assays or dual-label antibody labeling have severe limitations. Westerns are inherently denaturing, thus cause to miss functionally important reactions. On the other hand, co-localization by fluorescently coupled antibodies is diffraction-limited to 200 nm at best, which is large compared to the dimensions of proteins. Furthermore, immuno-electron microscopic co-localization greatly improves spatial resolution. Nonetheless, the technique is difficult and sometimes impossible in which epitopes are lost in the embedding process. Therefore, FRET emerged as a good method to demonstrate co-localization of protein species on a nanometer scale, preferably in living cells [5].

There are many fluorescent probes to label specific molecules in vivo or vitro FRET applications. However, the discovery and cloning of the green fluorescent protein from the jellyfish, *Aequorea victoria*, opened a new era in cell biology by allowing them to be used indicators or sensors of biological activities and protein interactions. When coupled to recent technical advances in widefield fluorescence and confocal microscopy, the green fluorescent protein (GFP) and its color-shifted genetic derivatives have been used in many thousands of live-cell imaging experiments [34].

Modified versions of GFP family proteins have seen extensive recent use in FRET studies. A recently used FRET pair is GFP-RFP, in which GFP that emits in the green, interacts with Red Fluorescent Protein (RFP), which emits in the red.

Fusion proteins of GFP and RFP can readily be constructed in laboratories and transfected in to an expression system. It is highly desirable, especially in living cells, to have fluorescent labels directly attached to the proteins whose interactions are in consideration [35].

Light is sensed by eye and transmitted to suprachiasmatic nuclei (SCN) for resetting the clock (Fig. 6.1). The SCN is located in the hypothalamus; it gives rise to numerous oscillators all through the body and regulates the biological functions such as; sleep-wake cycles, neuroendocrine levels, mental alertness, physical strength, body temperature, blood pressure, and blood viscosity [36, 37]. These functions can be affected such as; feeding, stress and temperature.

The circadian photoreception occurs in the inner retinal cell within the eye. The mammalian cryptochromes (Cry) and melanopsin (Mel), or possibly other opsin family pigments, are proposed as circadian photoreceptor pigments that start signal transduction to SCN [38]. Experimental studies imply that the cryptochromes, in addition to the melanopsin, may act as circadian photoreceptor.

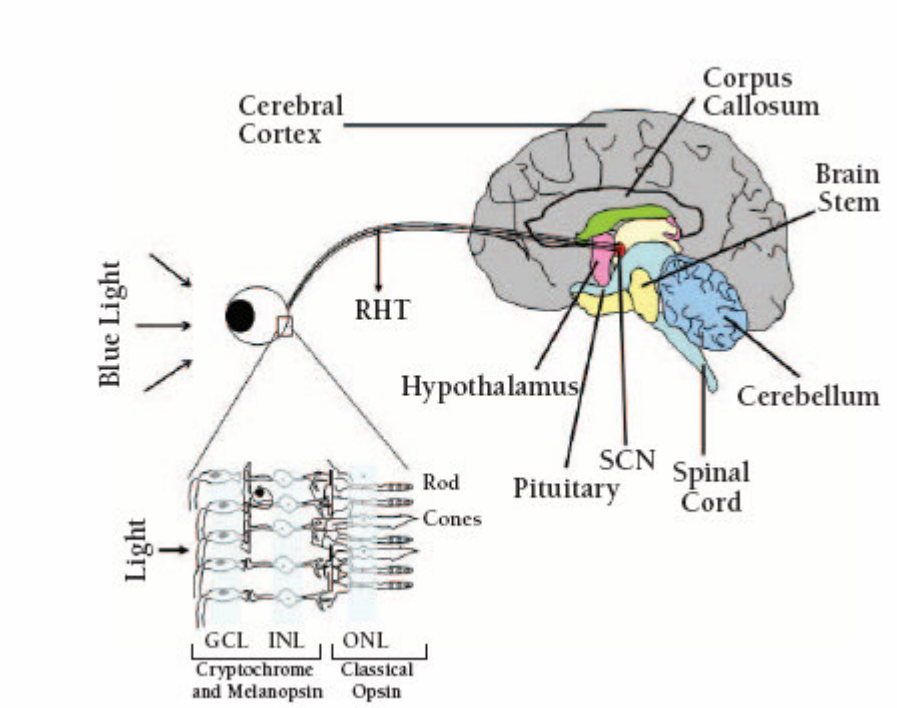

Figure.6.1 Light reception by eye and signal transduction to SCN [38]. The cryptochromes Cry1 and Cry2 are expressed in the inner nuclear layer (INL) and ganglion cell layer (GCL), and melanopsin is expressed in a small fraction of ganglion cells

It was discovered that mice lacking visual perception cells (rods and cones) could still respond to photoperiod by entrainment of their circadian rhythms [39]. Consequently, circadian photoreception pathway should be different from visual perception pathway. Melanopsin and cryptochromes are the only known photopigments in the inner retina of mice and humans, so they are possible photoreceptors for circadian rhythms. The knock-out studies imply that cryptochromes and melanopsin are essential for the circadian rhythms [40].

The studies of our collaboration group have shown that circadian photoreception depends primarily on cryptochromes and melanopsin [33].

It is not clear whether CRYs are in the pathway of melanopsin mediated light response in mammals. E.B.Ünal and her coworkers have taken computational approaches to investigate such a possible interaction between these proteins (personal communication). Computational works were performed by Hex 4.4 and AutoDock 3.0.5 tools. It was shown that the melanopsin binds to the part of human Cry2 that is indicated by yellow color (Fig 6.4) by computational dock analysis. It seems to be light may be mediated through interaction between 3 cytosolic loops of melanopsin and N-terminal of cryptochrome2 in humans. The interaction between those 2 proteins is hypothesized to give rise to the activation of signal-pathway from retinal cells to SCN for restarting biological clock.

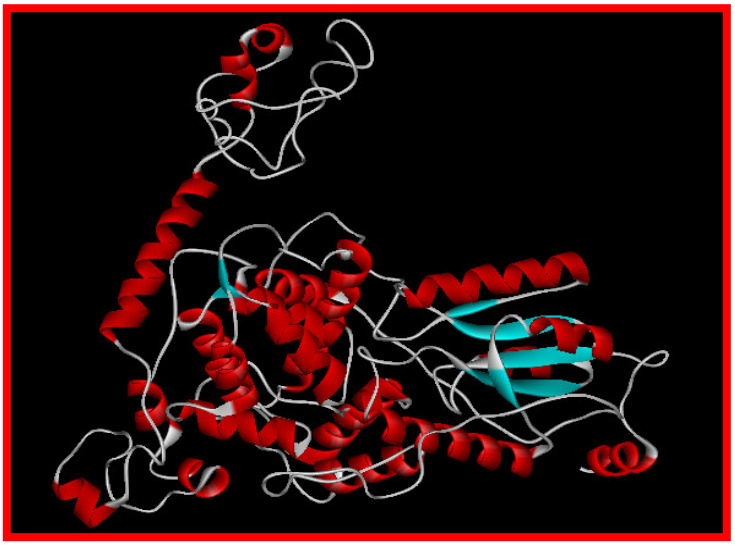

Figure 6.2 The computational modelling of human cryptochrome2 (by Evrim Besray Ünal Koç University Computational Sciences and Eng. Department)

Figure 6.3 The computational modeling of melanopsin (R. Hermann et al; Neuroscience Letters (2005) 36:76

Figure 6.4 The binding of Melanopsin to the part of human Cry2 that is indicated by yellow color (by Evrim Besray Ünal, Koç University Computational Sciences and Eng. Department)

In this study, we are going to study possible interaction between these two proteins using FRET *in vivo*. To do that we have fused both cryptochrome and melanopsin with GFP and RFP, respectively. Our preliminary data indicated that both proteins interact by FRET using human cell line 293T.

6.2 Materials and Methods

6.2.1 Construction of Expression Vectors and DNA Expression

By using mouse Cry2 and mouse Melanopsin as template, were amplified by PCR. PCR products of both CRY2 amd melanopsin were digested and cloned into a pEGFP and into a pDSRed2 mammalian expression vectors, respectively.

The *E. coli* DH5-alpha strain transformed with expression plasmids (pEGFP only, pDSRed2 only, pEGFP+Cry2, pDSRed2+Melanopsin) using electroporation technique. pEGFP+Cry2 transformed bacteria was used to obtain "Cry2 + GFP"; pDSRed2+Melanopsin transformed bacteria was used to obtain "Mel + RFP"; only pEGFP transformed bacteria was used to obtain "only GFP"; and finally only pDSRed2 transformed bacteria was used to obtain "only RFP" DNA.

The transformed bacteria were grown at 37°C shaker in LB medium for 30 minutes. The LB medium containing pEGFP was spread onto LB plates with kanamycin; and LB medium containing pDSRed2 was spread onto LB plates containing ampicillin. Colonies were picked by toothpick the day after spreading and grown overnight in LB containing appropriate antibiotic. Mini-prep was performed to extract the plasmid the next day. The control for pEGFP was performed by EcoRI digestion and gel-electrophoresis techniques. The control for pDSRed2 was performed by BamHI digestion and gel-electrophoresis techniques. Maxi-prep was performed to extract plasmids in high amount. The DNA was

obtained by digestion and agarose gel purification techniques and stored at -20^{o}C. The DNAs were used for HEK293 transfection afterwards.

6.2.2 The Preparation of Cells

293 T cells were used in our experiments. 293 T is a derivative of 293 human renal epithelial cell line that is transformed by adenovirus E1A gene product. They were prepared by the transient transfection method according to $Ca_3 (PO_4)_2$ transfection protocol [59]. The cells taken from a definite line are grown in cell culture. The cell culture is DMEM supplemented with 10% FCS (Fetal Calf Serum), 2 mM Glutamine and 1000 IU Penicillin/Streptomycin. Furthermore, they are put into 37 ºC, % 95 air, %5 CO_2 incubator. Because of the fact that the cells do not attach tightly, the cells can be detached with EDTA alone. For 10 cm dish, 10 ml medium is needed. If one wants to use 6-well or 12 well plates the volume of the medium will be 3 ml and 1,5 ml, respectively. The following protocol is for 10 cm dish. The cells are plated the night before to give 60-70 % confluence at the day of transfection. Then 10 µg DNA is added to ddH_2O in 15-ml sterile tube, then 155 µl 2M $CaCl_2$ is added. After that, while mixing gently, 1250 µl of 2×HEBS dropwise is added. This mixture is added directly to the cells dropwise evenly over the entire area through the medium within 10 min. The medium turns to orange. Then, it is incubated for 7-11 h. Very fine, dust like precipitate will be observed. After incubation, it is rinsed once and changed to fresh medium, again 10 ml/dish. Cells are harvested 24-48 h after transfection. The proteins are produced as long as the cells are alive. As the cells are ready with proteins in them, they are put into two cover glasses and sealed with epoxy.

6.2.3 Selecting suitable fluorophores

A group in USA [41] working on the interaction of phytochrome B and cryptochrome 2 in plants used GFP-RFP pair as a FRET pair for the first time and showed that these fluorophores are suitable pair by calculating the spectral overlap between donor emission and acceptor absorption J_{da}= 1.67× 10^{-13} M^{-1} cm^3 and R_0 is 5 nm which allows FRET detection over distances ~1.6×5=8 nm [50]. The spectral overlap of donor emission with acceptor absorption is seen in Fig. 6.5. FRET can be an accurate measurement of molecular proximity at distances (1–10 nm) and highly efficient if the donor and acceptor are positioned within the Förster radius [21].

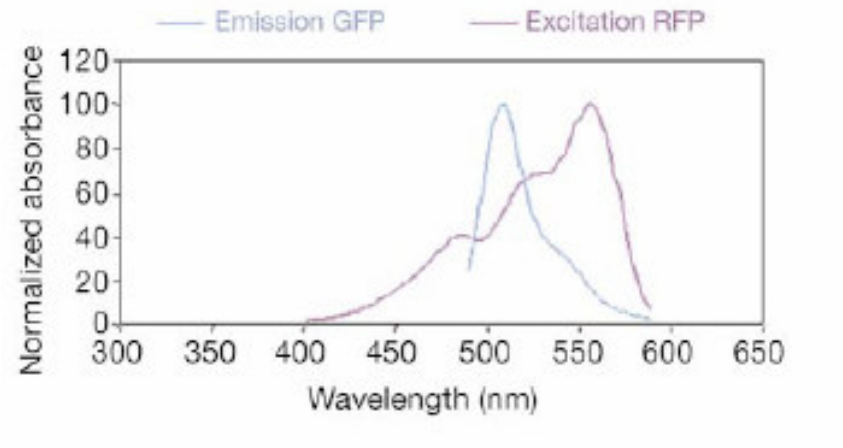

Figure 6.5 The spectral overlap of donor emission and acceptor absorption

Furthermore, there is a sufficient separation in excitation spectra of fluorophores that the excitation maximum of green fluorescent protein EGFP is 488 nm, while RFP's excitation maximum range from 548 nm to 595 nm according to the type of red fluorescent protein fused. In addition, there is reasonable separation in emission spectra of these flurophores that GFP emits green, which corresponds to wavelengths between 520-570, on the other hand, RFP, emits in the range of 585-650 nm corresponding to orange and red wavelength range. Therefore, one can use filters for separating emissions from donor and

acceptor in the range of their emission wavelengths. We have collected light emitted from the fluorophores with the HQ Chroma filters 620/60 for RFP, 525/50 for EGFP.

6.2.4 The localization of Proteins in Cells

By using fluorescence microscopy, it is possible to find the locations of proteins that are tagged with fluorescent proteins. We have used confocal microscopy which scans the whole cell point by point thus gives a better result about the localizations of proteins in cell. We have used 488 nm Ar ion laser as an excitation source for donor fluorophore, GFP and 532 nm diode pumped Nd-YAG laser as an excitation source for acceptor fluorophore, RFP. For collecting the light emission from fluorescent molecules, we have used HQ Chroma band pass filters allowing to pass light between 500-550 nm for donor molecule which emits in the range of green and 590-650 nm for acceptor molecule emitting in the range of orange and red. The fluorescence emitted from donor and acceptor molecules was collected by a microscope objective (N.A.=1.4, 60x oil), and a 1.5x magnification element was used for further magnification. For the confocal microscopy experiments an avalanche photodetector was used to detect fluorescence emission from fluorescent proteins. A piezoelectric translation stage was used for confocal scanning. For the total internal wide-field microscopy experiments a cooled CCD camera were used to detect signals emitted from fluorescent proteins.

6.2.5 FRET Experiment

We have used total internal wide-field microscopy to measure FRET between RFP-Mel and GFP-Cry by exciting donor and acceptor tagged samples by 488 nm Ar ion laser. The angle of incidence of the laser beam to the sample interface where the living cells are sealed between two cover glasses was adjusted to observe total internal reflection. The fluorescent light collected by the same microscope objective (N.A.=1.4, 60x oil), and a

1.5x magnification element. Afterwards the fluorescent light passed through dichroic mirror and band pass filters (HQ Chroma filters 620/60 for RFP, 525/50 for EGFP) and a cooled CCD camera were used to detect signals emitted from fluorescent proteins.

6.3 Results and Discussion

It was observed that the melanopsin protein where RFP is fused with its C-terminal, is localized in cell membrane shown in Fig. 6.6 Melanopsin was observed to be localized in cell membrane. The image (Fig. 6.6c) was obtained simply subtracting cells, which do not express RFP-Mel constructs. The fluorescence observed in control cells can result from the some intrinsic aminoacids such as tryptophan, tyrosine existing in fetal Calfserum put into cell culture as well as Ca $(PO_4)^{-3}$ calcium phosphate were used to transfect DNA into cell. Beside these, some antibiotics such as penicillin put into cell culture to avoid bacterial infusion can cause contamination light in control cells. However, in the following FRET experiments the preparation of cells was altered to diminish background light as much as possible by not using antibiotics in cell culture. Additionally, the cells were prepared without fetal Calfserum.

The aggregation of melanopsin proteins was observed in Fig.6.6c. This can be explained with the oligomerization properties of melanopsin [42] as well as red fluorescent proteins. Because it was shown that red fluorescent protein shows oligomerization even at subnanomolar concentrations by many researchers [24]. For future work, in order to be sure whether RFP or melanopsin is making oligomerization, the cells with only RFP can be used as a control. The subtraction of RFP fused with melanopsin cells from only RFP cells can be a proof of oligomerization of melanopsin. If melanopsin is able to oligomerize, the interaction of Cry2 and melanopsin may be possible by those oligomers.

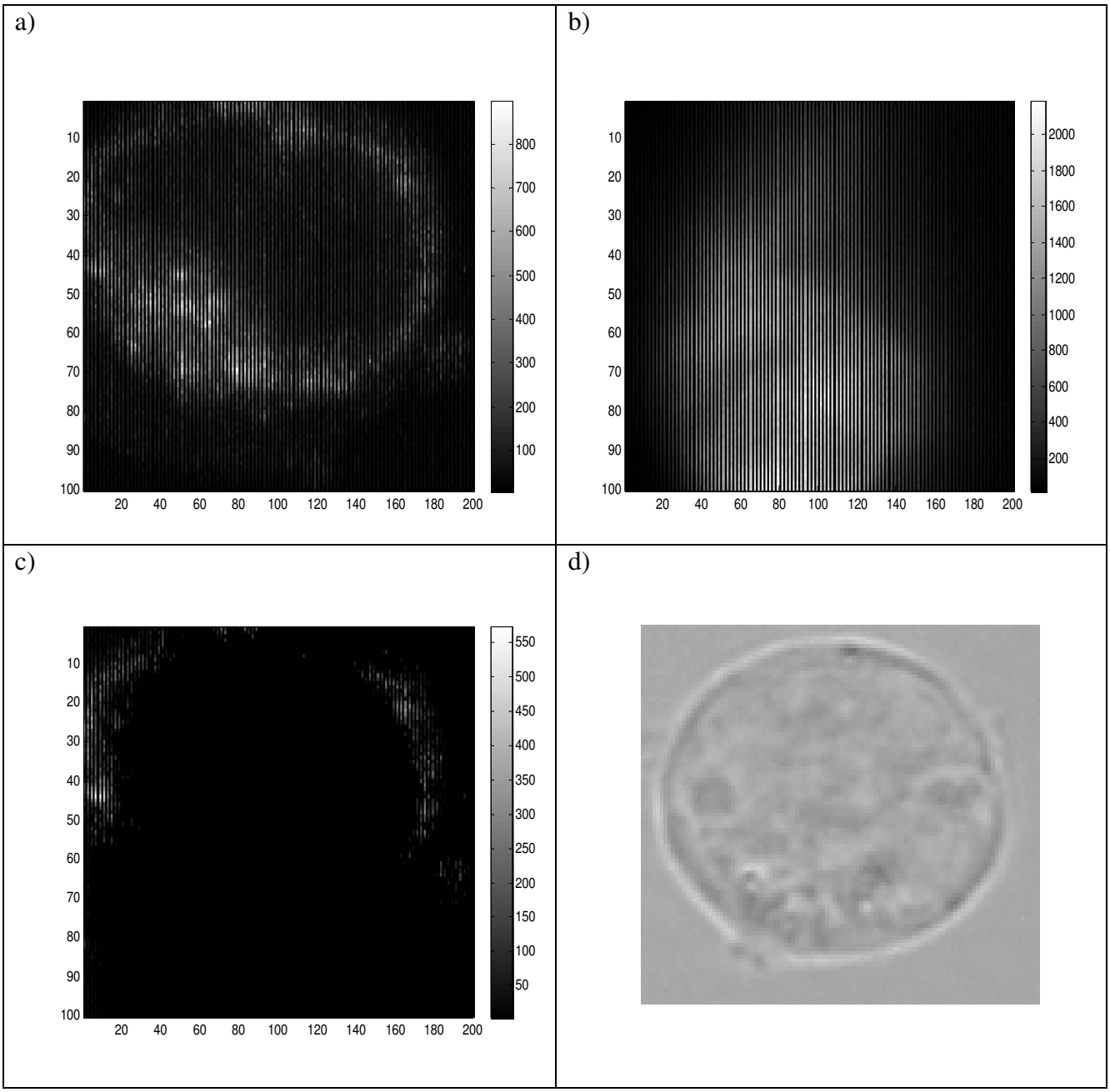

Figure 6.6 a) The confocal image of Melanopsin labeled with RFP **b)** Untransfected cell **c)** RFP tagged Melanopsin containing cell free of background light **d)** The transmission image of the cell.

Cry, which is fused with GFP at their C terminal, seems to be localized in the cytoplasm (Fig. 6.7c). The background light (Fig.6.7b) were subtracted from the cells expressed with GFP tagged cryptochrome (Fig.6.7a). In Fig.6.7c the cell free of background light shows that the Cry proteins are distributed in cytoplasm of cell as it is verified from the transmission image of the cell (Fig. 6.7d).

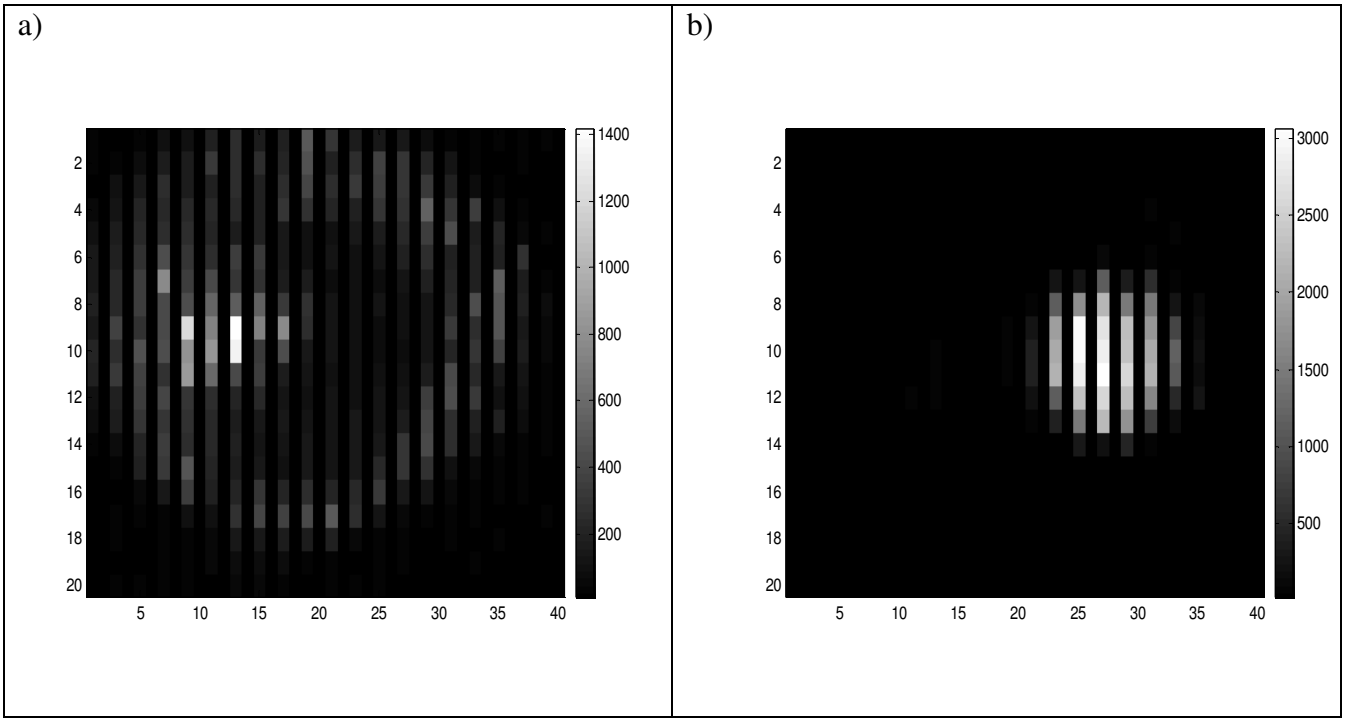

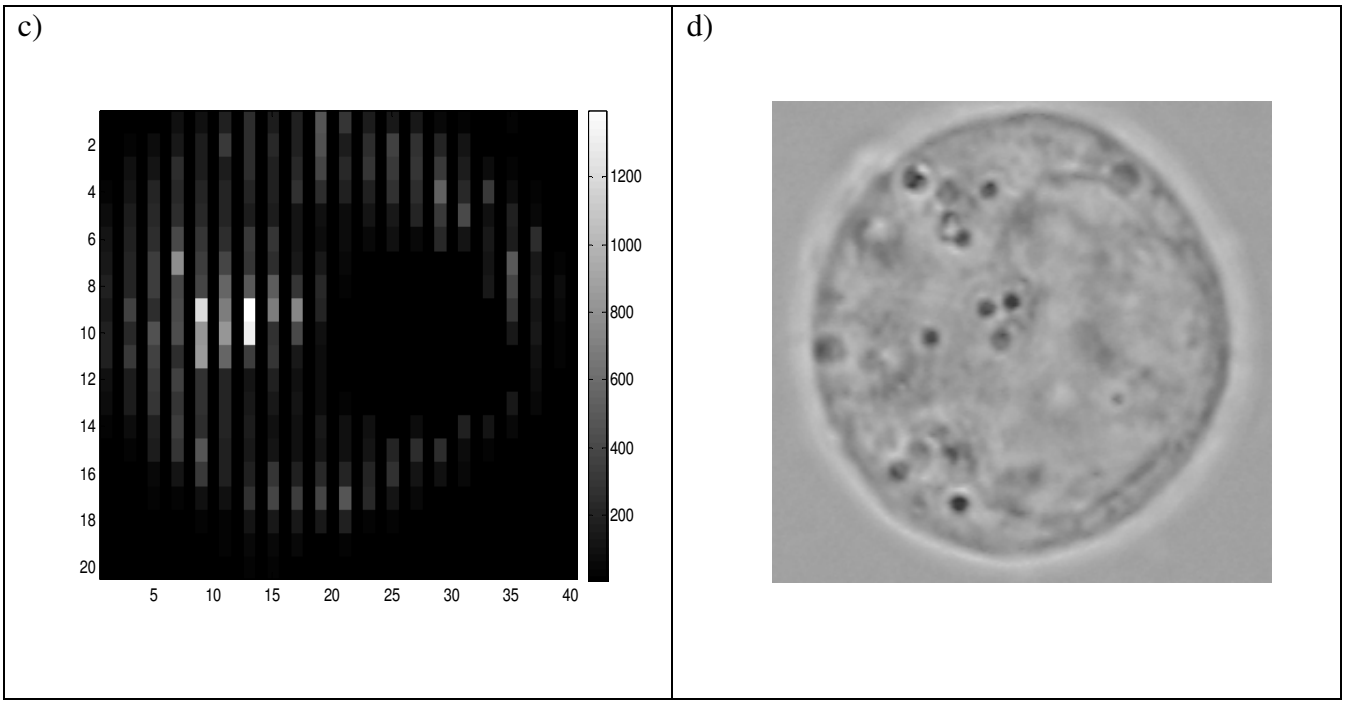

Figure 6.7 a) Cryptchrome labeled with GFP. **b)** Control cell. **c)** GFP tagged Cry cell free of background light. **d)** Transmission image of a cell with Cry labeled GFP

In the previous chapter, the results of the FRET efficiency between Fluorescein Na and Rhodamine B were given by analyzing the data based on decrease in FRET emission developing a method inspired by spectra FRET technique. However, we had difficulty to apply this technique to our samples containing proteins fused with fluorescent proteins since the lasers we are using have different powers. The 532 nm diode pumped Nd:YAG laser which is the excitation light of acceptor fluorophore (RFP) is stronger than the 488 nm Ar ion laser which is the excitation light of donor fluorophore (GFP). As the power of excitation light increases, the average distance between unassociated donor and acceptor fluorophores decreases. Hence, the probability of finding a donor and an acceptor within the FRET distance increases. Thus the fluorescence emission obtained from RFP tagged melanopsin only and GFP tagged cryptochrome only will not be reliable so as to use them

as controls in our experiments. In addition, it is hard to equate the power of the lasers for exciting the GFP tagged Cry and RFP tagged melanopsin. Thus, we could not obtain the data of the fluorescence emissions of the donor tagged only proteins (Cry-GFP) and the acceptor tagged only proteins (Mel-RFP) with their own excitation light, which would be our controls to determine if there is an energy transfer between the GFP fused with cryptochrome and RFP fused with melanopsin.

We have observed that the donor emission from cells both transfected with Mel-RFP and Cry-GFP and acceptor emission from cells both transfected with Mel-RFP and Cry-GFP positioned around cell membrane, which is observed in Figures 6.8a, 6.8b and 6.9a and 6.9b. Figure 6.8a shows the acceptor emission from a cell transfected with Mel-RFP and Cry-GFP obtained with FRET filter while Fig. 6.8b shows the fluorescence emission from the same cell transfected with both Mel-RFP and Cry-GFP obtained with donor filter. This is the indication of co-localizations between Cry and melanopsin proteins in cells. Furthermore, Figures 6.10, 6.11, and 6.12 show the co-localizations of fluorescent proteins and an increase in the intensity of acceptor fluorescence emission. We obtained the substraction of donor emission from acceptor emission by Labview program. Figures 6.10c, 6.11c, 6.12c show the difference between donor and acceptor fluorescence where the intensity of light emitted from RFP-Mel is more than the intensity of light emitted from GFP-Cry. These images indicate that there are some points on the sample where the acceptor chromophore emits more fluorescence light than the donor chromophore does. It can result from energy transfer from GFP to RFP. Since if there is an energy transfer from donor chromophore to acceptor chromophore, the intensity of donor decreases whereas the intensity of acceptor fluorophore increases. Even though we obtain good results with the samples containing Mel-RFP and Cry-GFP by observing that the acceptor emission is higher than the donor emission, we could not be sure about the energy transfer from donor to acceptor molecule. Since there is always light contaminations resulting from overlap

between emission and absorption spectra of chromophores. That is to say, GFP can emit light in the range of acceptor emission and RFP can be excited by donor excitation light thus contributes more emission to the FRET channel. Additionally, uncoupled fluorophores and pairs of like fluorophores contributes to the total fluorescence intensity and reduces the apparent FRET efficiency. Nonetheless, in order to find exact energy transfer from GFP to RFP chromophore we need to remove contaminating signals from competition with fluorescent signal of interest.

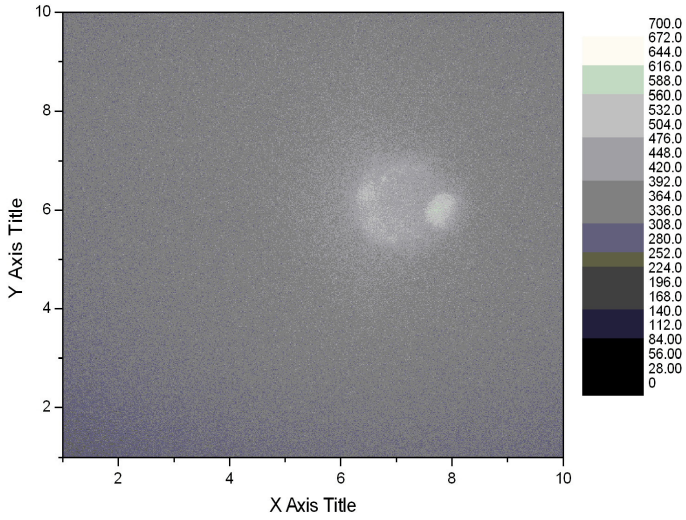

Figure 6.8a Acceptor emission in a cell both transfected with RFP-Mel and GFP-Cry

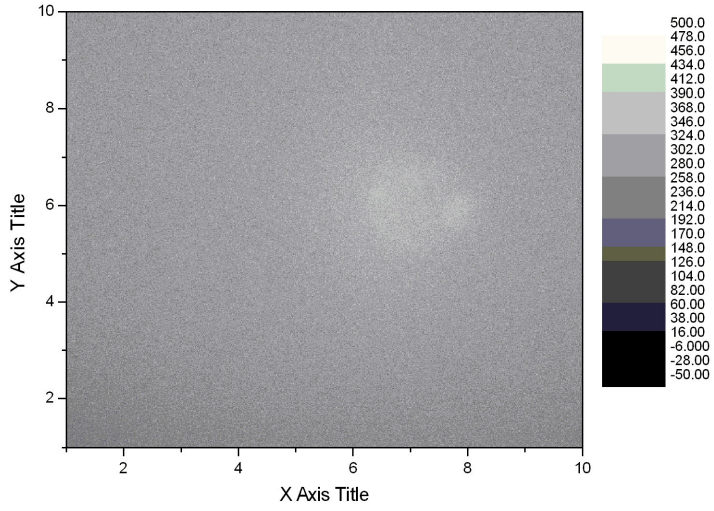

Figure 6.8b Donor Emission in a cell both transfected with both RFP-Mel and GFP-Cry

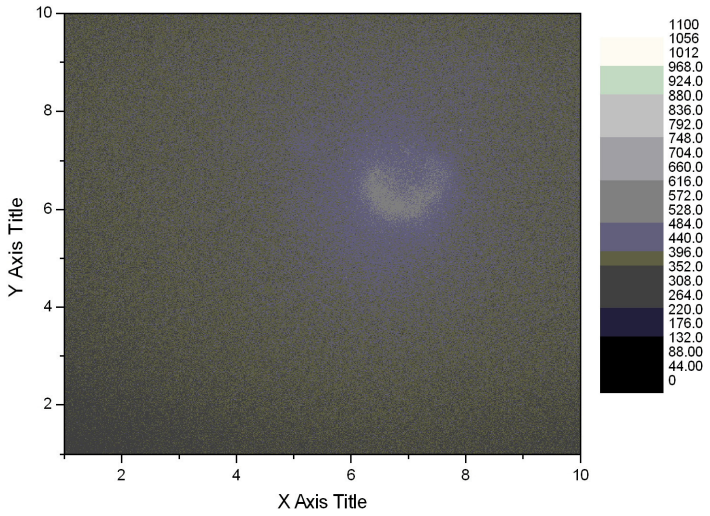

Figure 6.9a Acceptor emission in a cell both transfected with RFP-Mel and GFP-Cry

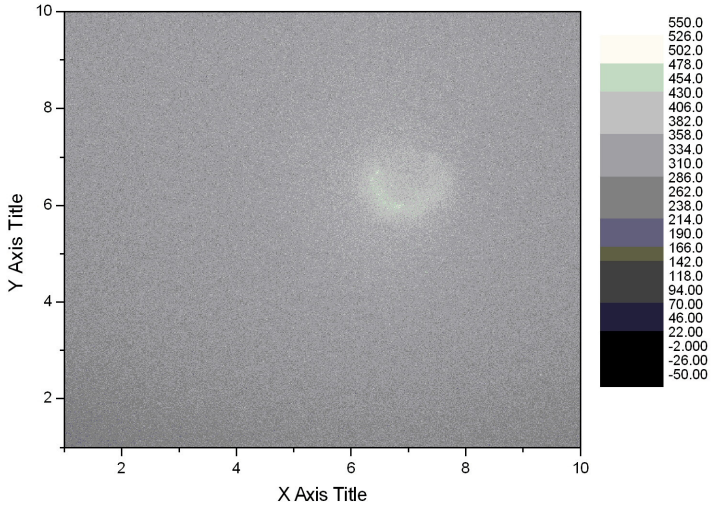

Figure 6.9b Donor Emission in a cell both transfected with both RFP-Mel and GFP-Cry

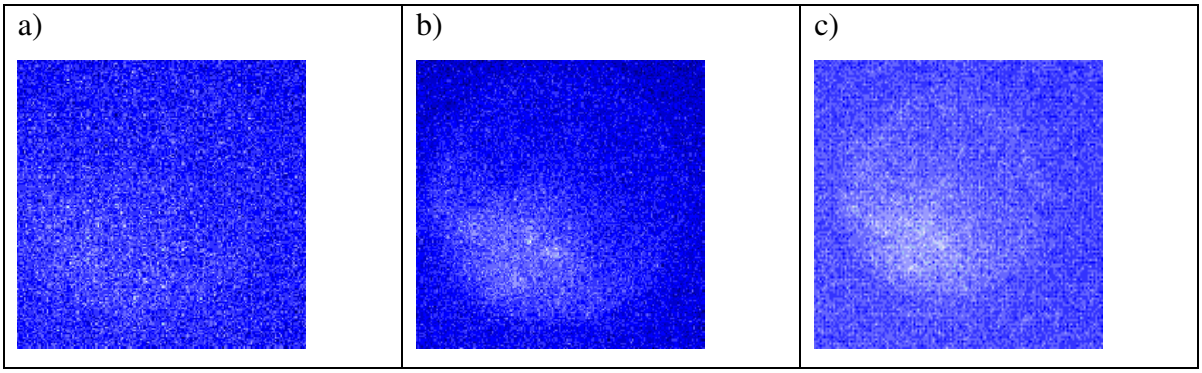

Figure 6.10 a) The image of donor and acceptor tagged molecules obtained with donor filter **b)** The image of donor and acceptor tagged molecules obtained with FRET filter **c)** The substraction of donor emission from acceptor emission

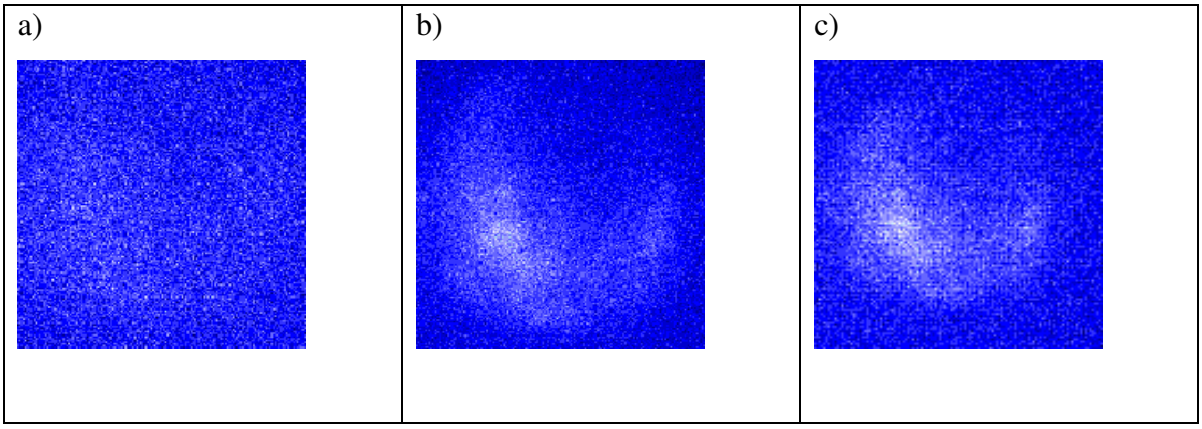

Figure 6.11 a) The image of donor and acceptor tagged molecules obtained with donor filter **b)** The image of donor and acceptor tagged molecules obtained with FRET filter **c)** The substraction of donor emission from acceptor emission

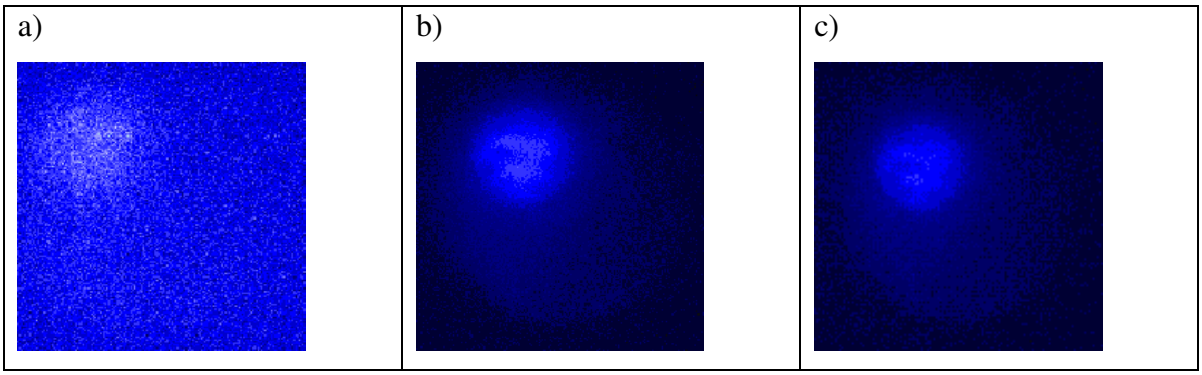

Figure 6.12 a) The image of donor and acceptor tagged molecules obtained with donor filter **b)** The image of donor and acceptor tagged molecules obtained with FRET filter **c)** The substraction of donor emission from acceptor emission

There is also background light problem in our experiments including autofluorescence from aminoacids in proteins such as tryptophan, tyrosine, detector noise, optical noise, and photobleaching in intensity-based FRET imaging microscopy. These light contaminations can be removed from the observed FRET signal by several approaches as explained in Chapter 5, Sec. 5.4.

Moreover, the co-localizations of Cry fused with GFP and melanopsin fused with RFP around cell membrane gives a strıong indication about their vicinity. Since if melanopsin transmits light signal together with Cry, the Cry protein will bind to melanopsin protein. Then we expect them to be localized at the same place in cells. FRET allows for the detection of energy transfer between donor and acceptor chromophores separated with maximum 10 nm distance. Consequently, if there is an energy transfer between RFP and GFP, the melanopsin and Cry proteins fused with these fluorophores must be in close proximity, i.e. apposed to each other, as a result of the interaction of Cry with melanopsin protein.

Futhermore, in order to be sure about the interaction of Cry with Melanopsin the apparent energy transfer must be calculated in numerous cells transfected with Mel-RFP and Cry-GFP. Since the FRET efficiency depends on the concentration of the donor and acceptor molecules, the problem arises when the expression levels of the donor and the acceptor fluorophore vary from one sample to another. In experiments with transfected cells we can not calculate the expression levels of proteins in cells. Since gene transfection do not produce consistent fluorophore ratios even both the donor and acceptor are encoded in the same plasmid. Thus donor-to acceptor ratio vary at each cell and we can not evaluate exact energy transfer efficiency statistically.

Lastly, in order to be sure if the Cry protein really interacts with melanopsin protein, the energy transfer must be measured in cells containing RFP-Mel and GFP only which is not fused to Cry. Since if Cry interacts with melanopsin we will expect it to bind to melanopsin protein i.e. close proximity (in nanometers). In the absence of Cry if there is energy transfer from GFP-RFP then we can conclude that the Cry protein is not functioning with Melanopsin in circadian clock to transmit light signals to SCN. The detection of FRET can be used to infer that the fluorophores, and therefore the targeted proteins are closely located to each other. However, the absence of FRET should not be used to infer that the fluorophores are more widely separated.

Chapter 7

CONCLUSIONS

FRET detection and measurement are important new tools in structure-function studies. We have used confocal and wide field microscopy in our experiments.

We have used total internal reflection fluorescent microscopy to look for the molecular interactions i.e. energy transfer between two fluorescent molecules Rhodamine B and Fluorescein Na in PMMA thin films. In order to find actual FRET signal, we used a technique following the steps of spectra FRET method to subtract bleed through and cross talk from the observed FRET signal. The efficiency of FRET was quantified by the decrease in donor intensity after energy transferred from donor to acceptor molecule. In addition, te total internal reflection fluorescent microscopy technique was used to examine whether melanopsin interacts with Cry. Our preliminary data indicates that both proteins interact by FRET. Since we have observed an increase in the intensity of acceptor fluorescence emission as well as co-localizations of the proteins labeled with RFP and GFP in living cells.

Furthermore, we have used confocal microscopy to determine the exact localization of proteins in cells. The melanopsin protein that belongs to the group of transmembrane proteins is located in cell membrane as expected, while the cry proteins are distributed in cytoplasm of the cell.

Lastly, we observed sudden and complete photobleaching as well as blinking in the fluorescent spots of Rhodamine B in the confocal images, which are the photophysical

properties of single molecules. In addition, we observed the single molecule behavior of Rhodamine B molecules in PMMA thin films by wide field microscopy.

Biology and imaging provide powerful tools for research and clinical applications. FRET techniques can become more powerful when combined with recent advances in fluorescent probes, instrumentation, and methodologies. FRET will revolutionize scientific research in the near future.

BIBLIOGRAPHY

[1] K. T. a. M. Ikura, "The use of FRET imaging microscopy to detect protein-protein interactions and protein conformational changes in vivo," *Current Opinion in Structural Biology*, vol. 11, pp. 573-578, 2001.

[2] B. Valeur, *Molecular Fluorescence Principles and Applications*: WILEY-VCH, 2002.

[3] H. Taekjip, "Single-Molecule Fluorescence Resonance Energy Transfer," *METHODS*, vol. 25, pp. 78-86, 2001.

[4] N. K. Andrew H. A. Clayton, Stephen H. Cody, Edouard C. Nice, "Dual-channel photobleaching FRET microscopy for improved resolution of protein association states in living cells," *Eur Biophys J*, vol. 34, pp. 82-90, 2005.

[5] E. Golemis, *Protein-protein interactions : a molecular cloning manual*: NY : Cold Spring Harbor Laboratory Press, 2002.

[6] L. S. a. R. P. Haugland, "Energy Transfer: A Spectroscopic Ruler," *Biochemistry: Stryer and Haugland*, vol. 68, 1967.

[7] B. C. Richard Hallworth, Michael G. Nichols, Xudong Wu, Jian Zuo, "Studying inner ear protein-protein interactions using FRET and FLIM," *BRES-35283, 4C:2*, 2006.

[8] L. R. Joseph, *Principles of Fluorescence Spectroscopy*, Third edition ed: Plenum Press Newyork and London, 1986.

[9] V. Rheenen, *Biophysical Journal*, vol. 86, pp. 2517-2529, 2004.

[10] N. J. Emptage, "Fluorescent imaging in living systems," *Current Opinion in Pharmacology*, vol. 1, pp. 521-525, 2001.

[11] T. H. Matthew P. Gordon, and Paul R. Selvin, "Single-molecule high-resolution imaging with photobleaching," *PNAS*, vol. 101, pp. 6462-6465, 2004.

[12] A. L. D. a. D. A. Andrey, *Resonance Energy Transfer*: John Willey& Sons, 1999.

[13] R. H. Webb, "Confocal optical microscopy," *Rep. Prog. Phys. 59*, pp. 427-471, 1996.

[14] T. Ha, "Structural Dynamics and Processing of Nucleic Acids Revealed by Single-Molecule Spectroscopy," *American Chemical Society*, vol. 43, 2004.

[15] L. Kubínová, in: Proceedings: 2nd Annual Meeting of CSMS, *Vranovská Ves,* 2002.

[16] H. T. M. v. d. V. G.J. Brakenhoff, E.A. van Spronsen, W.A. Linnemans, and N. Nanninga, "Three-dimensional chromatin distribution in neuroblastoma nuclei

shown by confocal scanning laser microscopy," *Nature*, vol. 317, pp. 748-749, 1985.

[17] J. E. Ch. Zander, R. A. Keller, *Single Molecule Detection in Solution*: *WILEY-VCH*, 2002.

[18] D. W. Piston, "Choosing Objective Lenses: The Importance of Numerical Aperture and Magnification in Digital Optical Microscopy," *Biol. Bull.*, vol. 195, pp. 1-4, 1998.

[19] A. Yariv, *Optical Electronics in Modern Communications*, Fifth Edition ed: Oxford University Press, 1997.

[20] N. C. a. L. P. Lee, "Total internal reflection-based biochip utilizing a polymer-filled cavity with a micromirror sidewall," *Lab Chip*, vol. 4, pp. 125-130, 2004.

[21] R. B. S. a. A. Periasamy, "Fluorescence resonance energy transfer (FRET) microscopy imaging of live cell protein localizations," *The Journal of Cell Biology*, vol. 160, pp. 629-633, 2003.

[22] E. T. S.A. McKinney, T.J. Wilson, M.K. Nahas, A.C. Declais, R.M. Clegg, D.M.J. Lilley and T. Ha, "Single-molecule studies of DNA and RNA four-way junctions," *Biochemical Society Transactions*, vol. 32, pp. 41-45, 2004.

[23] R. K. a. H. Piwon´ski a, A. Meixner b, J. Sepiol, "Optimal oxygen concentration for the detection of single indocarbocyanine molecules in a polymeric matrix," *Chemical Physics Letters*, vol. 405, pp. 352-356, 2005.

[24] J. H. Mircea Cotlet, Fabian Köhn, Jan Michiels, Gunter Dirix, Maarten Van Guyse, Joys Vanderleyden, Frans C. De Schryver, "Collective effects in individual oligomers of the red fluorescent coral protein DsRed," *Chemical Physics Letters*, vol. 336, pp. 415-423, 2001.

[25] J. E. M. Böhmer, "Orientation Imaging of Single Molecules by Wide-field Epifluorescence Microscopy," *J. Opt. Soc. Am. B.*, vol. 20, 2003.

[26] L. R. Joseph, *Topics in Fluorescence Spectroscopy*: Plenum Press Newyork and London, 1991.

[27] R. E. C. Jin Zhang, Alice Y. Ting, Roger Y. Tsien, "Creating new fluorescent probes for cell biology," *Nature Publishing Group*, vol. 3, pp. 908-918, 2002.

[28] L. D. B. a. M. A. Behlke, "Spectra of DNA-Conjugated Fluorescent Dyes," *Integrated DNA Technologies*, 2005.

[29] S. S. H. C V Bindhu, Geetha K Varier, Riju C Issac, V P N Nampoori and C P G Vallabhan, "Measurement of the absolute fluorescence quantum yield of rhodamine B solution using a dual-beam thermal lens technique," *J. Phys. D: Appl. Phys. 29*, vol. 1074-1079, 1996.

[30] A. M. Clegg RM, A Zechel, C Carlberg, S Diekmann, and DM Lilley, "Fluorescence resonance energy transfer analysis of the structure of the four-way DNA

Junction," *Biochemistry 31*, pp. 4846-4856, 1992.

[31] S. C. Z. D. S. Corrêa, L. Misoguti, C. R. Mendonça, "Two-photon fluorescence excitation in fluorecein," *ANNALS OF OPTICS - XXV ENFMC*, 2002.

[32] E. A. B. Christina L. Takanishi, Wei Cheng, Jie Zheng, "GFP-based FRET analysis in live cells," *Brain Research-35197, 4C*, vol. 3, 2006.

[33] A. G. F. Baldini, "Optical chemical and biochemical sensors: new trends," *Proc. SPIE*, vol. 5826, pp. 485-499, 2005.

[34] E. H.-C. Nandini Hayes, William Gullick, "Green fluorescent protein as a tool to study epidermal growth factor receptor function," *Cancer Letters*, vol. 206, pp. 129-135, 2004.

[35] O. T. Robert E. Campbell, Amy E. Palmer, Paul A. Steinbach, Geoffrey S. Baird, David A. Zacharias, and Roger Y. Tsien, "A monomeric red fluorescent protein," *Proc Natl Acad Sci U S A.*, vol. 99, pp. 7877-7882, 2002.

[36] W. J. Schwartz, "A clinician's primer on the circadian clock: Its localization, function, and resetting," *Adv. Intern. Med. 38*, pp. 81-106, 1993.

[37] I. P. Tida Kumbalasiri, "Melanopsin and other novel mammalian opsins," *Experimental Eye Research*, vol. 81, pp. 368-375, 2005.

[38] A. S. İbrahim Kavaklı, "Circadian Photoreception in Humans and Mice," *Molecular Inventions*, vol. 2, 2002.

[39] L. P. Ralph Hermann, Sarolta Pilbak, Carolin Boden, Jochen Maurer, Susanne Weber, Alexander Lerchl, "Predicted 3D-structure of melanopsin, the non-rod, non-cone photopigment of the mammalian circadian clock, from Djungarian hamsters (Phodopus sungorus)," *Neuroscience Letters*, vol. 376, pp. 76-80, 2005.

[40] N. C. a. P. Sassoneorsi, "Environmental stimulus perception and control of circadian clocks," *Current Opinion in Neurobiology*, vol. 12, pp. 359-365, 2002.

[41] P. F. D. Paloma Mas, Satchıdananda Panda,Steve A. Kay, "Functional interaction of phytochrome B and cryptochrome 2," *Nature 408*, pp. 207 - 211, 2000.

[42] M. F. a. H. Weinstein, "The study of G-protein coupled receptor oligomerization with computational modeling and bioinformatics," *FEBS Journal*, vol. 272, 2005.